ΠΑΝΕΠΙΣΤΗΜΙΟ ΘΕΣΣΑΛΙΑΣ

ΤΜΗΜΑ ΒΙΟΧΗΜΕΙΑΣ ΚΑΙ ΒΙΟΤΕΧΝΟΛΟΓΙΑΣ

ΠΡΟΓΡΑΜΜΑ ΜΕΤΑΠΤΥΧΙΑΚΩΝ ΣΠΟΥΔΩΝ

«ΤΟΞΙΚΟΛΟΓΙΑ»

«Insights into alpha-synucleinopathies: The role of RNA binding protein TIA1. Development of an *in vivo* model»

Μεταπτυχιακή διπλωματική εργασία

ΤΣΑΡΝΑ ΟΛΓΑ

Επιβλέποντες: Δοξάκης Επαμεινώνδας

Κουρέτας Δημήτριος

Νέπκα Χαριτίνη

ΛΑΡΙΣΑ 2020

ΠΑΝΕΠΙΣΤΗΜΙΟ ΘΕΣΣΑΛΙΑΣ

ΤΜΗΜΑ ΒΙΟΧΗΜΕΙΑΣ ΚΑΙ ΒΙΟΤΕΧΝΟΛΟΓΙΑΣ

ΠΡΟΓΡΑΜΜΑ ΜΕΤΑΠΤΥΧΙΑΚΩΝ ΣΠΟΥΔΩΝ

«ΤΟΞΙΚΟΛΟΓΙΑ»

«Insights into alpha-synucleinopathies: The role of RNA binding protein TIA1. Development of an *in vivo* model»

Μεταπτυχιακή διπλωματική εργασία

ΤΣΑΡΝΑ ΟΛΓΑ

<u>Επιβλέποντες</u>:

Δοξάκης Επαμεινώνδας, ερευνητής Γ' στον Τομέα Βασικών Νευροεπιστημών του Ιδρύματος Ιατροβιολογικών Ερευνών της Ακαδημίας Αθηνών (Ι.Ι.Β.Ε.Α.Α.).

Κουρέτας Δημήτριος, καθηγητής Φυσιολογίας Ζωικών Οργανισμών και Τοξικολογίας, διευθυντής του προγράμματος μεταπτυχιακών σπουδών «Τοξικολογία».

Νέπκα Χαριτίνη, ιατρός-κυτταροπαθολόγος, διδάσκουσα στο πρόγραμμα μεταπτυχιακών σπουδών «Τοξικολογία»

ΠΡΟΛΟΓΟΣ

Η παρούσα πτυχιακή εργασία εκπονήθηκε στον Τομέα Βασικών Νευροεπιστημών του Ιδρύματος Ιατροβιολογικών Ερευνών της Ακαδημίας Αθηνών (Ι.Ι.Β.Ε.Α.Α.). Την επιστημονική επίβλεψη της πτυχιακής εργασίας είχε αναλάβει ο κύριος Επαμεινώνδας Δοξάκης τον οποίον ευχαριστώ θερμά για την ευκαιρία που μου έδωσε να αποτελέσω μέλος της επιστημονικής του ομάδας, για την καθοδήγηση και τις συμβουλές που μου παρείχε καθώς και για την εμπιστοσύνη που μου έδειξε σε κάθε βήμα κατά τον σχεδιασμό και την εκτέλεση των πειραματικών διαδικασιών.

Ευχαριστώ θερμά τον επιβλέποντα καθηγητή κύριο Κουρέτα Δημήτριο, καθηγητή Φυσιολογίας Ζωικών Οργανισμών και Τοξικολογίας και διευθυντή του προγράμματος μεταπτυχιακών σπουδών «Τοξικολογία» για την τιμή που μου έκανε να συμμετάσχει στην τριμελή επιτροπή της πτυχιακής μου εργασίας.

Ευχαριστώ από καρδιάς την κυρία Νέπκα Χαριτίνη, ιατρό-κυτταροπαθολόγο και διδάσκουσα στο πρόγραμμα μεταπτυχιακών σπουδών «Τοξικολογία» που παρά τις δύσκολες συνθήκες και τις αυξημένες υποχρεώσεις με τίμησε με τη συμμετοχή της στην τριμελή επιτροπή της εργασίας μου.

Ιδιαιτέρως θα ήθελα να αναφερθώ και να ευχαριστήσω την Δήμητρα για την σύντομη αλλά άψογη συνεργασία μας καθώς και τον Φαίδωνα που υπήρξε πολύτιμος φίλος και πάντα παρών να συνδράμει και να προσφέρει τη βοήθειά του σε κάθε επίπεδο. Ευχαριστώ την Αλεξία για την εκπαίδευση μου στο στερεοτάκτορα, την Μαρία που επέβλεψε και βοήθησε στις στερεοτακτικές εγχύσεις των ιικών φορέων στους τέσσερεις ενήλικες επίμυες και τον Στέλιο με τον οποίον πραγματοποιήσαμε αυτά τα χειρουργεία.

Από καρδιάς ευχαριστώ την Ελένη για τις πολύτιμες συμβουλές της και την εκπαίδευση μου στη χρήση όλων των μικροσκοπίων και την Άννα για την εκπαίδευση μου στη χρήση του κρυοστάτη και την αδιάκοπη αρωγή που μου παρείχε απλόχερα σχετικά με την λήψη τομών από τους ιστούς που διαχειρίστηκα. Ειδική μνεία και τις πιο ειλικρινείς μου ευχαριστίες οφείλω στη Βάσω και τον Βαγγέλη που ως υπεύθυνοι για την

ευζωία και την φροντίδα των ζώων εργαστηρίου με στήριξαν με ενδελεχή ενημέρωση και πρακτικές συμβουλές αναφορικά με τη βέλτιστη διαχείριση των ζώων που μου εμπιστεύτηκαν για την πραγματοποίηση των πειραματικών διαδικασιών.

Οφείλω να ευχαριστήσω συνολικά το Ίδρυμα για τη δυνατότητα που μου έδωσε να συμμετάσχω σε δεκάδες επιστημονικά σεμινάρια συμπεριλαμβανομένου και του ετήσιου συνεδρίου του RSPCA καθώς και για τη συνεχή μου επιμόρφωση και εκπαίδευση.

Τέλος, ευχαριστώ από τα βάθη της ψυχής μου τους δικούς μου ανθρώπους που στάθηκαν δίπλα μου και με στήριξαν με κάθε δυνατό μέσο και τρόπο ώστε, παρά τις δύσκολες υγειονομικές συνθήκες που αποτέλεσαν τροχοπέδη για την πραγματοποίηση αυτής της εργασίας, να μείνω στοχοπροσηλωμένη και να καταφέρω να ολοκληρώσω την εργασία μου.

Contents

Abstract

α-synuclein is a presynaptic neuronal protein that is considered to play a key role in synaptic function such as neurotransmitter release, dopamine regulation, synaptic activity, plasticity, and vesicular trafficking. α-syn pathology and aggregation, which is attributed to point mutations, post-translational modifications, and environmental factors, has been linked to neurodegenerative disorders including Parkinson's Disease, Dementia with Lewy Bodies, Multiple System Atrophy, Lewy body variant of Alzheimer's disease and others. Several RNA binding proteins, upon mutation or abnormal expression, are implicated in neurodegenerative diseases. RNA binding protein TIA1, deregulation of which correlates with neurodegeneration in cases of amyotrophic lateral sclerosis (ALS), ALS associated frontotemporal dementia (ALS/FTD), distal myopathy, Alzheimer's disease (AD) and FTD-tau, has been shown to promote post-translational phosphorylation of α-syn in *in vitro* experiments by members of our lab. It was therefore essential to develop an appropriate animal model in order to determine if these finding could be confirmed *in vivo*. The aim of this thesis was to generate such a model and develop the optimal techniques, procedures, and protocols for the analysis of the results. The primary goal in the experimental model development was to simultaneously over-express both α-syn and TIA1 at the dopaminergic neurons of the substantia nigra pars compacta.

Herein we present the process of generating a rodent model including failures and complications along with the possible explanations for these impediments but also breakthroughs and solutions to overcome the difficulties. With regard to neonates' models, where AAV vectors encoding for α-syn, TIA1, and a fluorescent control protein were delivered via intracerebroventricular injections, we report insufficient diffusion of the viral vectors. Specifically, the AAV vectors were diffused throughout the cerebellum, the cortex and the olfactory bulb but did not reach the substantia nigra region of the brain which was our target area. Mediocre infectivity of the viral vectors was observed in the hippocampal area where, upon immunofluorescence analysis, we present ambiguous findings that may indicate an interaction between α-syn and TIA1. The adult rat-model, where AAV vectors were delivered via stereotactic injection directly to the substantia nigra area, disclosed that the viral vectors' titer was high enough to cause massive cell death and

fragmentation. However, we were able to report successful TIA1 over-expression and possibly α-syn over-expression. Taking into consideration these findings, we propose an experiment based on stereotactic injection with three different dilutions of the viral vectors in order to determine the optimal titer in adult rats.

In conclusion, developing in vivo models is an invaluable tool in understanding the interactions between RNA binding proteins and α-syn through which we aim to shed light in the underlying mechanisms of α-syn aggregation, an approach essential for developing new strategies for early diagnosis and effective treatment of synucleinopathies.

I. Introduction

1. <u>RNA-binding proteins</u>

RNA-binding proteins (RBPs) are around 42kDa protein molecules that interact with mRNA targets either alone or along with non-coding RNAs, such as microRNAs, forming ribonucleinoprotein complexes and ultimately regulate gene expression (Doxakis, 2014; Hentze et al., 2018). Interaction between RBPs and RNA targets is achieved via highly conserved RNA Binding Domains (RBD) which are found in numerous copies throughout their genome (Hentze et al., 2018; Ravanidis et al., 2018). Specificity, affinity, and strong selective binding to RNA target require multiple RBDs that recognize short sequences, or the RNA molecule as a whole, or even secondary and three dimensional structures (Abbas et al., 2013; Järvelin et al., 2016; Ravanidis et al., 2018). Typically non-binding areas consist of specific amino acids in monotonous repeats that prevent the formation of stable secondary structures but enable the interaction with other RBPs (Järvelin et al., 2016; Ravanidis et al., 2018). An RNA molecule can be targeted by multiple RBPs at different binding areas or even at the same binding site leading to competition among RBPs (Doxakis, 2014; Lal et al., 2004). RBPs are involved in many aspects of RNA metabolism. They regulate alternative splicing of the pre-mRNA giving rise to different gene products with structural and functional modifications (Zheng & Black, 2013). RBPs play a key role in alternative polyadenylation (APA) resulting in the formation of RNA isoforms with different 3'UTR length and hence with more or less regulatory elements from the same pre-mRNA or the generation of different length proteins if APA occurs in introns or protein-coding exons (Curinha et al., 2014). RBPs are implicated in RNA stability (Grigull et al., 2004; Keene, 2007; Mukherjee et al., 2011)translation efficiency, mRNA localization (Johnstone & Lasko, 2001), and transport along axons and dendrites (Doxakis, 2014). RBPs are also essential factors for embryonic development and cell lineage specification (Brinegar & Cooper, 2016). Research in C.elegans identified several RBPs to be implicated in germline but also in early embryonic development and somatic tissue formation such as neuron, muscle, hypodermis (M. H. Lee

& Schedl, 2001). The significant role of RBPs in RNA metabolism could suggest that deregulation of RBPs strongly affect RNA pathways resulting to disruption of protein homeostasis and consequently cellular function. Mutations in RBPs or abnormal expression are directly linked to pathogenesis and diseases of the nervous system (Brinegar & Cooper, 2016; Ibrahim et al., 2012). They have been implicated in the field of neurodegenerative diseases such as Frontotemporal Dementia (FTD), Amyotrophic Lateral Sclerosis (ALS), Spinal Muscular Atrophy, Fragile-X Syndrome, Alzheimer's disease, Huntington's disease and others(Ibrahim et al., 2012; Ravanidis et al., 2018).
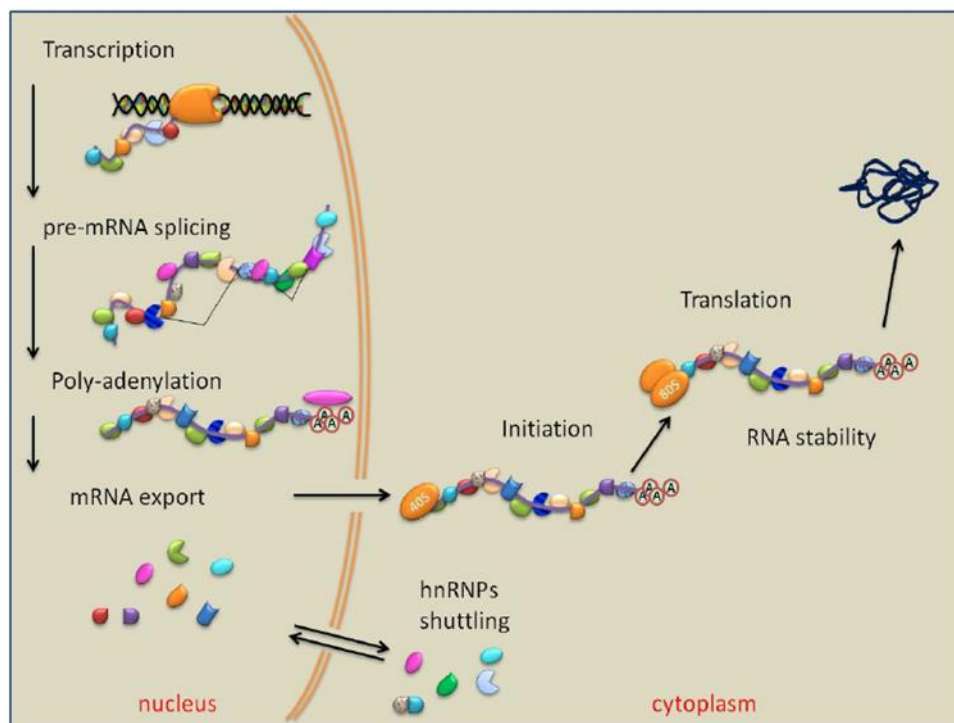
Figure I. RBP interaction with RNA at different steps of RNA biogenesis and metabolism (Romanelli et al., 2013).

2. <u>TIA1</u>

T-cell Intracellular Antigen 1 (TIA1) is a 40kDa RNA Binding Protein that contains three RNA Recognition Motifs (RRM) and a glutamine rich carboxyl terminal region structurally related to prion like protein (Kawakami et al., 1992; Tian et al., 1991). With respect to its subcellular localization, research has shown that TIA1 shuttles between the nucleus and the cytoplasm depending on the cell's transcriptional activity and

stress (T. Zhang et al., 2005). Primarily, TIA1 is expressed in brain, testis, and spleen (Beck et al., 1996) but also in other tissues such as the endometrium (Karalok et al., 2014).

TIA1 is a major factor in the regulation of alternative mRNA splicing associated with U-rich intronic motifs which is estimated at a total of 15% of the overall alternative cassette exons (Aznarez et al., 2008). It has been reported that TIA1 and TIAR (TIA1 related protein) auto-regulate their own mRNA, leading to preferential expression of their isoforms in human tissue and cell lines; TIAR influences the ratio of TIA1 isoforms whereas the opposite does not seem to take place (Izquierdo & Valcárcel, 2007).

Under cell stress TIA1 promotes the formation of distinct cytoplasmic inclusions known as Stress Granules (SG) via TIA1 prion like aggregates (Gilks et al., 2004). However, in cases of oxidative stress, when TIA1 is oxidized, inhibition of SG formation linked with cell death and apoptosis was reported (Arimoto-Matsuzaki et al., 2016). The implication of TIA1 in apoptosis is also supported by evidence indicating that DNA fragmentation can be induced by TIA1 leading to cellular apoptosis (Tian et al., 1991).

Recent studies have revealed that TIA1 can function as a translation silencer for several mRNAs. Under normal conditions TIA1/TIAR seem to regulate the amount of Tumor Necrosis Factor-α protein by silencing its translation rather than affecting the stability of its mRNA like other ARE-binding proteins (adenine and uridine rich element in the 3'UTR of TNF-α transcript). However, in cases of inflammation (LPS stimulation of macrophages) TNF-α protein is abundantly produced indicating that TIA1/TIAR are implicated in TNF-α translation and cell response to stress (Förch & Valcárcel, 2001; Gueydan et al., 1999; Piecyk et al., 2000). Research on COX-2 enzyme, which can lead to carcinogenesis when overexpressed, showed that TIA1 is implicated in the COX-2 ARE binding complex and is a major factor in COX-2 posttranscriptional regulation. Consequently, TIA1 can normally function as a tumor suppressor whereas when its levels are downregulated, COX-2 overexpression may take place leading to cancer progression (Dixon et al., 2003). Analysis of TIA1/RNA complexes identified a U-rich motif of 30-37 nucleotides in the mRNA targets. This motif, according to the UniGene database, is relatively common indicating that TIA1 can repress the translation of several

proteins and thus function as a general translation silencer (López de Silanes et al., 2005). Meyer et al. observed that TIA1 regulates the alternative splicing of the PRKRA protein and promotes ds-RNA triggered stress response thus leading to a global translation silencing (Meyer et al., 2018).

With regard to mitochondrial morphology and function, TIA1 is a key factor in MFF (mitochondrial fission factor) translational regulation. MFF normally recruits the Dynamin-1-like protein (DNM1L) that mediates mitochondrial membrane fission. In vitro studies showed that TIA1 overexpression resulted in elevated mitochondrial fragmentation whereas TIA1 silencing led to mitochondrial elongation (Tak et al., 2017). Similarly, two TIA1 isoforms (TIA1b/TIARb) were found to downregulate the expression of the Optic Atrophy 1 protein (OPA1) and promote mitochondrial fission and clustering (Carrascoso et al., 2017).

Several studies have indicated the importance of TIA1/TIAR in embryonic development. Double knockout resulted in high rates of embryonic lethality (Kharraz et al., 2010), whereas TIAR deficiency alone lead to infertility for both sexes caused by spermatogonia or oogonia absence (Beck et al., 1998). In coordination with these findings, knockout of both genes in murine embryonic fibroblasts (MEFs) caused major alterations in cell homeostasis and affected the signaling pathways and the developmental program of the MEFs (Sánchez-Jiménez & Izquierdo, 2013). The hypothesis that TIA1/TIAR could be involved in the developmental process of the early embryonic stages, based on the results mentioned above, needs further research that includes *in vivo* experimental models. Interestingly, similar results were reported following *in vivo* TIAR overexpression; low embryonic viability and abnormal embryonic development were observed (Kharraz et al., 2010).

Recently, TIA1 has been associated with fear memory processing (Rayman et al., 2019) and also with stress triggered psychopathology predisposition in cases where single-nucleotide polymorphisms were detected (Rayman et al., 2020).

A major aspect of TIA1 biology is its implication with several neurodegenerative diseases such as amyotrophic lateral sclerosis (ALS), ALS associated frontotemporal dementia (ALS/FTD), distal myopathy, Alzheimer's disease (AD) and FTD-tau. Whole-exome sequencing to

ALS/FTD patients revealed mutations in TIA1 gene which were not detected in the control group. Post-mortem analysis of TIA1 mutation carriers disclosed round, hyaline inclusions positive for TAR DNA-binding protein 43 (TDP-43) suggesting a strong connection between mutations in TIA1, TDP-43 pathology, and ALS/FTD pathogenesis (Mackenzie et al., 2017). Analogous results were provided for Welander Distal Myopathy; multiple sequencing techniques showed a specific mutation in TIA1 gene in the prion-like domain present in all the patients' samples but absent in the control group. Analysis in biological material also revealed increased stress granules formation in the patients group compared to the control. Taken together, these observations could indicate TIA1 mutation as a major factor behind Welander Distal Myopathy possibly by changing SG dynamics (Hackman et al., 2013). In the field of myopathy research, another TIA1 mutation was detected along with an SQSTM1 mutation in muscle tissue of three unrelated patients with distal myopathy (Niu et al., 2018). With respect to taupathies including AD and FTD-tau, interesting findings have been recently reported. Tau protein is normally found in the axons where it stabilizes microtubules, in pathological conditions however tau is relocated to the somatodendritic region of the neuron where it aggregates and forms oligomers and fibrils (Y. Wang & Mandelkow, 2016). Vanderweyde et al. showed that tau is responsible for TIA1 distribution and SG formation but also pointed that alterations in TIA1 expression strongly affect tau function. Specifically, in TIA1 knockout models tau misfolding and consequently tau toxicity was reported whereas in TIA1 overexpression models tau misfolding and neurodegeneration was observed demonstrating a valid interaction between the two proteins (Vanderweyde et al., 2016). However, when TIA1 expression is reduced but not eliminated (as in knockout models) Apicco et al. reported increased neuronal survival in transgenic tau mice and significant improvement in behavioral tests and lifespan indicating a potential protective role against tau neurodegeneration (Apicco et al., 2018).

3. α-SYNUCLEIN

3.1 α-syn structure

α-synuclein (α-syn) is a 140 amino-acids protein with a molecular weight of approximately 15kDa which is encoded by the SNCA gene localized in the long arm of chromosome 4 (Bernal-Conde et al., 2019). α-syn is a member of the synuclein family of proteins along with β- and γ-synuclein. With respect to its primary sequence, α-syn is characterized by three distinct, major domains. The positively charged N-terminal region (residues 1-60) consists of seven imperfect repeats of the conserved KTKEGV segment and is essential for membrane-induced amphipathic a-helix formation thus playing a role of "membrane-anchor" (Fusco et al., 2014; Pirc & Ulrih, 2015; Villar-Piqué et al., 2016). This motifs are common among proteins that bind to membranes such as the apolipoproteins. The hydrophobic central region (residues 61-95), known as non-amyloid component (NAC), is proposed to be a key factor in α-syn folding to β-sheets of amyloid fibrils, in α-syn aggregation, in α-syn transport through larval axons (Anderson et al., 2019) and even function as a "membrane-sensor" (Fusco et al., 2014). α-syn interacts preferentially with considerably curved membranes rich in acidic phospholipids via two antiparallel a-helixes with a small linking region formed by amino acids 3-37 and 45-92 (Mor et al., 2016; Ulmer et al., 2005; Zhu et al., 2003). Interaction with low curvature membranes results in the formation of a single extended helix derived by the same regions (Ferreon et al., 2009). The C-terminal region (residues 96-140), which is enriched in negative charged and proline residues, is reported to be unstructured (lack of secondary folds), highly flexible, and also the least conserved domain among synuclein isoforms α-, β-, γ- and across species (Bendor et al., 2013). This region forms interactions with the N-terminal domain resulting in compact monomeric structures preventing α-syn aggregation. However, in high temperatures this interaction is disrupted and α-syn is prone to aggregation (Dedmon et al., 2005; Mor et al., 2016). Whereas the first two domains mediate the membrane binding, the C-terminal appears to facilitate protein-protein interaction (Breydo et al., 2012).

repeat 1   repeat 2   repeat 3

MDVFMKGL SKAKEGVVAAA EKTKQGVAEA**A** GKTKEGVLYVG

repeat 4   repeat 5   repeat 6   repeat 7

SKTK**E**GVVHGV **A**TVA EKTKEQVTNVG GAVVTGVTAVA QKTVEGAGSIA

AATGFVKKDQLGKNEEGAPQEGILEDMPVDPDNEAYEMPSEEGYQDYEPEA

N	Amphipathic N-terminal region	Central region (NAC domain)	Acidic C-terminal region	C
1	↓ α-helix	61 ↓ β-sheet	95 ↓ unstructured	140

Figure II. α-syn structure. Image modified by (Pirc & Ulrih, 2011)

α-syn exists in a dynamic equilibrium between soluble state and membrane bound state with different secondary structure in each case. Native α-syn is generally considered to be an intrinsically disordered protein (IDP) that can adopt different conformations, depending on the external stimuli, such as β-sheet fibrils, oligomers linked with toxicity, structured monomers associated with membrane bound, and α-helical tetramers resistant to aggregation (Lucas & Fernández, 2020). However, in human brain α-syn is thought to exist in a stable monomeric conformation (Burré et al., 2013) and occasionally form metastable multimers (Gould et al., 2014). α-syn interactions with lipid membranes and its consequent structure is probably a key factor for its cellular functions (Burré, 2015).

3.2 α-syn tissue distribution

α-syn is mainly expressed in the Central Nervous System (CNS) and peripheral nerves but also in a subset of cells in bone marrow. Research has shown that during prenatal development α-syn is abundant in several tissues apart from the brain such as kidney, liver, heart, lung, adrenal gland, and testis. However, in adult human tissues α-syn is highly expressed solely in brain tissue and can still be detected in kidney, adrenal gland, and testis (Ltic et al., 2004). With respect to its distribution in the brain, α-syn is highly expressed in almost all brain regions and localizes preferentially in presynaptic terminals. Studies have shown that in the neocortex α-syn is detected in axons and terminals, while in the region of frontoparietal sensory and motor cortex is also detected in somata and

dendrites. In the midbrain α-syn is abundant in substantia nigra pars compata (SNc) in large somata, dendrites, axons and terminals from where it projects in substantia nigra pars reticulata. Some α-syn positive axons from SNc also project to striatum and globus palidus region of the basal ganglia whereas in the ventral tegmental area (VTA) it is expressed in large neurons. In the dorsal hippocampal region of the brain α- syn is detected only in granule cells in the dentate gyrus, but in retrohippocampus (ventral and caudal area) it is also expressed in the pyramidal cell layer along with dentate gyrus neurons. In the olfactory region of the piriform cortex α-syn positive neurons and fibrils are present. Amygdala only receives projections of other positive for α-syn regions whereas basal cholinergic forebrain consists of numerous α-syn positive neurons. Thalamus and hypothalamus are highly heterogenus regarding α-syn expression; the protein can be detected in neurons, somata, or fibrils, and in some areas it is not expressed at all. Finally, in the brainstem α-syn is found mainly in cell nucleus and some neuronal cell bodies (Andringa et al., 2003; Brenz Verca et al., 2003; Taguchi et al., 2016; Totterdell et al., 2004).

3.3 α-syn function

Normal function of α-syn remains controversial despite three decades of research dedicated in this field. The ability to form different conformations and exist in both soluble and membrane bound state is only one of the many obstacles for the researchers. Experimental models designed to study α-syn function reveal only moderate effects when silencing its translation whereas, in overexpression models the toxicity caused by α-syn aggregation is apparent in several brain regions resulting in neuronal death thus, making it difficult to differentiate between function and pathology of the protein. The attempt to understand α-syn normal function using knockout models for all synuclein isoforms also produced very complicated findings. However, the preferential localization of α-syn in presynaptic terminals and its ability to interact with membranes and proteins indicates a role in synaptic function such as neurotransmitter release, synaptic activity and plasticity, dopamine regulation, synaptic vesicle trafficking (Benskey et al., 2016; Bernal-Conde et al., 2019; Burré, 2015; Villar-Piqué et al., 2016).

α-syn role in lipid metabolism

α-syn similarity with class A2 apolipoproteins suggests a possible role in lipid metabolism. Research data however, have been inconsistent and even contradictory in some cases. α-syn has been shown to bind to phospholipase Cβ (PLCβ) and increase PLCβ1 cellular levels as it protects it from digestion and degradation (Y. Guo et al., 2012). On the contrary, α-syn probably acts as an inhibitor for phospholipase D2 based on accumulative data from both in vitro and in vivo experiments (Ahn et al., 2002; Gorbatyuk et al., 2010; Payton et al., 2004). However, other researchers did not confirm the inhibitory role of α-syn on PLD and proposed that the observed inhibition derived from endoplasmic reticulum stress upon α-syn overexpression (Rappley et al., 2009). Due to its structure α-syn has been suggested to function as a fatty acid transporter or even be a member of the fatty acid binding proteins (FABPs), whereas, other studies have shown that the protein does not likely act as an FA transporter and the binding to negatively charged membranes is one of its physiological properties (Fecchio et al., 2018). α-syn has also been reported to affect lipid packing and even sense lipid packing defects (Burré, 2015).

Interactions within the nucleus

In vitro studies have recently revealed that monomeric α-syn can bind directly to DNA, either as small clusters, when the protein to DNA ratio is low, or by fully covering the DNA molecule, when the protein to DNA ratio is high, leading to an increase in its persistence length (Jiang et al., 2018). Pinho et.al observed that reduced α-syn binding to DNA is associated with transcriptional deregulation of several cell cycle related genes among others thus, providing indications of a potential role of α-syn on gene expression(Pinho et al., 2019). Other studies, including transgenic mouse model expressing wild type human α-syn, showed that α-syn associates with the DNA methylotransferase 1 enzyme (Dnmt1) leading to its retention to the cytoplasm and consequently to DNA reduced methylation (Desplats et al., 2011). α-syn has also been reported to interact with histones forming a tight complex; this interaction, *in vitro*, resulted in high rates of α-syn fibrillation which is linked with the protein's pathophysiology (Goers et al., 2003). Kontopoulos et al. confirmed both

in vitro and *in vivo* this interaction and pointed out that α-syn can inhibit histone acetylation thus leading to neurotoxicity (Kontopoulos et al., 2006).

Interaction with mitochondrial components

It has been shown that α-syn has high affinity for mitochondrial membranes and its translocation to these organelles is mediated by the N-terminal of the protein. Researchers have proposed a regulating role for α-syn in mitochondrial fusion, electron transport chain, VDAC (voltage dependent anion channel) permeability and other functions (Bernal-Conde et al., 2019). It has also been suggested that α-syn could have a protective role in mitochondria against oxidative stress (OS) (Seo et al., 2002); specifically in cases of ROS induced OS, low levels of α-syn overexpression can lead to decrease of the fission factor Drp1 (dynamin-related protein 1), prevent Caspase3 activation and as a result reduce apoptosis (Menges et al., 2017).

Recent data support the hypothesis that α-syn influences mitochondrial size either through reduction of outer mitochondrial membrane curvature upon binding, leading to decreased fusion vehicle dynamics and fusion rate that results to smaller mitochondrial size, or, in case of mutant α-syn, through inhibition of mitofusins Mfn1 and Mfn2 along with inhibition of Drp1 which is linked with a decrease in mitochondrial size (Pozo Devoto & Falzone, 2017).

With respect to α-syn role in cell respiration and mitochondrial bioenergetics, Ludtmann et al. 2016 reported that α-syn interacts with ATP synthase subunit α and regulates the enzyme's function by increasing its efficiency. Specifically, they observed that α-syn deficiency leaded to lower ATP synthase efficiency and reduced ATP levels, whereas the phenotype was rescued upon exogenous monomeric α-syn administration (Ludtmann et al., 2016). By contrast, α-syn oligomers induce oxidation of the ATP synthase subunit β and lipid peroxidation, resulting in opening of the permeability transition pore (PTP), mitochondrial swelling, and cell death (Ludtmann et al., 2018).

Interaction with cytoplasmic organelles involved in vesicular trafficking

Various studies have provided evidence that α-syn, upon overexpression or mutant α-syn, can accumulate in the ER disrupting

normal protein folding and inducing ER stress by destabilizing Ca^{2+} homeostasis and impairing intracellular protein trafficking and vesicles release (Colla, 2019; Melo et al., 2018). ER and mitochondria share several membrane contact sites through which transit of metabolites and signaling molecules is achieved; as a result, in case of ER malfunction, caused by α-syn induced stress, excessive Ca^{2+} can leak to mitochondria triggering mitochondrial outer membrane permeabilization, opening of the PTP, mitochondrial swelling, and cell apoptosis (van Vliet & Agostinis, 2018).

With respect to lysosomal function, Mazzulli et al. showed that α-syn overexpression and accumulation could result in reduction of multiple lysosomal hydrolases enzymatic activity and disruption of their trafficking through ER and Golgi apparatus (Mazzulli et al., 2016).

Other studies provide evidence that overexpression of either wild type or mutant α-syn promotes alterations in the Golgi apparatus morphology and significant fragmentation (Paiva et al., 2018).

These observations do not point directly to the normal functions of α-syn, but they could indeed highlight its importance in cell homeostasis, cycle, and death.

α-syn in pre-synaptic terminal

Neurotransmitter release in presynaptic terminals requires a fine coordination of the membrane fusion machinery that consists of soluble N-ethylmaleimide-sensitive factor (NSF), attachment protein receptor (SNARE), and Sec1/Munc18-like proteins (SM) (Burré et al., 2010; Südhof & Rothman, 2009). The SNARE proteins are in fact three separate proteins, syntaxin-1 and SNAP-25 located in the presynaptic plasma membrane and vesicle-associated membrane protein-2(VAMP2), also called synaptobrevin-2, located in the synaptic vesicle (SV). Neurotransmitter release occurs thousands of times per minute and each time individual unfolded SNARE proteins assemble into a stable four-helix SNARE-complex (Südhof & Rothman, 2009). Burre et al.2010 showed that the C-terminal of α-syn binds directly to the N-terminal of synaptobrevin-2 promoting SNARE-complex assembly. α, β, γ- synuclein triple knockout mice developed neurological impairment during aging and had shorter lifespan; furthermore, they presented lower levels of synaptobrevin-2

upon time but higher levels of cysteine string protein α [CSPα is a presynaptic vesicle protein implicated in neurodegeneration-(Sheng & Wu, 2012)] indicating that synuclein family regulate normal SNARE-complex assembly (Burré et al., 2010). Similarly, in TKO neuron cultures SNARE assembly deficit was observed and then restored by reintroducing α-syn (Burré et al., 2010). α-syn binding to synaptobrevin-2 was also found to promote SV clustering but not to affect Ca^{2+} triggered membrane fusion indicating that α-syn may regulate the accumulation of synaptic vesicles at the synapse rather than affecting the neurotransmitter release itself (Diao et al., 2013).

On the opposite, other researchers have reported that moderate α-syn overexpression leads to decreased SV recycling and trafficking and inhibition of neurotransmitter release thus proposing a role of physiological attenuator of neurotransmitter release for the protein (Nemani et al., 2010; L. Wang et al., 2014).

In order to reconcile those seemingly incompatible views in one unified model of α-syn function Sun et al proposed that α-syn binding to synaptobrevin-2 is essential both for SV clustering and their recycling attenuation (Sun et al., 2019). Moreover, Atias et al suggested that α-syn reduces SV mobility and restricts their egress to the active zone thus attenuating exocytosis; they proposed that these interactions are mediated by synapsine (a cytosolic protein that is involved in SV clustering and mobilization) either locally or by facilitating α-syn axonal transport (Atias et al., 2019).

α-syn impact on dopamine system

α-syn has been implicated in many aspects of the dopamine system including synthesis, storage, neurotransmission, clearance and efflux. At dopamine biosynthesis level, the tyrosine hydroxylase enzyme plays a key role as it catalyzes the rate limiting step of converting L-tyrosine to L-DOPA along with O_2, Fe^{2+} and tetrahydrobiopterin as cofactors, L-DOPA is then converted to dopamine by the aromatic-l-amino-acid decarboxylase. Overexpression of α-syn has been shown to inhibit tyrosine hydroxylase by reducing its activity, rather than altering its levels (Perez et al., 2002). Peng et al. proposed that the underlying mechanism through which α-syn decreases tyrosine hydroxylase activity is based upon α-syn impact on its dephosphorylation, a process that deactivates the enzyme. Specifically,

they observed increased activity of protein phosphatase PP2A, that almost exclusively dephosphorylates tyrosine hydroxylase, upon α-syn overexpression whereas, the AMP-dependent protein kinase PKA-responsible for the Ser40 phosphorylation that contributes to tyrosine hydroxylase activation- was unaffected (Peng et al., 2005).

Upon biosynthesis, dopamine is stored in synaptic vesicles through the activity of vesicular monoamine transporter-2 (VMAT2). *In vitro* studies have shown that overexpression of α-syn led to lower levels of VMAT2 protein and consequently to reduction of its activity, which in turn resulted in inhibition of VMAT2 mediated dopamine uptake and accumulation in cytoplasm (J. T. Guo et al., 2008).

With respect to dopamine transporter DAT, which is responsible for dopamine transport from the synaptic cleft back into the cytoplasm, the existing information on its regulation by α-syn is contradictory. Some studies show that α-syn overexpression is followed by increased DAT levels on cell surface while other studies have found decreased DAT levels (Butler et al., 2017). On the other hand, Swant et al reported that α-syn overexpression inhibited DAT activity and reduced dopamine uptake but did not affect DAT levels (Swant et al., 2011). Ninkina et al however, in triple synuclein knockout mice found decreased efficiency of dopamine uptake but no changes in DAT function (Ninkina et al., 2019). These incompatible results suggest that further research should be pointed to this direction in order to understand α-syn role in DAT modulation and the mechanism through which dopamine uptake is impaired upon α-syn deregulation.

In vivo experiments have shown that α-syn overexpression in rat substantia nigra led to reduced dopamine release in the striatum, reduced vesicles density, reduced VMAT2 and tyrosine hydroxylase density, early signs of neurodegeneration, and neuronal loss (Gaugler et al., 2012).

3.4 α-Synucleinopathies

Three decades of research on α-syn have led to the conclusion that α-syn pathology is part of the underlying cause in a broad spectrum of neurodegenerative disorders collectively referred to as synucleinopathies. Among these disorders are included Parkinson's

disease (PD), dementia with Lewy bodies (DLB), multiple system atrophy (MSA), pure autonomic failure, Lewy body variant of Alzheimer's disease, and neurodegeneration with brain iron accumulation (Benskey et al., 2016). α-syn pathology is thought to derive upon protein's misfolding and aggregation caused by point mutations, post-translational modifications , and/or environmental factors (Villar-Piqué et al., 2016). The location of α-syn aggregates corresponds with the symptomatology observed in each case; this remark explains the different phenotypes of the disorders mentioned above but also the similarities among some symptoms.

PD is associated with motor symptoms that include resting tremor, bradykinesia, rigidity, shuffling gait, postural instability, hypomimia, decreased eye blink rate, blurred vision, dystonia, speech impairment and non-motor symptoms that include cognitive changes, behavioral changes, sensory and sleep disturbance, autonomic system failure, and others (Beitz, 2014). The PD symptomatology is partly attributed to α-syn aggregation which leads gradually to the loss of dopaminergic neurons in substantia nigra pars compacta (SNc) in the midbrain; although deposits in Lewy bodies are detected in these brain areas, their small number cannot explain the outspread neuronal loss nor the clinical symptoms (Schulz-Schaeffer, 2010). Remarkably, all known point mutation in the SNCA gene associated with PD-A53T, A30P, E46K, G51D, H50Q, A53E, A53V- are located in the N-terminal (Bendor et al., 2013; Meade et al., 2019). Collectively, α-syn mutants are linked with higher aggregation rate leading to early onset PD however, some of them increase the fibril formation rate while others slow it down. Although this observation may seem controversial, some researchers believe that the prefiblilar oligomers are in fact more toxic than the mature aggregated fibrils (Meade et al., 2019). Furthermore, there are examples where duplication or triplication of the SNCA gene resulted in more severe PD manifestation accordingly, indicating that increased levels of intracellular α-syn lead to higher probability of misfolding, toxicity and ultimately to disease onset (Goedert et al., 2017).

MSA manifests either as the Parkinsonian variant (MSA-P), formally designated striatonigral degeneration, or as the cerebral variant (MSA-C), formally designated olivopontocerebellar degeneration. In MSA-P case, patients exhibit parkinsonism with typical bradykinesia, rigidity, tremor and balance loss due to degeneration in the striatum and the substantia

nigra pars compacta and pars reticulata. In MSA-C case, symptomatology include gait ataxia, dysarthria, limb ataxia upon cerebellum and brain stem degeneration (Ramirez & Vonsattel, 2014). In patients brains α-syn deposits in glial cytoplasmic inclusions (GCI) that involve oligodendrocytes where the protein is not normally expressed (Goedert et al., 2017).

DLB is categorized as a major neurocognitive disorder distinguished from PD dementia although they present numerous similarities (McKeith et al., 2017). DLB patients experience dementia, cognitive impairment, progressive parkinsonism, fluctuation in early stages, visual hallucinations, REM sleep behavioral disorder (Bendor et al., 2013; McKeith et al., 2017). Lewy bodies-the hallmark of the disease-in DLB are mainly located in cortex and brain stem but, as mentioned also in PD, they do not correlate with the severity of the symptoms nor the disease duration. α-syn aggregates in presynapse, on the other hand, are detected in large numbers throughout these brain regions indicating a causative relation between α-syn aggregation and DBL neurodegeneration (Kramer & Schulz-Schaeffer, 2007).

3.5 α-syn aggregation

As already mentioned, α-syn aggregates are directly linked to neurodegeneration and manifestation of synucleinopathies. Aggregation takes place in three steps starting with the rate-liming step when soluble α-syn monomers are converted into partially soluble oligomers which, in turn, are subjected to nucleation-dependent polymerization (Wood et al., 1999; J. Zhang et al., 2019). Among these large oligomers-also described as pre-fibrillar aggregates-some will eventually form insoluble fibrils and thus they are commonly referred to as protofibrils (Lindström et al., 2014; Walsh et al., 1997). Finally, the mature insoluble fibrils coalesce into amyloid fibrillar aggregates. α-syn pathological form is structurally related to prion proteins which are misfolded forms of native cellular proteins; this observation generated the hypothesis that α-syn aggregates may spread in α prion-like manner throughout the brain leading to synucleinopathies. Although accumulating evidence support this suggestion, further research is necessary to shed light to the mechanism of α-syn aggregation and propagation before confirming the prion hypothesis (Vargas et al., 2019).

3.6 Post-translational modifications of α-syn

It is established thus far, that α-syn aggregation results in toxicity and neurodegeneration hence, understanding the underlying mechanisms of this process is essential for developing new strategies for early diagnosis and effective therapeutic treatment for α-synucleinopathies. The role of point mutations has already been mentioned in accordance with the specific disorders they are linked to. With regard to post-translational modifications of α-syn, phosphorylation, ubiquitination, truncation, nitration, and O-GlcNAcylation should be reported.

<u>Phosphorylation</u>

Apart from phosphorylation at serine 129, which has proven to be very common among α-synucleinopathies and especially PD, α-syn can also be phosphorylated at serine 87, tyrosine 125, 133, and 136. However, the tyrosine phosphorylation have not yet been linked to the protein's aggregation (J. Zhang et al., 2019). The kinases that have been shown to induce the serine 129 phosphorylation are mainly casein kinase I and II (Okochi et al., 2000), polo-like kinase II (Inglis et al., 2009), G protein-coupled receptor kinases (Pronin et al., 2000), and Leucine-rich repeat kinase II (Li et al., 2014). Although α-syn in Lewy bodies is phosphorylated at serine 129 at a percentage of 90%, the scientific community has not yet reached a consensus regarding the effects of this modification. Numerous studies have produced incompatible, dissenting results regarding ps129 effect on α-syn aggregation, fibril formation, and neuronal loss. Recently, it was suggested that phosphorylation at serine 129 may occur post-fibrilization as a step to clear aggregated α-syn from the cell (Samuel et al., 2016).

<u>Ubiquitination</u>

It has been reported that α-syn in patients' brains suffering from α-synucleinopathies is highly phosphorylated and partially ubiquitinated (Hasegawa et al., 2002). α-syn ubiquitination has be shown to be mediated via three E3 ubiquitin-protein ligases, the seven in absentia homolog (SIAH) (J. T. Lee et al., 2008), the co-chaperone carboxyl terminus of Hsp70-interacting protein (CHIP) (Kalia et al., 2011), and the

neural precursor cell expressed developmentally down-regulated protein 4 (Nedd4) (Tofaris et al., 2011).

With respect to mammalian homologs of Drosophila seven in absentia 1 (SHIA-1), it has been reported to induce mono- and di-ubiquitination of α-syn and, interestingly, to promote aggregation of the protein leading to apoptosis and cell death (J. T. Lee et al., 2008).

CHIP has been found to co-localize with α-synuclein in Lewy Bodies and intracellular inclusions and mediate α-syn degradation via either the proteasomal degradation, through the tetratricopeptide repeat domain, or the lysosomal degradation, through the U-box domain (Shin et al., 2005). Furthermore, CHIP overexpression results in lower α-syn levels and inhibition of α-syn inclusion formation (Shin et al., 2005).

Ubiquitin ligase Nedd4 recognizes the C-terminal of α-syn and upon ubiquitination drives the protein to the endosomal-lysosomal pathway for clearance from the cell. Nedd4 overexpression has been linked with enhanced α-syn clearance from the cell and thus lower levels of the protein, whereas, down-regulation of Nedd4 led to increased α-syn content (Tofaris et al., 2011). Although, the A53T α-syn mutation has been reported to be less efficient substrate for Nedd4 ligases and thus more toxic due to accumulation (Mund et al., 2018), other studies did not confirm lower levels of ubiquitination for A53T and A30P α-syn mutants (Nonaka et al., 2005).

α-syn is also conjugated to small ubiquitin-like modifier (SUMO) at lysine residues. Some Lewy bodies in the substantia nigra region of PD patients' brains were stained positive for SUMO1 indicating a possible role in the disease's pathogenesis. Research has shown that after SUMOylation, induced by SUMO ligase PIAS2, reduced ubiquitination of α-syn was reported, followed by increased aggregation and release from the cell. These findings, along with previous data showing that α-syn secretion form the cell is mediated via the ESCRT complex (endosomal sorting complexes required for transport) upon SUMOylation, support the hypothesis that deficiently ubiquitinated and degraded α-syn molecules are partially secreted from the cell through SUMOylation (Stefanis et al., 2019).

Truncation

Apart from the full length α-syn, there have been detected some truncated forms of the protein with molecular masses of 10-15kDa (J. Zhang et al., 2019). Although truncation in N-terminal and C-terminal of the protein is a normal event that can be observed in healthy brain tissue (Muntané et al., 2012), there is significantly more truncated α-syn in the insoluble disease fractions (Sorrentino & Giasson, 2020). It has been reported that some C-truncated variants of the protein can shift the pH range where autocatalytic proliferation of fibrils occurs into physiological values, hence promoting conversion of protofibrils to mature fibrils and α-syn aggregation (van der Wateren et al., 2018). Other researchers have shown that some C-truncated forms promoted full-length α-syn aggregation through co-polymerization and others induced seeded aggregation of the protein (Sorrentino et al., 2018).

Nitration

α-syn has four tyrosine residues that are susceptible to nitration: Y39, Y125, Y133, Y136. It has been reported that nitration of α-syn led to oligomerization and aggregation of the protein while, other researchers observed that nitrated α-syn formed dimers which coalesced into fibrils even in low concentrations. It has also been shown that nitrated α-syn monomers have lower rate of degradation compared to native α-syn (He et al., 2019).

O-GlcNAcylation

O-GlcNAcylation is a form of protein glycosylation where β-d-N-acetlyglucosamine (GlcNAc) is added via the O-linkage to serine or threonine residues; the reaction is catalyzed by two enzymes: O-GlcNAc transferase (OGT) and O-GlcNAcase (OGA). α-syn O-GlcNAcylation has been shown to reduce the protein's aggregation and toxicity *in vitro* (Wani et al., 2017). Threonine 72 and serine 87 O-GlcNAcylation, among others, have been found to inhibit α-syn aggregation whereas, threonine O-GlcNAc modification also block the extension of α-syn fibers to larger aggregates and reduce its toxicity even upon adding exogenous α-syn to neuron culture (Levine et al., 2019; Lewis et al., 2017) thus emerging as potential therapeutic strategies for PD and other synucleinopathies.

II. Aim and purpose of the study

Collective data from our lab have shown, in *in vitro* studies, that overexpression of the RNA binding protein TIA1 correlates with higher levels of α-syn phosphorylation and aggregation. We, therefore, decided to generate an experimental model in order to determine if these findings could be confirmed *in vivo*. The purpose of this study was to choose the appropriate animal model and the optimal analyzing techniques for our cause. Furthermore, it was essential to develop, test and refine all the protocols that were necessary for studying the outcomes of the experimental procedures. Each aspect from the first up to the last step of the experimental protocols was applied, upon the initial development, tested and optimized before finalizing in order to ensure high-quality results.

Regarding the animal model, we focused on developing an experimental model where we could simultaneously overexpress both α-syn and TIA1 protein at the dopaminergic neurons of substantia nigra pars compacta. Our aim was to achieve co-localization of the overexpressed proteins in order to study the possible aggregation of α-syn, fibrils formation, and neuronal loss at SNc. For this purpose, it was essential to develop appropriate immunofluorescence (IF) and immunohistochemistry (IHC) protocols for quality and quantity analysis. Specifically, through IF we aimed to detect α-syn aggregates and filaments but also markers of inflammation, immune response, and neurodegeneration such as astrocytes and microglia. On the other hand, through IHC we would proceed to quantification of our results by calculating the number of viable dopaminergic neurons stained positive for tyrosine hydroxylase enzyme.

Conclusively, we wanted to develop the animal model and the appropriate methods, which would allow us to study the effect of TIA1 overexpression on α-syn phosphorylation, conformations, and levels in SNc, in order to confirm or reject our initial hypothesis regarding the interaction between the two proteins. In this assay, we will describe the process of developing and refining the experimental model and the protocols and eventually present preliminary data from our study.

III. ANIMAL MODELS

All animals were housed in accordance to the European Legal framework that exists for the protection of animals used for experimental and other scientific purposes (European Convention 123/Council of Europe and Directive 86/609EEC). Specifically, animals were housed in individual ventilated cages (47.5cm length, 20.5cm height, and 27cm width) in climate-regulated environment at a temperature of 22°C±2 under a 12h light/dark circle with free access to food and water in accordance to the guidelines of the Federation of European Laboratory Animal Science Associations (FELASA) and the International Council of Laboratory Animal Science (ICLAS). All experiments and procedures were approved by the Official Veterinary Service and the Institutional Bioethics Committee in compliance with the principle of the 3Rs. Effort was made to reduce the levels of pain and discomfort.

1. Mouse models

1.1. The first experimental model

1.1.1 The first viral vectors construction

In our first attempt to generate an experimental model we constructed three different viral vectors following the protocol described in the materials and methods section, before the refinement steps. We chose to use the PHP.eb variant of the AAV9 serotype of adeno-associated virus based on recent literature that shows higher infectivity in lower concentrations of this variant (Dayton et al., 2018). We constructed the plasmids for the transfection procedure using TH promoter for the inserted genes in order to achieve localized overexpression of the proteins to the substantia nigra region of the brain. Each viral vector carried only one gene which was GFP, human SNCA or TIA1 accordingly. GFP is a non-reactive green fluorescent protein that was chosen for the control group. The experimental group would receive a 1:1 mixture of the viral vector with the SNCA gene and the viral vector with the TIA1 gene

whereas, the control group would receive a 1:1 mixture of the viral vector with the SNCA gene and the viral vector with the GFP gene.

1.1.2. The first mouse model

We chose to develop an experimental model based on neonates instead of adult mice although there were indications in literature that in adult rodents preferential transduction in neurons is achieved whereas, in neonates transduction is mainly observed in astrocytes (Gholizadeh et al., 2013). However, the procedure in adult mice required special training in stereotactic injection technique which would not be available until fifteen months later. Furthermore, neonates are generally easier to handle and usually develop phenotype in a shorter period of time compared to adults (Jackson et al., 2016).

We were granted two litters of CD1 mice, namely twenty neonates, a few hours after birth to perform bilateral intracerebroventricular injection with the viral vectors. The neonates were placed into ice to achieve deep anesthesia and then they were transferred to the surgical surface. Ten mice pups were randomly assigned to receive the control group mixture-GFP/SNCA, and ten mice pups were randomly assigned to receive the experimental group mixture-TIA1/SNCA. During or shortly after the procedure four mice pups, three of the experimental group and one of the control group, died. The mice were eventually euthanized nineteen weeks post-surgery while no apparent phenotype was observed.

After harvesting the brain, we applied the cryo-embedding technique with OCT to freeze and preserve the tissue. However, when we were ready to proceed to section cutting, we realized that the tissue was frozen in a direction appropriate for horizontal sections but not for coronal sections which are recommended for substantia nigra studying. Once we were at the cryostat, each tissue was left in room temperature until most of the OCT melted, then it was repositioned vertically and once again cryo-embedded with fresh OCT. We recognized the possibility of alterations and damages to the tissue due to this process; however, the other viable option was to insert the frozen tissue to the cryostat without being able to check or adjust its position appropriately which could lead to sections partially coronal and partially sagittal. The tissue was indeed "brittle" and some sections were destroyed. We collected forty 35μm thick sections of the substantia nigra region and transferred them to the

antifreeze medium in a 48well plate in order to store them at -20°C until we use them.

1.1.3. Developing the immunofluorescence protocol

In our first attempt to create an immunofluorescence protocol for free floating sections we performed three 5'-minute washes with PBS, 1-hour blocking with 5%BSA (bovine serum), and 48-hours incubation with primary antibodies for TH and synuclein followed by three 5'-minute washes with PBS and 1-hour incubation with secondary antibodies. Finally, the sections were subjected to another round of three 5'-minute washes with PBS and eventually transferred to positively charged slides and covered with Mowiol mounting medium.

Under fluorescent microscope we were able to detect only the TH staining (Figure 1.1) whereas, neither synuclein nor GFP- in the control group- gave any signal. Upon this observation, we decided to apply an antigen retrieval step before the blocking step which translated to 1-hour incubation in citric acid solution of pH 6.0 at 80°C followed by 15'-minute ice incubation. However, this antigen retrieval protocol almost completely destroyed the sections so we had to readjust it by reducing the heating incubation time from 1-hour to 45'-minutes and leaving the sections to gradually revert to room temperature instead of the ice incubation step. In order to further refine the protocol and after several attempts we realized that the sections should not be folded during the antigen retrieval steps in order to prevent cracking of the tissue.

Upon applying the refined IF protocol we were still not able to detect α-syn or GFP. At this point numerous explanations were plausible and could partly account for our observations: a) other researchers had also noted that upon more than six weeks after intracerebroventricular injection in neonates with AAV vector carrying the GFP gene, they could not detect the GFP fluorescent protein. They attributed it to the CMV promoter and to the fact that the neonate's brain is developing and changing drastically (Hammond et al., 2017). However, we did not find in literature similar results for TH promoter, which was the one we used, and even if that was the case it still did not account for the complete absence of α-syn signal, b) to address the issue of the non-detectable synuclein we wondered about the primary antibody that was used in the IF staining. We had chosen the BD synuclein antibody which is developed in mouse

host and thus it could give strong enough background signal to mask the protein's signal. Although in literature many researchers choose this antibody for IF staining in rodent's tissue, we repeated the protocol three times using an antibody for total synuclein that was created in rabbit host, a rabbit raised antibody for phosphoserine-129 α-syn to target only the phosphorylated form of the protein, and finally a rabbit-raised antibody for filamentous α-syn that would target α-syn fibrils. None of these antibodies gave us specific α-syn signal under the fluorescent microscope. After several attempts, we detected a weak signal from α-syn BD antibody that corresponded to the endogenous protein c) in light of total failure to detect either the GFP or overexpressed α-syn protein we examined the possibility of unsuccessful intracerebroventricular injection. Although this approach would indeed explain our observation, statistically some of the injections should have been successful or partially successful and so the question remained d) we finally considered the fact that our viral vectors could be inactive, however the protocol we had followed to construct them had been used by members of our lab numerous times before and hence this explanation was rather weak.

The solution to this puzzling problem emerged months later and will be analyzed properly in the rat experiment section. In short, upon intracerebroventricular injection the viral vector solution was diffused throughout the cortex, the cerebellum, the olfactory bulb, and to a certain extent to the hippocampus. However, the inserted genes had a TH promoter which would lead to overexpression only upon transduction to dopaminergic neurons in substantia nigra where tyrosine hydroxylase enzyme is abundant. Consequently, the inserted genes with the TH promoter could not be expressed at the infected brain regions because tyrosine hydroxylase enzyme is not normally expressed in these cells.

With respect to the difficulty of detecting the endogenous or over-expressed α-syn, we eventually realized that the handling of the sections was a crucial factor that determined the background signal and thus, after gaining the necessary experience, we were able to achieve proper staining (Figure 1.2).

We also applied the IF protocol with the GFAP and Iba1 antibodies. The GFAP (glial fibrillary acidic protein) antibody stains astrocytes and is indicative of immune response to trauma or neurodegeneration. We

indeed detected a few GFAP positive astrocytes, not enough to imply inflammation, and thus confirmed that the protocol and the dilution of the antibody was appropriate (Figure 1.3). The Iba1 (ionized calcium binding adaptor molecule 1) antibody is a marker of microglia activation which is a hallmark of brain pathology and acute inflammation. We did not detect any Iba1 positive signal at this point (Figure 1.4); however, months later, the datasheet of the antibody was refined and suggested eight fold higher concentration of the antibody for IF protocols.

Furthermore, we applied the IF protocol with the TIA1 antibody by Everest (EB07741) in two dilutions either 1:100 or 1:50 but no signal was detected. We repeated the staining with another TIA1 antibody by Proteintech (12133-2-AP) in 1:200 dilution in which case we were ambiguous about the results. We made another attempt applying the protocol to sections of the experimental group with the TIA1 antibody by Proteintech in 1:100 dilution and achieved good staining results (Figure 1.5).

Finally, we decided to apply the IF protocol in order to detect co-localization of α-syn with either TH or TIA1 protein in the substantia nigra of mice injected with AAV encoding for α-syn and TIA1 (experimental group)(Figure 1.6 and Figure 1.7). At this point, it was obvious that we had failed to over-express the proteins however, we concluded that it was necessary to ensure that the protocol we had developed was appropriate for co-localization as we would use this technique to the forthcoming experimental models.
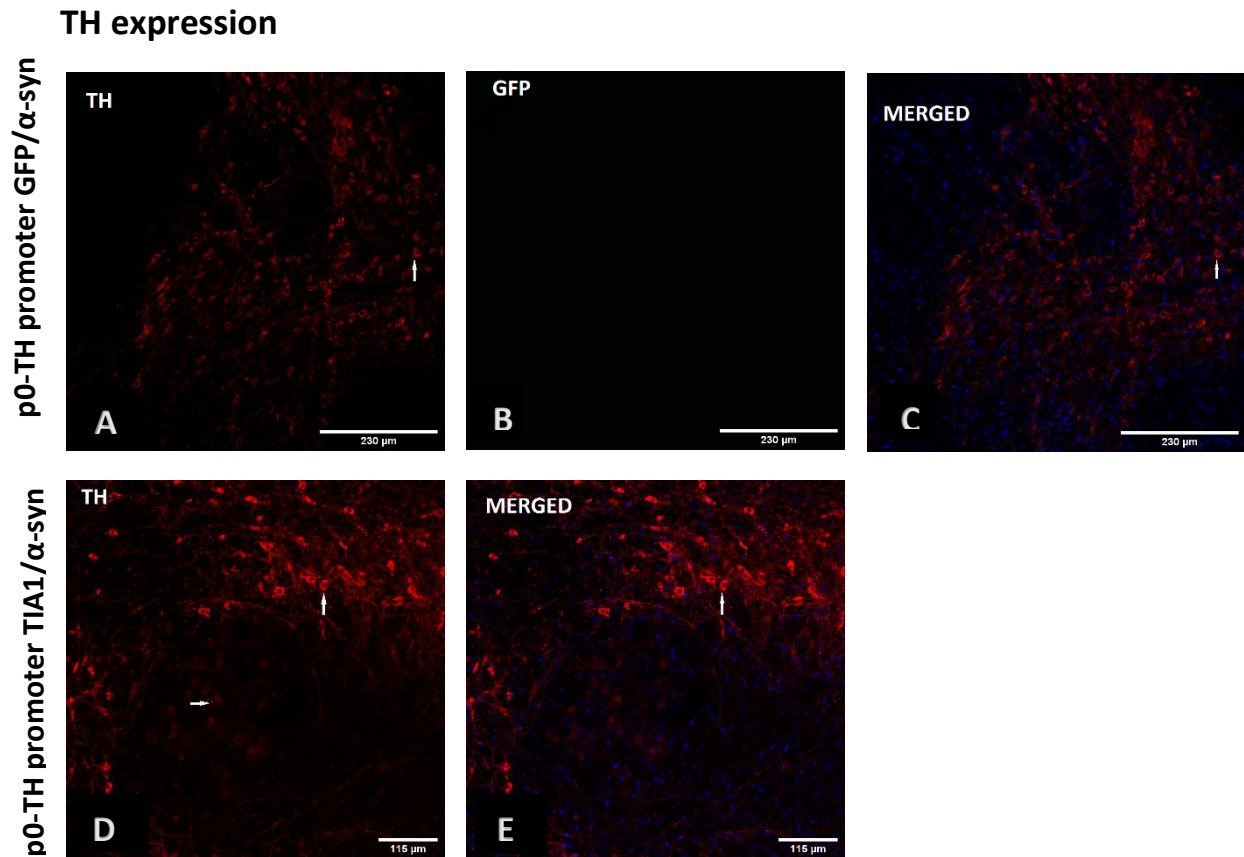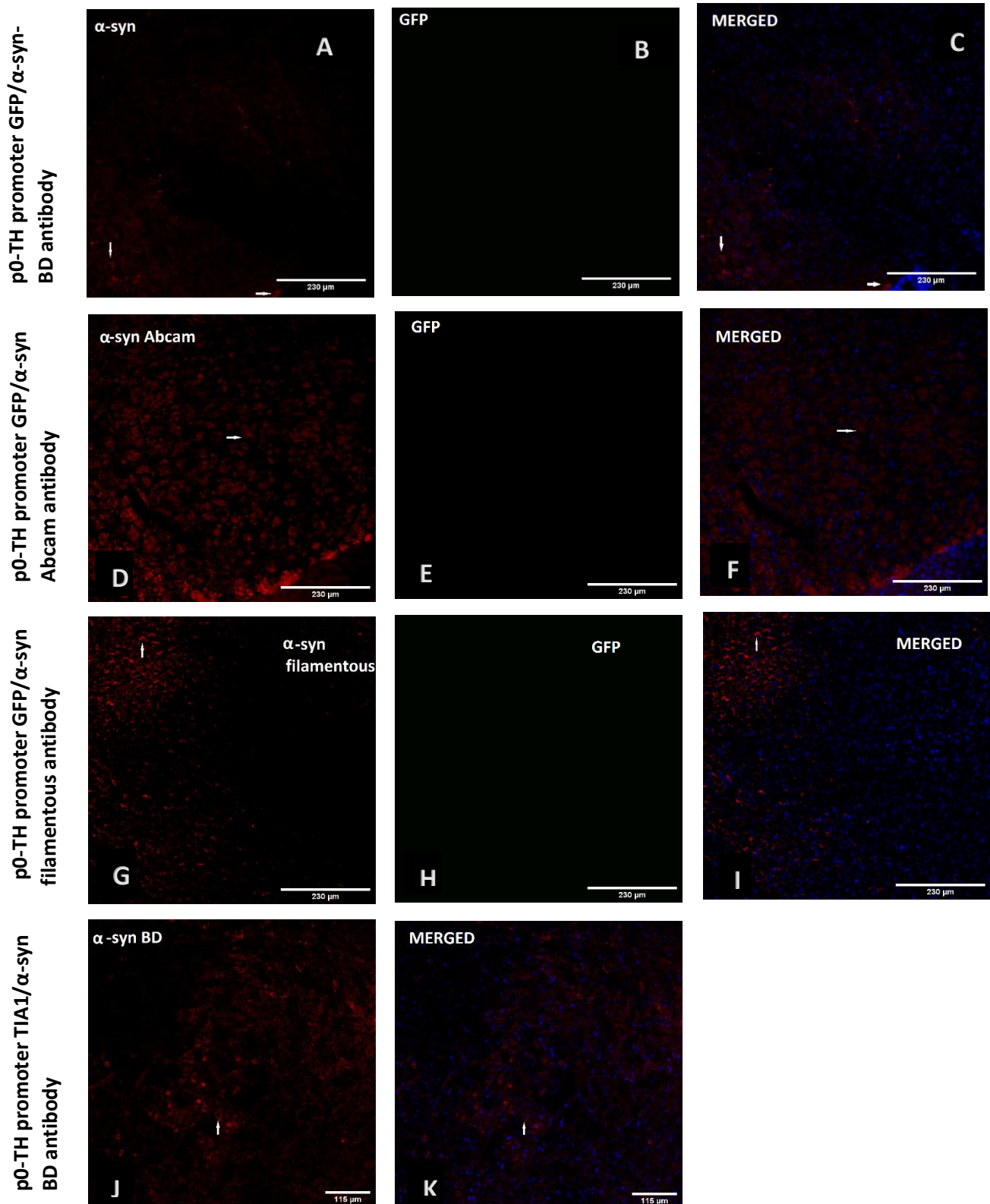
TH expression
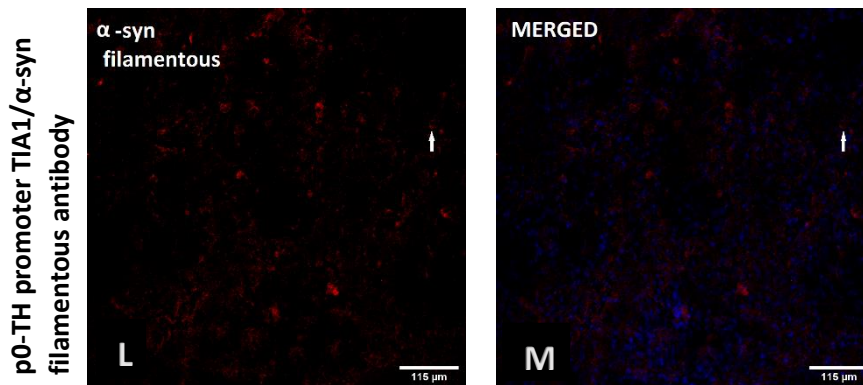

Figure 1.1

Dopaminergic specific marker TH (tyrosine hydroxylase) expression in the substantia nigra of mice injected with AAV vectors encoding for GFP and wild type human α-syn **(A-C)** or for TIA1 and wild type human α-syn **(D-E)** upon intracerebroventricular injection to neonate mice p0. The TH staining is good in both groups; arrows point to characteristic TH-positive neurons. Blue fluorescence refers to nucleic acids upon DAPI staining, red fluorescence refers to TH staining. We report absence of GFP positive cells in the control group **(B)**.
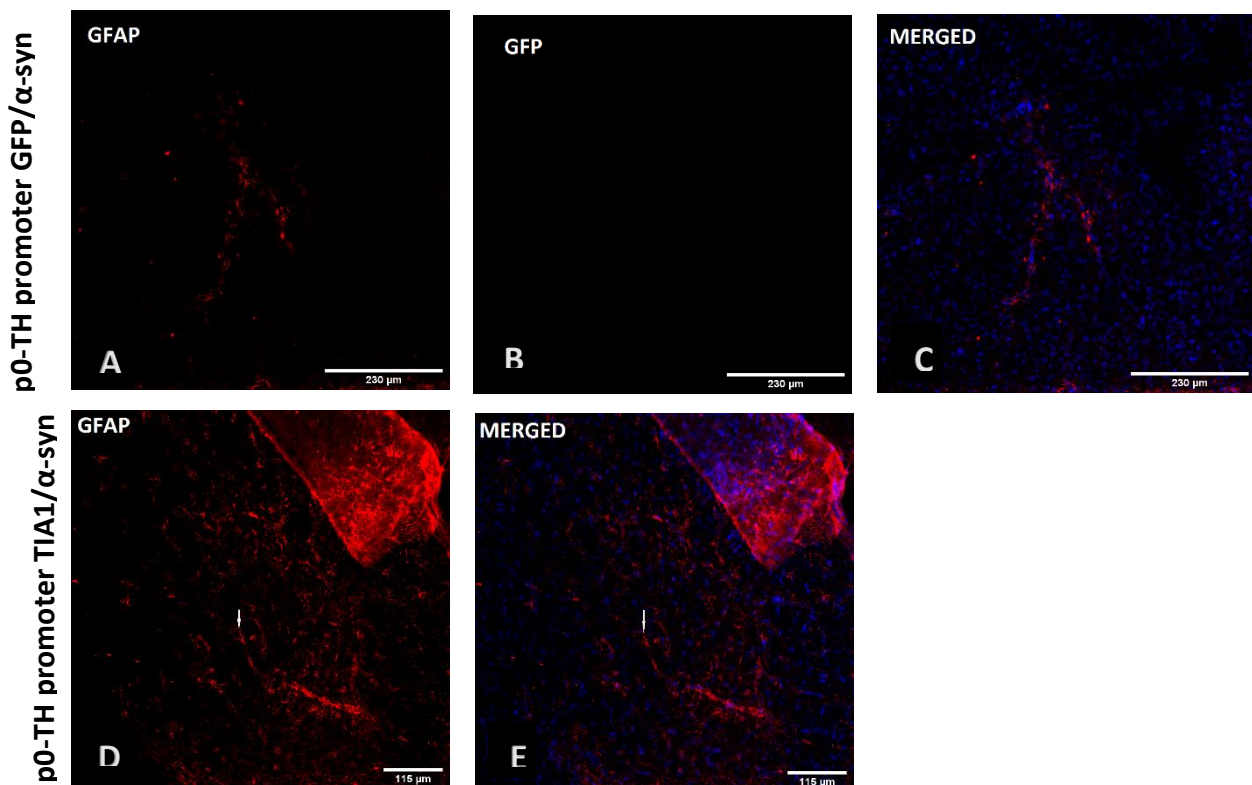
α-syn expression

Figure 1.2

α-syn expression in the substantia nigra of mice injected with AAV vectors encoding for GFP and wild type human α-syn **(A-I)** or TIA1 and wild type human α-syn **(J-M)** upon intracerebroventricular injection to neonate mice p0. Antibodies used to detect α-syn: α-syn BD 610787 **(A-C, J-K),** α-syn Abcam 138501 **(D-F)**, α-syn filamentous Abcam 209538 **(G-I, L-M)**. Blue fluorescence refers to nucleic acids upon DAPI staining. The staining for α-syn where the BD antibody was used **(A-C),** is weak but in line with existing literature, whereas in **(J-K)** staining is strong; arrows point to characteristic α-syn positive neurons. In **(D-F)** where the Abcam antibody was used, there is strong non-specific signal but α-syn positive neurons are detectable as pointed by the arrows. In **(G-I, L-M)**, where the filamentous antibody was used, there is strong non-specific signal; arrows point to possibly positive cells. We report absence of GFP positive cells in the control group **(B, E, H)**.
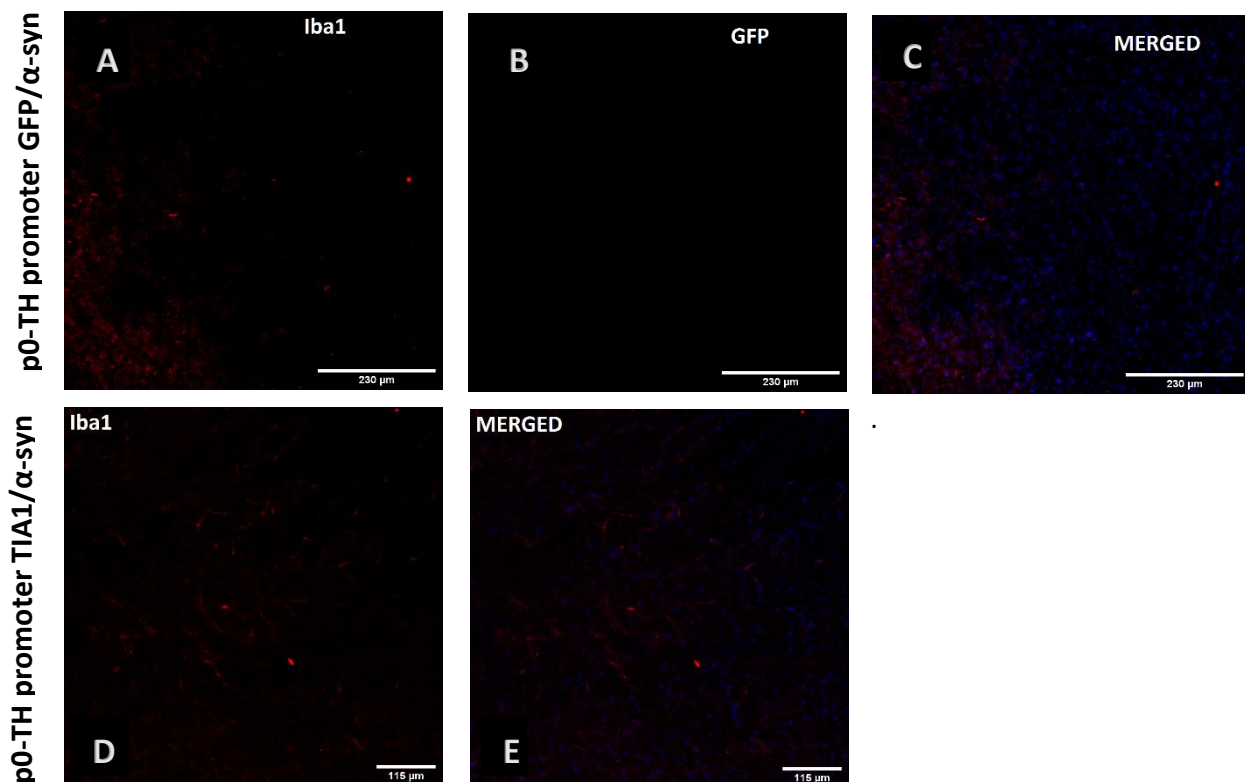
GFAP expression

Figure 1.3

Astroglial injury marker GFAP expression in the substantia nigra of mice injected with AAV vectors encoding for GFP and wild type human α-syn **(A-C)** or TIA1 and wild type human α-syn **(D-E)** upon intracerebroventricular injection to neonate mice p0. Blue fluorescence refers to nucleic acids upon DAPI staining. In **(A-C)** the GFAP staining does not correspond with typical astrocytes and is probably a result of non-specific binding of the antibody, whereas in **(D-E)** arrow point to a single astrocyte, however we report strong non-specific signal. We report absence of GFP positive cells in the control group **(B)**.

Iba1 expression

Figure 1.4

Microglial activation marker Iba1 in the substantia nigra of mice injected with AAV vectors encoding for GFP and wild type human α-syn **(A-C)** or TIA1 and wild type human α-syn **(D-E)** upon intracerebroventricular injection to p0 mice. Blue fluorescence refers to nucleic acids upon DAPI staining. The Iba1 staining does not correspond with typical microglia or macrophages and is probably a result of non-specific binding of the antibody. We report absence of GFP positive cells in the control group **(B).**

TIA1 expression

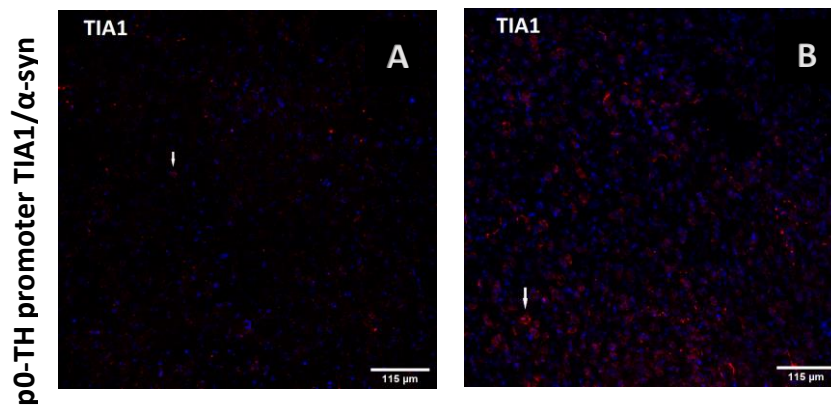
p0-TH promoter TIA1/α-syn

 Figure 1.5

TIA1 expression in the substantia nigra of mice injected with AAV vectors encoding for TIA1 and wild type human α-syn upon intracerebroventricular injection to p0 mice. Antibody used to detect TIA1: anti-TIA1 EB07741 by Everest in 1:50 dilution **(A)**, anti-TIA1 12133-2-AP by Proteintech in 1:100 dilution **(B).** Blue fluorescence refers to nucleic acids upon DAPI staining. Arrows point to characteristic TIA1 positive cells. We report weak staining in **(A),** whereas proper good staining in **(B).**

α-syn and TH co-localization

p0-TH promoter TIA1/α-syn
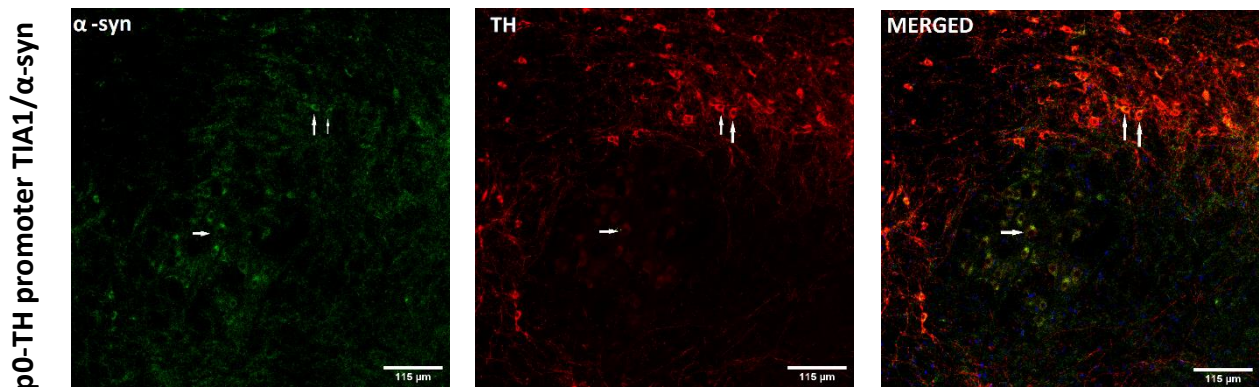
Figure 1.6

Co-localization of α-syn and TH positive neurons in the substantia nigra of mice injected with AAV vectors encoding for TIA1 and wild type human α-syn upon intracerebroventricular injection to p0 mice. We report co-localization of all α-syn positive cells with TH enzyme as expected in dopaminergic neurons; arrows point to characteristic cells.
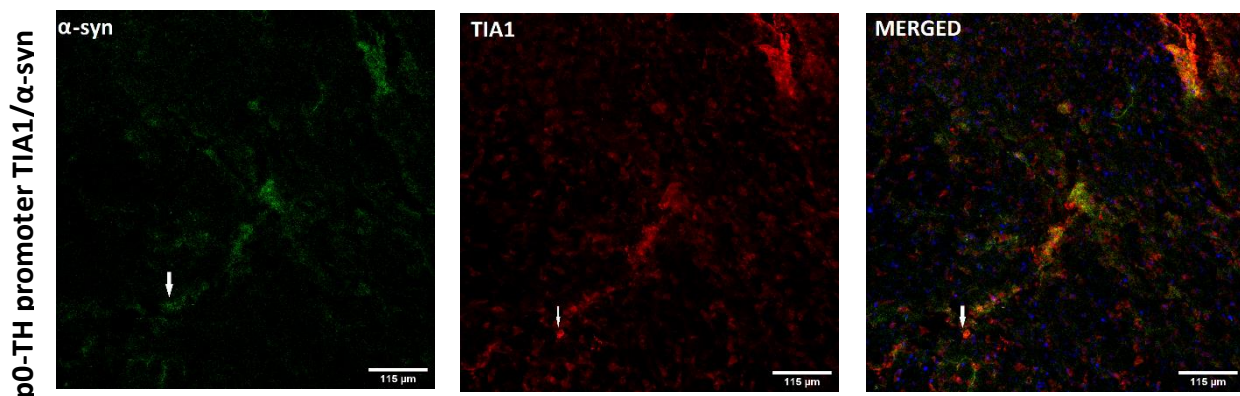
α-syn and TIA1 co-localization

Figure 1.7

Co-localization of α-syn and TIA1 protein in the substantia nigra of mice injected with AAV vectors encoding for TIA1 and wild type human α-syn upon intracerebroventricular injection to p0 mice. We report co-localization of α-syn positive cells with TIA1 expressing cells as expected; arrow point to characteristic cell.

1.1.4. Developing the immunohistochemistry protocol

Along with the IF protocol we had to develop an immunohistochemistry (IHC) protocol which is suitable for quantity analysis. The quantification, in our line of experiments, required several steps: a) we should develop an IHC staining protocol based on tyrosine hydroxylase enzyme as it is a very common and specific marker for dopaminergic neurons, b) we should develop the appropriate Nissl staining protocol for nucleic acids for our sections, c) we should adjust the steroinvestigator program for our experimental model. After inserting the parameters we would have to count and calculate the dopaminergic neurons in both groups and compare them with each other but also with the expected number of viable dopaminergic neurons in healthy mice. It is important to mention, that for a successful quantification of the neurons, we had to choose the sections carefully in order to represent all ten levels of depth in the substantia nigra region. For this purpose, while taking sections with the cryostat, we kept one every four sections for this protocol upon entering the substantia nigra.

For the first step, we had to decide whether quenching was necessary and if so what technique was more suitable for our sections. As described in the materials and methods section, we used para-formaldehyde, both in the perfusion/fixation protocol and in the preparation of the brain before freezing, which is known to block the endogenous peroxidase activity. However, it could still be possible that the para-formaldehyde had not covered successfully every single region of the brain, especially the substantia nigra region which is located deep in the midbrain. Upon that we decided that the quenching step was required. We chose to use a 3% H_2O_2/10% methanol mixture for this step rather than 0.1% sodium azide because the biotin antibody we would use later was sensitive to sodium azide and in its datasheet it was recommended to avoid it. For the 3,3-diaminobenzidine (DAB) test, after a few attempts, we found that the ideal incubation time with the working DAB solution was 10'-minutes in dark, although it was crucial to check the reaction after the seventh minute and if necessary, to stop it by adding double-distilled H_2O (γ- H_2O).

With respect to the Nissl staining protocol, it proved to be hard to finalize due to the fact that there are numerous significantly different approaches regarding the ethanol grades and the incubation time for each step. Upon discussion with other researches, we decided to follow the gradual transfer of the sections from 95° ethanol, to chloroform and to 70° ethanol, and finally to γ-H_2O. For the cresyl violet solution between the concentrations 0.1% up to 1%, that were suggested by other labs, we chose to proceed with the 0.3% cresyl violet/0.3% glacial acetic acid mixture as it seemed to be the most common choice among the researchers. However, in our first attempt to apply the protocol we realized that there was precipitate and some cresyl violet pellets in the solution, so we added a step of filtration upon heating before incubating the sections to the solution. In order to determine the incubation time in the cresyl violet solution, we repeated the protocol adjusting the incubation time upon our observations and eventually concluded to 3'-minutes and 30 seconds. We also found that it is necessary to wash under tap water the stained sections before transferring them to γ-H_2O so as to better control the intensity of the staining. We finally needed to decide the de-staining steps as they differentiated between the protocols we had found. We chose to follow the transfer of the section to gradually higher

ethanol grades starting from 50° up to 100° and finally to xylene with incubation time one to two minutes. It is important to note that the incubation time regarding the de-staining steps is not strict and needs adjusting each time as it depends on the intensity of the staining achieved from the previous steps.

Unfortunately, we did not have the chance to proceed to the last step with the stereoinvestigator program as it was made clear by this point, from the IF protocol, that the viral infection of the substantia nigra was unsuccessful.

1.2. The second experimental model

1.2.1. The second viral vectors construction

Following the first intracerebroventricular injections we decided to construct new viral vectors with a different promoter in order to repeat the experiment and compare the infectivity between the two models. We chose to use the CAGGS promoter, which is a strong synthetic promoter that drives high levels of gene expression, despite the fact that it cannot induce cell specific-overexpression as the TH promoter. We prepared two viral vectors one carrying the TIA1 gene and another carrying the mRuby2 protein gene-which is a red, fluorescent, photostable protein that does not bleach over time. The viral coat we used was, as previously, the PHP.eb variant of the AAV9 serotype of adeno-associated virus.

1.2.2. The second mouse model

We were granted one litter of CD1 mice, namely nine neonates, to perform bilateral intracerebroventricular injections with the viral vectors. After achieving deep anesthesia in ice, the pups were transferred to the surgical surface where five of them received the viral vector with the TIA1 gene (experimental group) and four of them received the viral vector with the mRuby2 gene (control group). After the injections the pups were returned to their cage where two of them did not survive. We did not separate the two groups nor mark the pups to eliminate bias in later steps. The mice were euthanized six weeks post-surgery while no apparent phenotype was observed.

After harvesting the brains, they were cryo-embedded in OCT and stored until we would use them. Unfortunately, this procedure was performed in parallel with the first experimental model and as a result the brains were, once again, placed in a position suitable for horizontal sections but not appropriate for coronal sections. When we were ready to proceed with the sectioning, we had the prior experience of the damage and the alterations in the tissue caused by leaving the brain in room temperature until OCT melts and cryo-embedding it with fresh OCT, so we decided to try a snap-freeze technique. Upon OCT partial melting,

each brain was placed in the peak of a 50ml falcon, covered with fresh OCT, and immersed for a few seconds in liquid nitrogen. We later discovered that some of the brain tissues were cracked as the preparation of the tissue with sucrose solution and para-formaldehyde solution was not completely successful and some moisture had remained. Of the non-damaged tissues we collected forty 35μm thick sections from the substantia nigra region, which were transferred in antifreeze medium in a 6well plate and stored at -20°C until we would need them. Before storing the sections we examined them upon an inverted fluorescent microscope and detected strong red signal from the mRuby2 protein in, at least, one of the wells.

1.2.3 Applying the IF protocol

As the protocol was already fixed, we had to decide upon the antibodies we would use, especially for the detection of TIA1. We concluded that we should try again with the anti-TIA1 by both manufactures (Everest and Proteintech). Regarding the antibodies for α-syn we decided to proceed with the BD antibody, as it is one of the most commonly used in studies similar to ours, and the filamentous antibody, hopping to detect abnormal conformations of the protein. We did not use the phosphoserine-129 antibody upon realizing that it was suitable only for the Western blot technique. Finally, we decided to use the GFAP antibody in order to establish that the staining was consistent with the previous experiment.

We observed the stained sections with a confocal microscope and concluded that the α-syn BD antibody gave strong signal but also strong background whereas, the α-syn filamentous antibody did not give any signal. α-syn was found to co-localize with tyrosine hydroxylase, however no aggregation was detected (Figure 2.2). Regarding the TIA1 antibody, we were able to detect strong signal only with anti-TIA1 by proteintech (Figure 2.1) whereas, with the Everest antibody we did not detect any signal. Upon careful examination, we concluded that the fluorescence intensity was almost equal in all stained cells and probably corresponded to the endogenous TIA1 and thus we had failed to overexpress the protein. With respect to the GFAP staining, we did not detect any astrocytes and received a weak non-specific signal (Figure 2.3).

It is important to note that we applied the protocol only in two brain tissues that we picked from storage in order to test our antibodies. We did not expect results from this line of experiment as its initial purpose was to study the infectivity with the CAGGS promoter and compare it to the TH promoter. At this point it was clear that we should proceed to our next experimental model with the CAGGS promoter. We also concluded that the mRuby2 protein was more suitable for the control group as it did not bleach and was easy to detect.

TIA1 expression
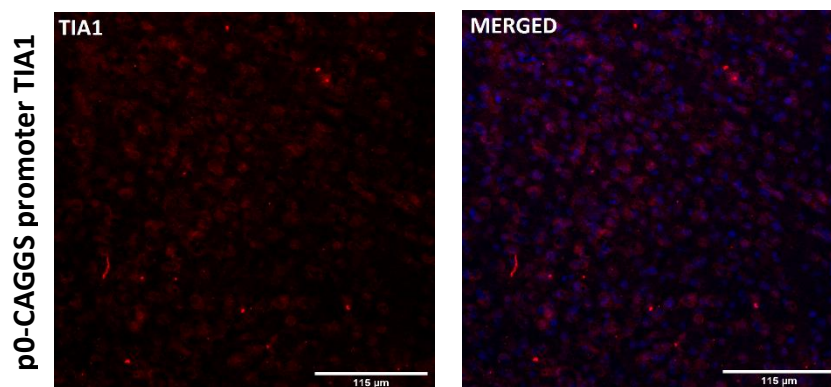
Figure 2.1

TIA1 expression in the substantia nigra of mice upon intracerebroventricular injection to p0 mice with AAV vectors encoding for TIA1. Antibody used to detect TIA1: anti-TIA1 12133-2-AP by proteintech in 1:100 dilution. Blue fluorescence refers to nucleic acids upon DAPI staining. We report good TIA1 staining but no overexpression of the protein in any cells.
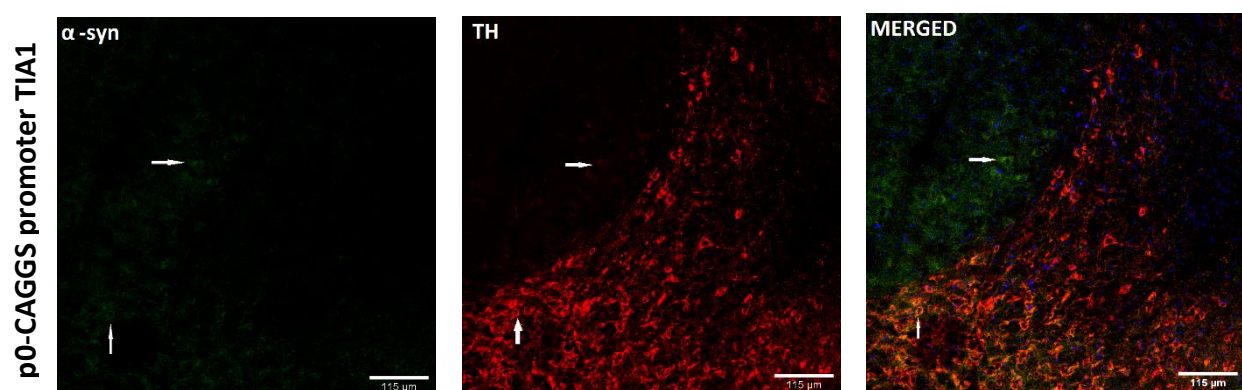
α-syn and TH co-localization

Figure 2.2

Co-localization of a-syn and TH positive neurons in the substantia nigra of mice upon intracerebroventricular injection to p0 mice with AAV vectors encoding for TIA1. Blue fluorescence refers to nucleic acids upon DAPI staining. We report co-localization of all α-syn positive cells with TH enzyme as expected in dopaminergic neurons; arrows point to characteristic cells.
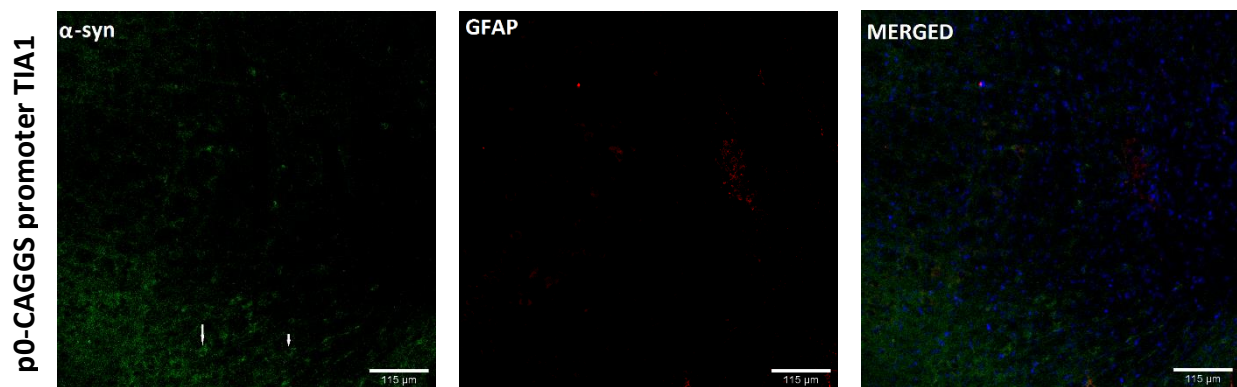
α-syn and GFAP co-localization

Figure 2.3

Co-localization of GFAP and α-syn positive neurons in the substantia nigra of mice upon intracerebroventricular injection to p0 mice with AAV vectors encoding for TIA1. Blue fluorescence refers to nucleic acids upon DAPI staining. The GFAP staining does not correspond with typical astrocytes and is probably a result of non-specific binding of the antibody. Arrows point to characteristic α-syn positive cells.

1.2.4. Applying the IHC protocol

Although we did not intent to quantify the neurons, as the purpose of this model was different, we decided to apply the IHC protocol in order to establish that no further refinement was needed. As expected, we achieved good staining intensity suitable for stereology analysis. The only optimization that took place was an extra step of chloroform incubation and the heating of the mounting medium that resulted in better distribution and in less air blisters.

2. Rat models

2.1. The first experimental model

2.1.1. The viral vectors construction

As we decided to proceed with the CAGGS promoter it was necessary to construct new viral vectors and if possible to achieve higher concentration. For this purpose we grew six 10cm plates with HEK-T cells, instead of four 10cm plates that we grew previously, in order to conduct the transfection procedure with the SNCA plasmid with the CAGGS promoter. When we retrieved the virus we noticed that the pellet was not pellucid but light brown which was indicative of deficient separation of the viral molecules from cell debris. Upon that we added several dilution steps throughout the procedure that resulted in clear, transparent viral pellet. However, we did not reach significantly higher concentrations and thus we decided in favor of the four or five 10cm plates as a starting point for the transfection. We, eventually, followed the refined protocol to construct viral vectors carrying the SNCA gene, the TIA1 gene, the mRuby2 gene; their titers, calculated upon real time PCR, were 9.53×10^9, 3.68×10^{10}, and 2.85×10^{10} respectively.

After constructing the viral vectors, we infected SH-SY5Y cells to determine if we could induce overexpression of the proteins in culture. When 80% of the cells expressed the mRuby2 protein we retrieved all the cell cultures and proceeded with Western blotting. Both α-syn and TIA1 were significantly overexpressed in the cells (Figure III)
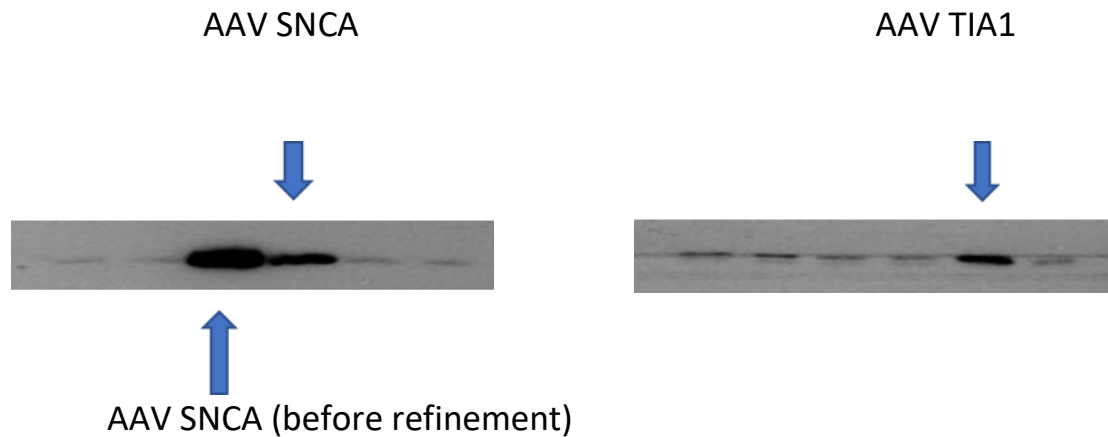
AAV SNCA   AAV TIA1

AAV SNCA (before refinement)

Figure III. Western blot representative immunoblotting images. Both α-syn and TIA1 were abundantly expressed in culture.

2.1.2. The first rat model

Upon studying the existing literature, in order to optimize our techniques and protocols, we noticed that in the majority of recent PD studies rat models are generally preferred compared to mouse models as they are more prone to α-syn toxicity (Creed & Goldberg, 2018); this observation led to the decision of changing our model from mouse to rat.

We were granted one litter of Sprague-Dawley rats, namely eleven neonates, to perform bilateral intracerebroventricular injections with the viral vectors. After achieving cryo-anesthesia, the rat pups were transferred to the surgical surface where six of them received a 1:1 mixture of the viral vectors carrying the SNCA and the TIA1 gene (experimental group) and five of them received a 1:1 mixture of the viral vectors carrying the SNCA and the mRuby2 gene (control group). The neonates were then returned to their cage to recover. The rat pups were not marked nor separated based on the viral vectors they received in order to avoid bias in later steps. All rats survived the procedure and were euthanized nine weeks post-surgery while no apparent phenotype was observed.

After harvesting the brains, they were transferred to 4% para-formaldehyde solution overnight, then to sucrose solution 15% and finally to 30% until they would sink. They were instantly washed with PBS, dried and eventually transferred to methyl-butane at -55°C for 30 seconds. This snap freeze technique allowed us to surmount the previous OCT cryo-

embedding challenges and also to prevent the cracking of the tissue as the temperature was not low enough to induce tissue damaging.

2.1.3. Applying the IF protocol

Hereby, we decided to analyze the brain tissues in pairs, one from the experimental group and one from the control group, each time in order to establish identical experimental conditions that would allow us well-grounded comparisons between the groups and reliable results. For this purpose, we took a small number of sections from the olfactory bulb and observed it under fluorescent microscope for mRuby2 red fluorescence. Upon identification, we chose the first pair and proceeded to the IF protocol.

We used the α-syn BD antibody, the filamentous α-syn antibody, and the TIA1 antibody by Everest. After applying the protocol we observed the substantia nigra region under fluorescent microscope and detected signal from the synuclein BD antibody and the TIA1 antibody. However, there was no signal from the mRuby2 protein which was unanticipated as we had detected the protein in the olfactory bulb sections.

We, therefore, had to question the distribution of the viral vectors in the brain tissue. In this regard, we chose a brain tissue from the control group and took coronal sections from the whole tissue, we then put the sections to slides and studied the infectivity and the distribution of the virus based on red fluorescence from the mRuby2 protein. This "mapping" demonstrated that the viral vector molecules had not reached the substantia nigra region of the brain-or any other region located in the midbrain-but they had successfully infected neuronal cells into the cerebellum, the cortex, the olfactory bulb, and to a certain degree to the hippocampus.

We, therefore, decided to repeat the IF staining and focus on the hippocampal area in an attempt to detect α-syn aggregates at this region. We used the α-syn BD antibody and the TIA1 antibody by Proteintech and studied the stained sections under a confocal microscope. Unfortunately, the diffusion of the viral vectors was not consistent among the rat brains and in the majority of the cases it had not reached the dentate gyrus

where synuclein is normally abundant. In some sections we detected possibly overexpressed α-syn that co-localized with overexpressed TIA1 which indicated a possibility of interaction between the proteins. However, these observations could be considered random and hence no conclusions should be drawn.

It is important to mention that, despite the insufficiency of this experimental model, we noticed that-contrary to mice-in the rat brain endogenous α-syn produces strong signal upon IF staining and thus it is easy to detect. This observation also applies for TIA1.
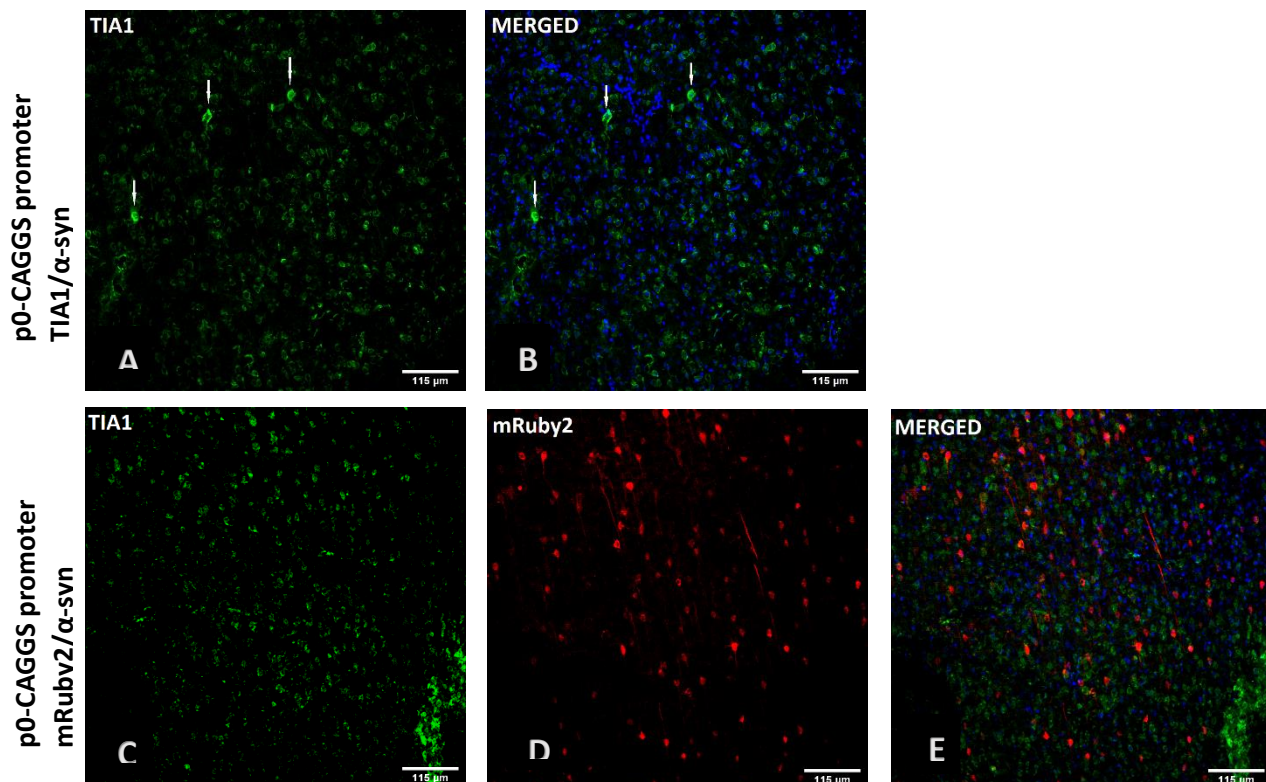
Rat 2 vs Rat 10

Figure 3.1.1

TIA1 expression in the hippocampal area of rat injected with AAV vectors encoding for TIA1 and wild type human α-syn **(A-B)** or mRuby2 and wild type human α-syn **(C-E)** upon intracerebroventricular injection in p0 rats. Antibody used to detect TIA1: anti- TIA1 12133-2-AP by Proteintech in 1:100 dilution. Blue fluorescence refers to nucleic acids upon DAPI staining We report good TIA1 staining; arrows point to cells where TIA1 is over-expressed **(A-B)**, whereas in **(C-E)** we report good TIA1 staining and good mRuby2 expression.
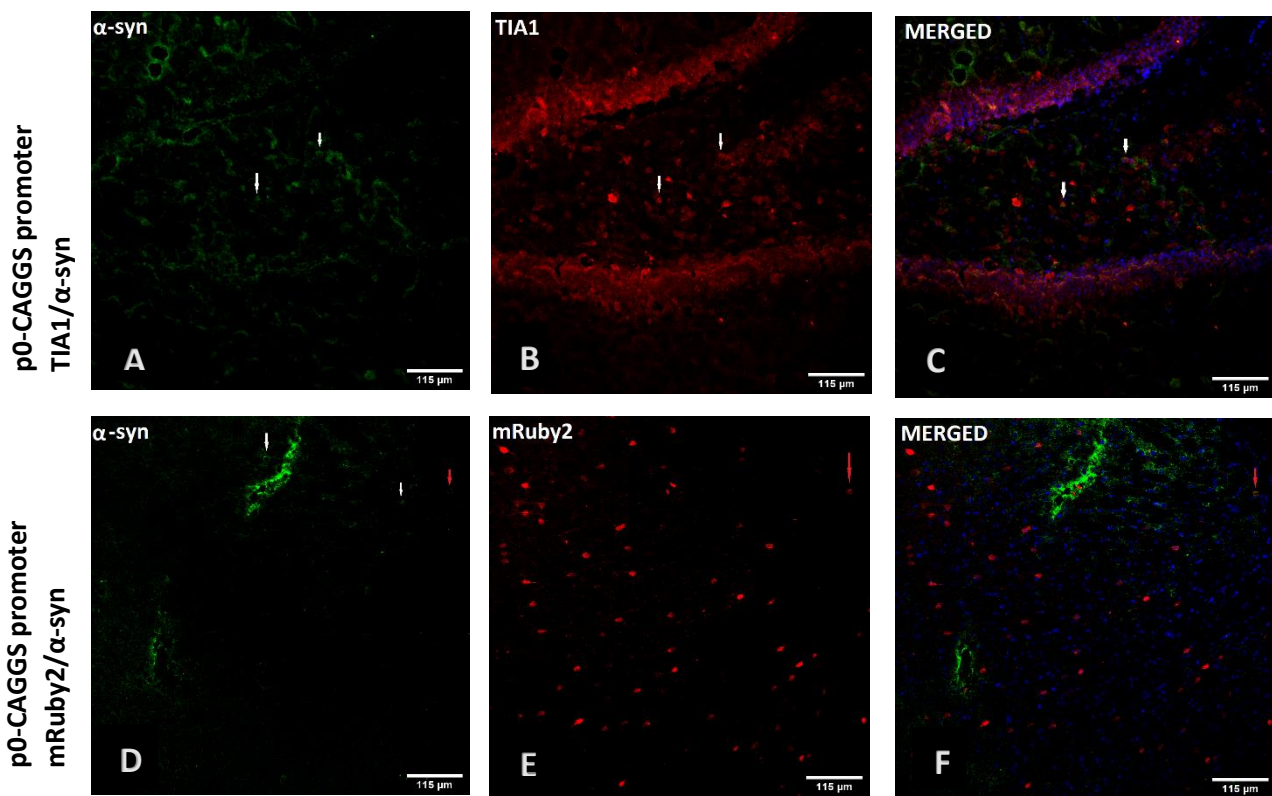
Rat 2 vs Rat 10

Figure 3.1.2

Images A-C: co-localization of α-syn and TIA1 protein in the hippocampal area of rat 2 upon intracerebroventricular injection to p0 rats with AAV vectors encoding for TIA1 and wild type human α-syn. Arrows point to sites of co-localization. We report presence of overexpressed TIA1 in a small number of cells but absence of overexpressed α-syn signal.

 Images D-F: co-localization of α-syn and mRuby2 protein in the hippocampal area of rat 10 upon intracerebroventricular injection to p0 rats with AAV vectors encoding for mRuby2 and wild type human α-syn. White arrows point to α-syn positive cells, red arrows point to sites of co-localization. We report good mRuby2 expression but absence of overexpressed α-syn signal.
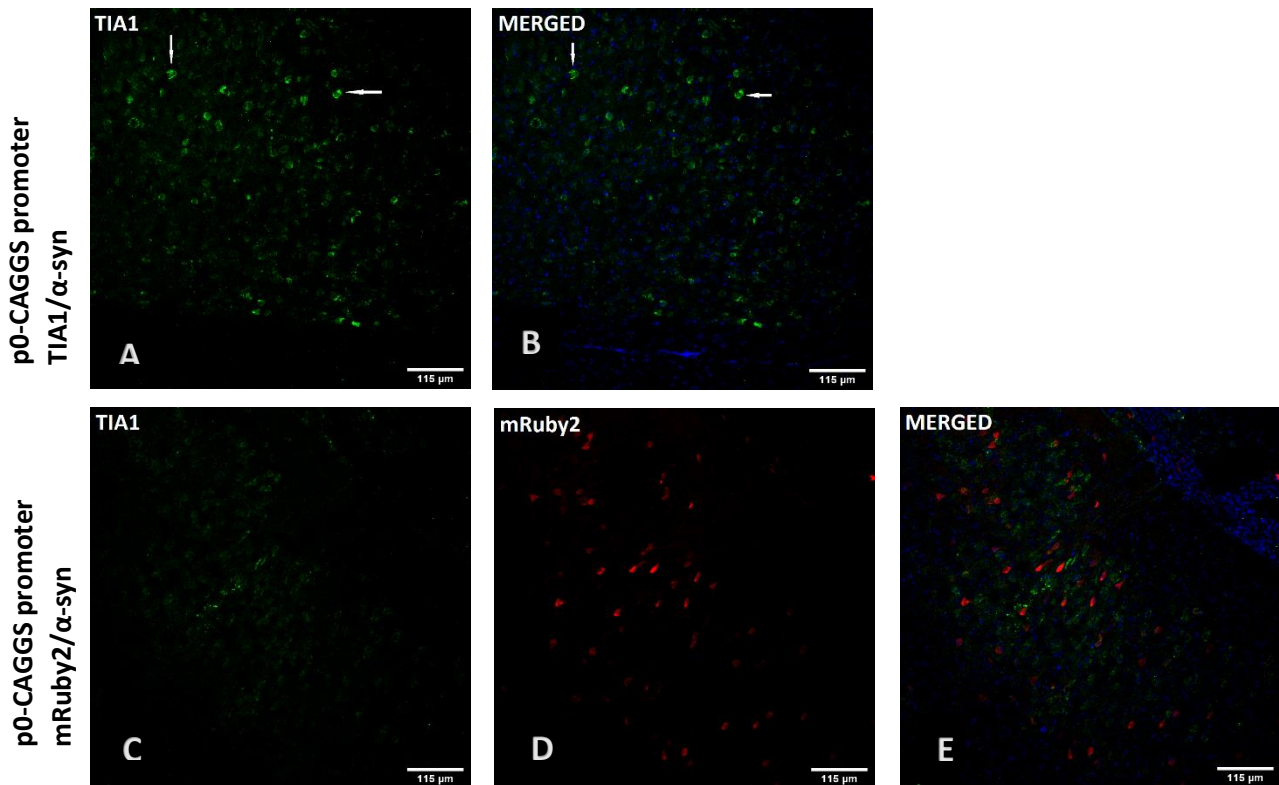
Rat 3 vs Rat 5

Figure 3.2.1

Image A-B: TIA1 expression in the hippocampal area of rat 3 upon intracerebroventricular injection in p0 rats with AAV vectors encoding for TIA1 and wild type human α-syn. Antibody used to detect TIA1: anti- TIA1 12133-2-AP by Proteintech in 1:100. We report good TIA1 staining; arrows point to cells where TIA1 is over-expressed.

Image C-E: TIA1 expression in the hippocampal area of rat 5 upon intracerebroventricular injection in p0 rats with AAV vectors encoding for mRuby2 and wild type human α- syn. Antibody used to detect TIA1: anti- TIA1 12133-2-AP by Proteintech in 1:100 dilution. We report good TIA1 staining and good mRuby2 expression.
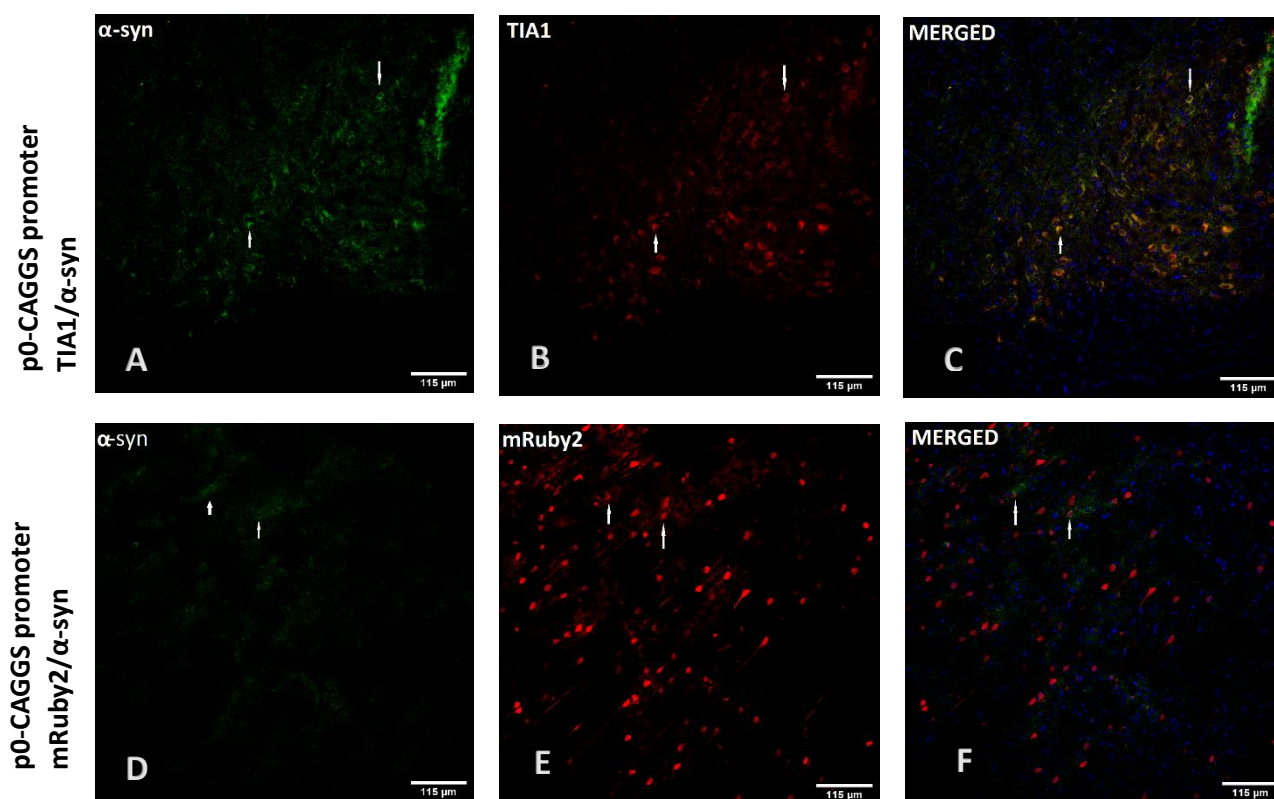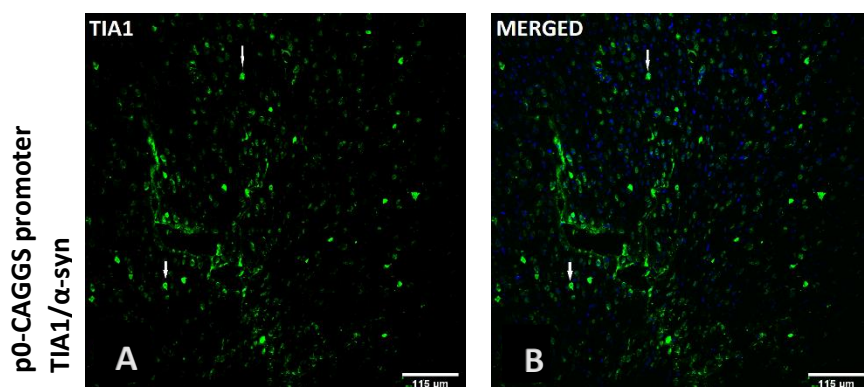
Rat 3 vs Rat 5

Figure 3.2.2

Image A-C: Co-localization of α-syn and TIA1 protein in the hippocampal area of rat 3 upon intracerebroventricular injection p0 rats with AAV vectors encoding for TIA1 and wild type human α-syn. Arrows point to sites of co-localization where both α-syn and TIA1 protein are possibly overexpressed.

Image D-F: Co-localization of α-syn and mRuby2 protein in the hippocampal area of rat 5 upon intracerebroventricular injection p0 rats with AAV vectors encoding for mRuby2 and wild type human α-syn. Arrows point to sites of co-localization. We report good mRuby2 expression but absence of overexpressed α-syn signal.
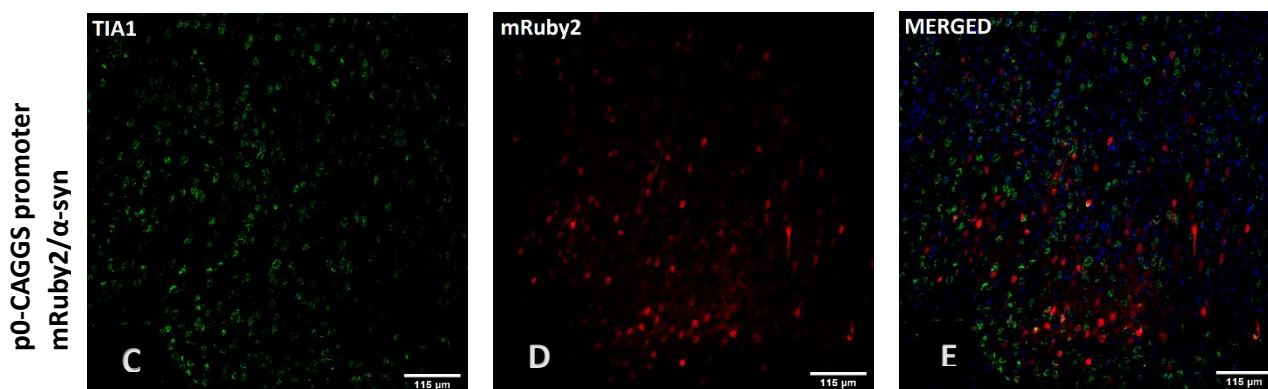
Rat 4 vs Rat 6

Figure 3.3.1

Image A-B: TIA1 expression in the hippocampal area of rat 4 upon intracerebroventricular injection to p0 rats with AAV vectors encoding for TIA1 and wild type human α-syn. Antibody used to detect TIA1: anti- TIA1 12133-2-AP by Proteintech in 1:100 dilution. We report good TIA1 staining; arrows point to cells where TIA1 is possibly over-expressed.

Image C-E: TIA1 expression in the hippocampal area of rat 6upon intracerebroventricular injection to p0 rats with AAV vectors encoding for mRuby2 and wild type human α-syn. Antibody used to detect TIA1: anti- TIA1 12133-2-AP by Proteintech in 1:100 dilution. We report good TIA1 staining and good mRuby2 expression.
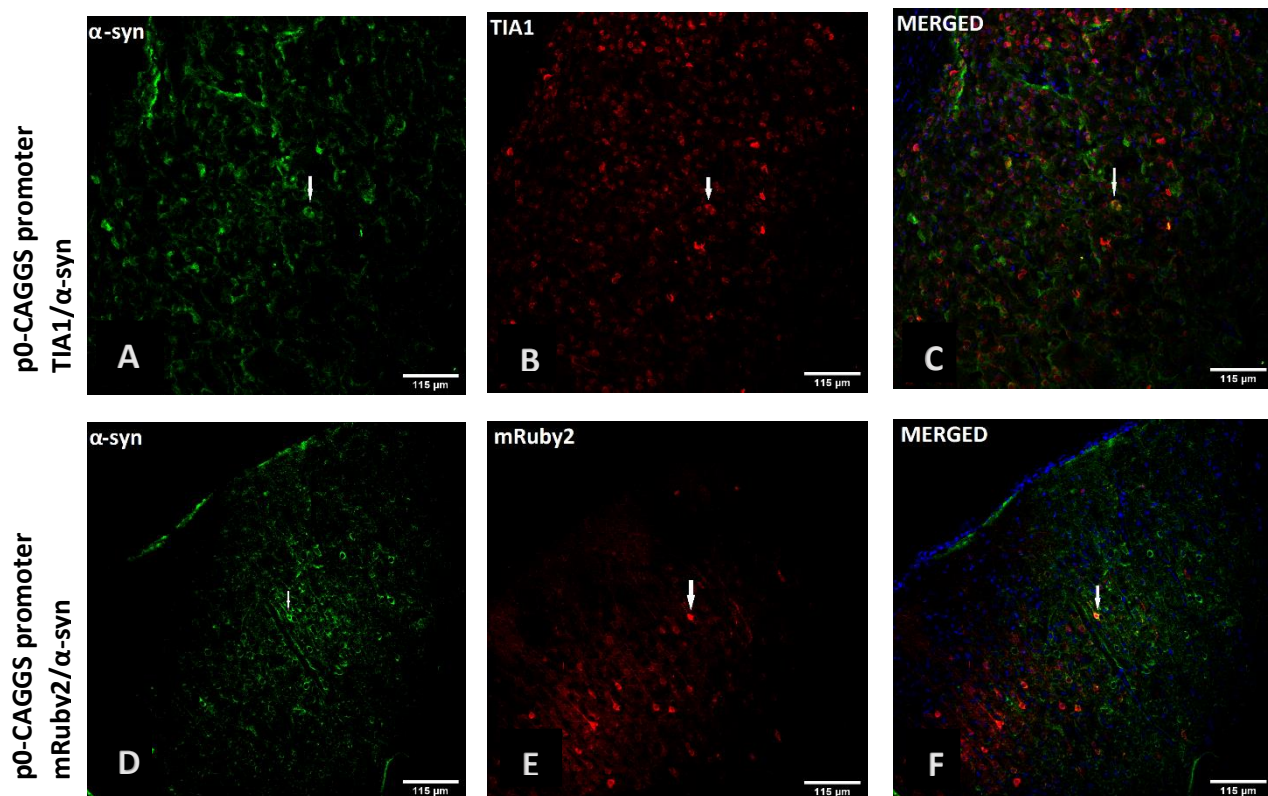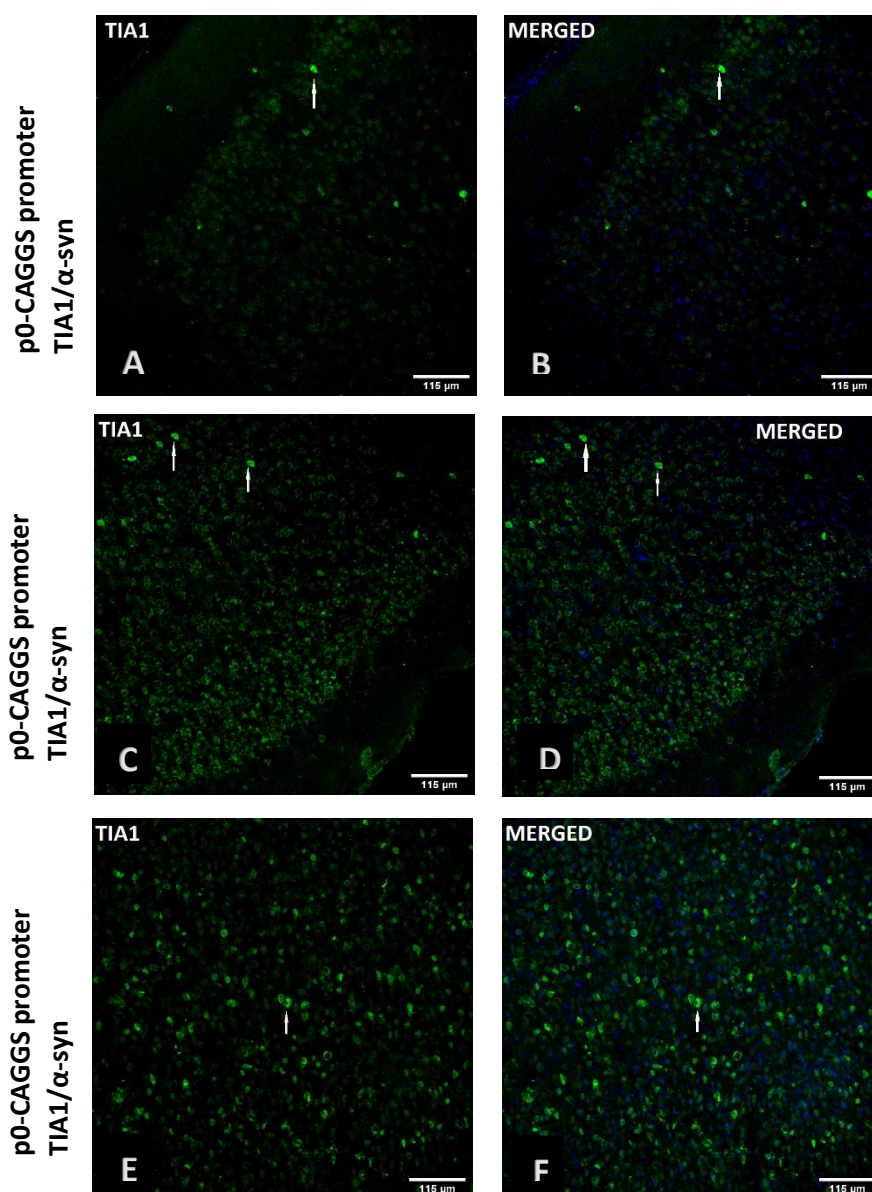
Rat 4 vs Rat 6

Figure 3.3.2

Image A-C: Co-localization of α-syn and TIA1 protein in the hippocampal area of rat 4 upon intracerebroventricular injection to p0 rats with AAV vectors encoding for TIA1 and wild type human α-syn. Arrows point to sites of co-localization where both α-syn and TIA1 protein are possibly overexpressed.

Image D-F: Co-localization of α-syn and mRuby2 protein in the hippocampal area of rat 6 upon intracerebroventricular injection to p0 rats with AAV vectors encoding for mRuby2 and wild type human α-syn. Arrows point to sites of co-localization where mRuby2 is expressed and a-syn is possibly overexpressed.

Rat 7, Rat 9, Rat 11 vs Rat 8
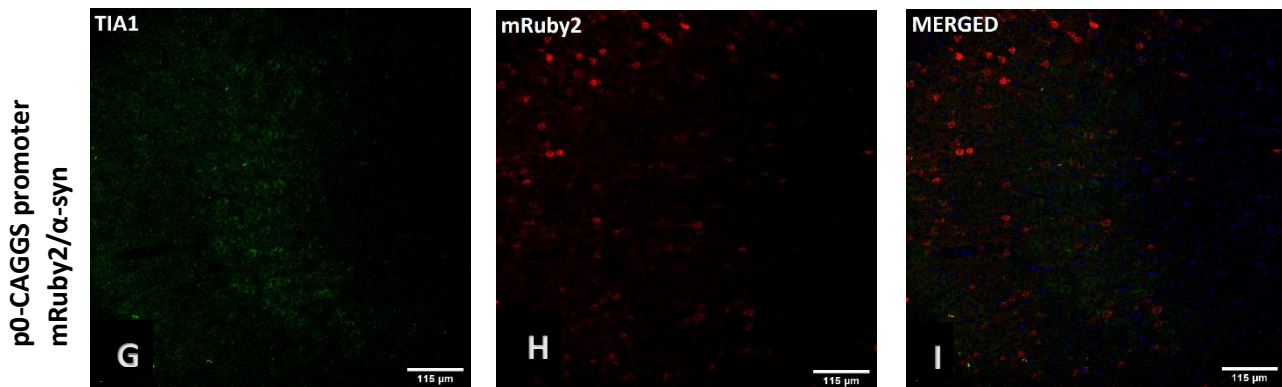
Figure 3.4.1

Image A-F: TIA1 expression in the hippocampal area of rat 7 **(A-B),** rat 9 **(C-D),** rat 11 **(E-F),** upon intracerebroventricular injection to p0 rats with AAV vectors encoding for TIA1 and wild type human α-syn. Antibody used to detect TIA1: anti- TIA1 12133-2-AP by Proteintech in 1:100 dilution. We report good TIA1 staining; arrows point to cells where TIA1 is over-expressed.

Image G-I: TIA1 expression in the hippocampal area of rat 8 upon intracerebroventricular injection to p0 rats with AAV vectors encoding for mRuby2 and wild type human α-syn. Antibody used to detect TIA1: anti- TIA1 12133-2-AP by Proteintech in1:100 dilution. We report mediocre TIA1 staining and good mRuby2 expression.

Rat 7, Rat 9, Rat 11 vs Rat 8
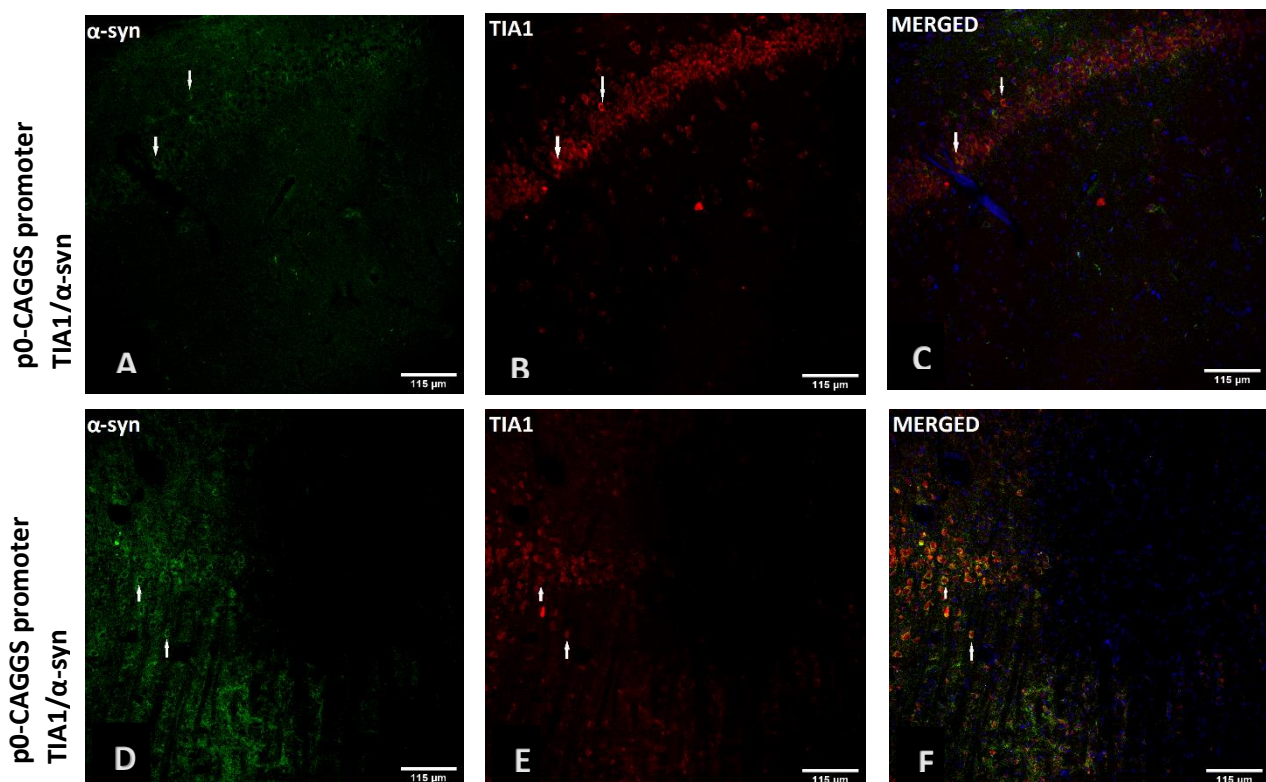
Figure 3.4.2

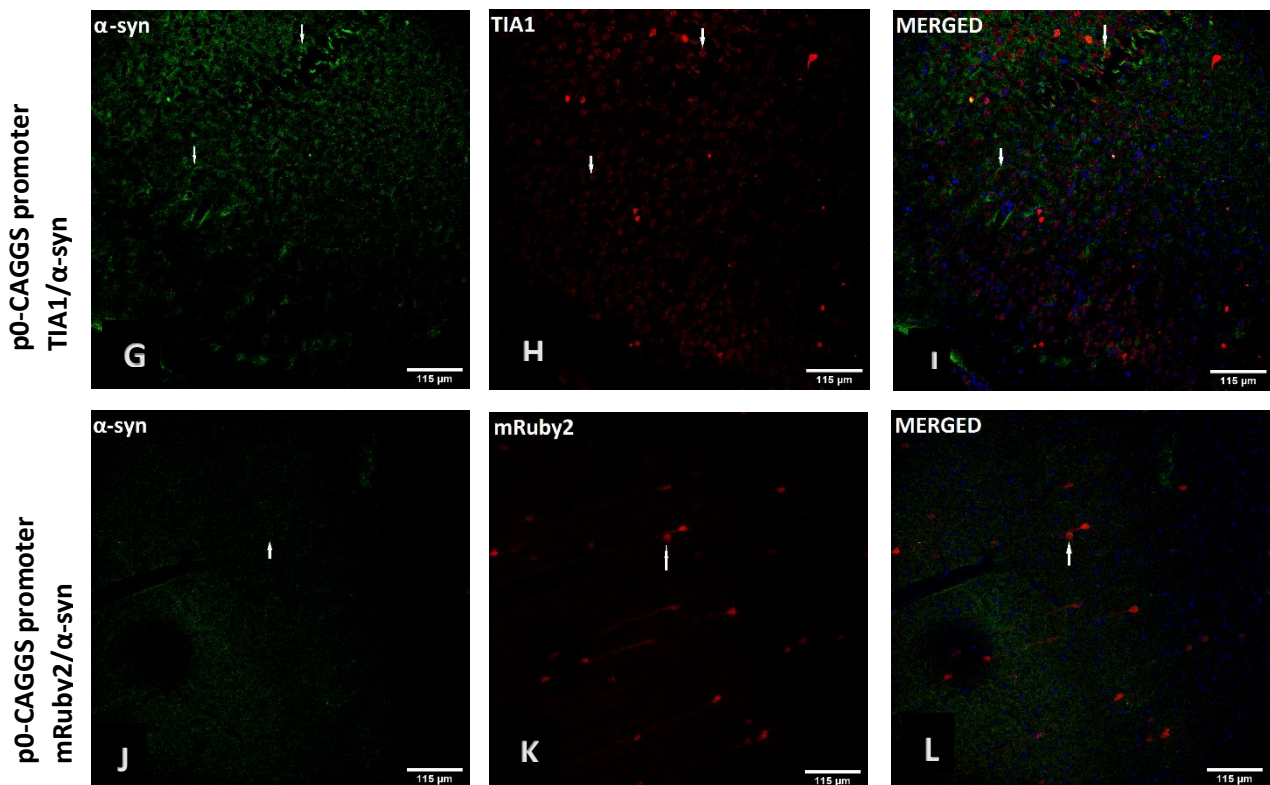**Image A-I:** Co-localization of α-syn and TIA1 protein in the hippocampal area of rat 7 **(A-C),** rat 9 **(D-F),** rat 11 **(G-I)** upon intracerebroventricular injection to p0 rats with AAV vectors encoding for TIA1 and wild type human α-syn. Arrows point to sites of co-localization where both α-syn and TIA1 protein are possibly overexpressed.

Image J-L: Co-localization of α-syn and mRuby2 protein in the hippocampal area of rat 8 upon intracerebroventricular injection to p0 rats with AAV vectors encoding for mRuby2 and wild type human α-syn. Arrows point to sites of co-localization where both mRuby2 and α-syn are expressed. We report absence of α-syn overexpression signal.

2.1.4. Applying the IHC protocol

As mentioned earlier, for the purpose of quantification of dopaminergic neurons, it is necessary to choose the sections for the IHC protocol carefully so as to represent all ten levels of depth in substantia nigra. In order to achieve that, while taking 35μm thick sections at the cryostat we kept one every six sections for the IHC protocol upon entering the substantia nigra region of the brain.

After applying the IF protocol, it was obvious that we had failed to infect substantia nigra and thus any attempt for quantification would be inapplicable. Therefore, we decided to perform the IHC protocol only once to establish that our prior conclusions and refinements, which were developed in mouse brain sections, were also suitable for rat brain sections. As anticipated, the staining had the appropriate intensity and no further optimizations were needed.

2.2 The second experimental model

2.2.1 The viral vectors construction

At this point, we did not need to construct new viral vectors as we would use those that were developed for the previous rat model. We discussed about the possibility that the different titers of the viral vectors might lead to different levels of gene expression and consequently to non-comparable results. However, the viral vector carrying the SNCA gene was the same in both mixtures and the other two viral vectors-carrying the TIA1 gene and the mRuby2 gene accordingly-had corresponding titers, hence we concluded that it was not necessary to construct new viral vectors and we would proceed as planned.

2.2.2 The second rat model

After failling to induce overexpression of the proteins in the substantia nigra region of the brain in neonate rodents, we decided to proceed with an adult rat model. We decided to develop an one-sex model in order to reduce the variables that could lead to different outcomes, so we debated about the rat gender we would choose to proceed with. Female rats present the advantage of smaller size and

weight and thus easier handling compared to the significantly larger size of male rats. However, literature on differences between rodent models based on sex did not collectively favor one sex over the other as the results were not consistent among the studies (Antzoulatos et al., 2010; Betancourt et al., 2017; Maguire et al., 2013; Niibori et al., 2020). On the other hand, Parkinson's disease is diagnosed to men more frequently than in women and also has an earlier age onset in men (Miller & Cronin-Golomb, 2010; Moisan et al., 2016). Taking these observations into consideration we concluded that a male rat model would probably be more appropriate for studying PD. Furthermore, we decided to inject the control mixture-mRuby2/SNCA-to one brain hemisphere of each rat and the experimental mixture-TIA1/SNCA-to the other hemisphere, thus utilizing each rat as both control and experimental individual. There are many advantages in using this technique, including reduction of the number of animals necessary for the study and more reliable results as it eliminates the differences among animals as a variable in the study.

We were granted four male Sprague-Dawley rats, four months old, to perform bilateral stereotactic injection to the substantia nigra pars compacta region of the brain. The rats were anaesthetized with ketamine/xylazine and then transferred to the surgical surface where, upon craniotomy, they received the TIA1/SNCA viral vectors mixture to the left hemisphere of the brain and the mRuby2/SNCA viral vectors mixture to the right hemisphere of the brain. During the stereotactic injection to the third rat, the Hamilton syringe malfunctioned and some portion of the viral vectors mixture was retracted. The rat was marked with a small cut on its right ear. Finally, during craniotomy to the right brain hemisphere of the fourth rat, the cortex was punctured causing a mild hemorrhage and significantly longer recovery time. All rats survived the procedure. Five weeks upon surgery two rats (the first and the second) presented symptoms of hypertension, fear to normal sound stimuli, disregard of everyday self-cleaning, significantly decreased food intake, up to 30% weight loss by the end of the sixth week, discomfort and pain. One of them developed spasms and died six weeks post-surgery, however, we proceeded to perfusion/fixation fifteen minutes upon death hopping to obviate possible hematoma formation to the brain. The second rat was euthanized the same day. Rats three and four did not

present any phenotype and thus we decided to observe them for a few more weeks.

After harvesting the brains of rat one and two, we followed the snap freeze technique described in the first rat model. In short, the brains were left overnight in 4% par-formaldehyde solution, then they were transferred to 15% and 30% sucrose solution until they would sink and finally to -55°C methyl-butane for 30 seconds.

Once in cryostat, we collected seventy 35μm thick sections from the substantia nigra region of the brain. We kept one every six sections for the IHC protocol and the remaining sections for the IF protocol. Unfortunately, the brain tissue of the rat that died prior to perfusion/fixation was brittle, probably due to blood clotting and impaired perfusion; hence we were able to collect only few intact sections but even so there were indications of hematoma that would give strong fluorescent signal at all wave lengths. We thus concluded that these sections were not appropriate for IF protocol.

2.2.3. Applying the IF protocol

For the IF protocol we decided to proceed with staining for

- α-syn using the BD antibody and the MJF by Abcam antibody (Figure 4.2.)

- TIA1 using the Proteintech antibody (Figure 4.4.)

- TH using the Millipore antibody (Figure 4.1.)

- GFAP using the Proteintech antibody (Figure 4.3.)

- Iba1 using the Proteintech antibody (data non-shown)

Under fluorescent microscope we noticed that the mRuby2 protein was abundantly expressed not only to the control hemisphere but also in regions of the experimental hemisphere. The excessive overexpression of the protein caused acute toxicity, massive cell death and fragmentation. Normally, the mRuby2 protein is not toxic however, the abnormally high overexpression probably overwhelmed the cells resulting in cell death and

neuronal loss. This observation, along with the diffusion of the viral vectors to neighboring brain regions apart from the substantia nigra, could provide an explanation for the apparent phenotype and the death of the first rat.

We detected in both hemispheres numerous astrocytes, upon GFAP staining, but we failed to detect activated microglia, upon Iba1 staining.

With respect to TIA1 protein, we noticed that there were several cells where the protein was overexpressed but considerably less in number compared to the cells expressing the mRuby2 protein. This was anticipated as there are indications in literature that TIA1, among other RNA binding proteins, auto-regulates its levels of expression and thus it might be challenging to induce significant overexpression (Dassi, 2017; Müller-McNicoll et al., 2019; Wollerton et al., 2004).

Finally, regarding α-syn, we were able to detect only a few cells overexpressing the protein in the experimental hemisphere and no cells where the protein is overexpressed in the control hemisphere. This was not expected as all viral vectors were tested in cell cultures and were found to induce expression of the proteins; furthermore, both TIA1 and mRuby2 genes were successfully transduced and expressed *in vivo*. One plausible explanation could be that the human α-syn plasmid was introduced to an inappropriate bacterial strain for transformation, thus resulting in a recombinant defective plasmid that could still drive strong expression in cell cultures but weak expression *in vivo*.

TH expression
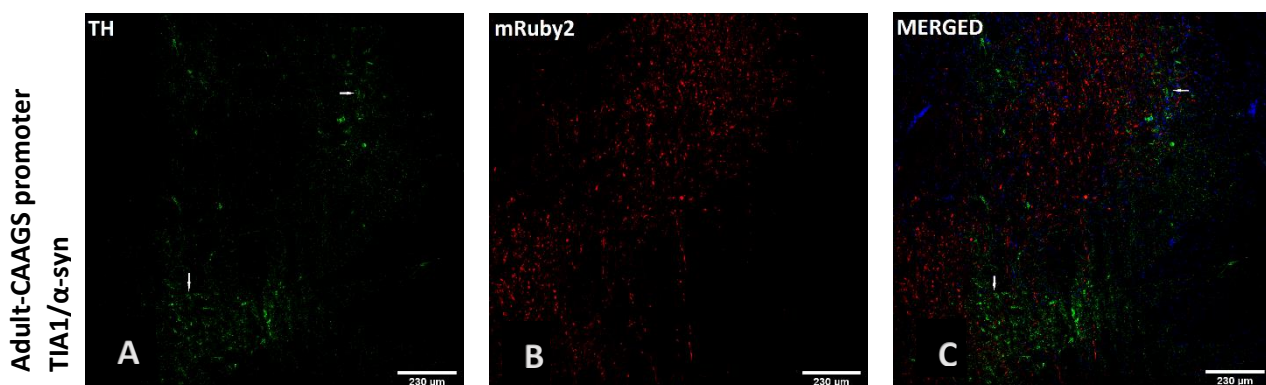
Figure 4.1

Image A-C: Dopaminergic specific marker TH (tyrosine hydroxylase) expression in the substantia nigra of rat in the experimental hemisphere upon stereotactic injection with AAV vectors encoding for TIA1 and wild type human α-syn. We report good TH staining in the SNc region and also in the VTA neurons. We report contamination of the experimental hemisphere with the AAV vector encoding for mRuby2 and numerous fragmented cells. Arrows point to characteristic TH positive neurons.

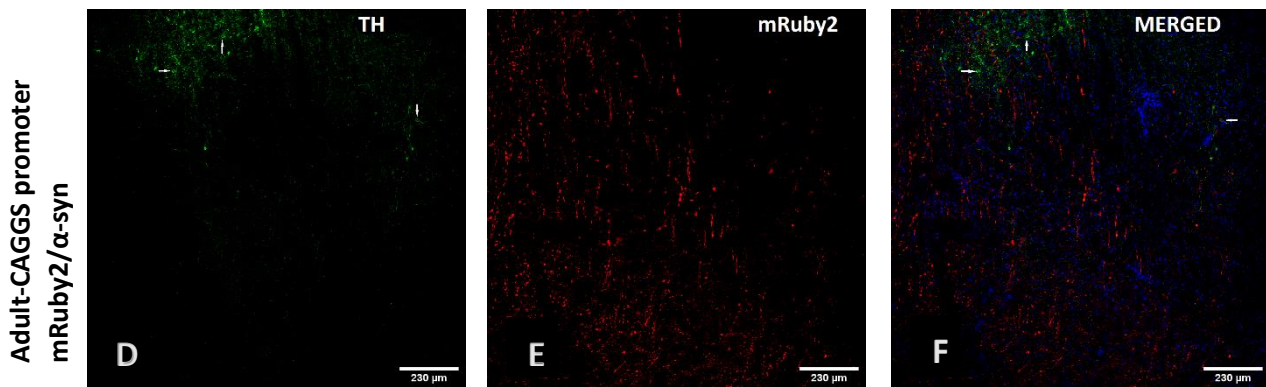**Image D-F:** Dopaminergic specific marker TH (tyrosine hydroxylase) expression in the substantia nigra of rat in the control hemisphere upon stereotactic injection with AAV vectors encoding for mRuby2 and wild type human α-syn. We report mediocre TH staining due to cell death. mRuby2 expression suggests massive cell death and fragmentation. Arrows point to characteristic TH positive neurons.
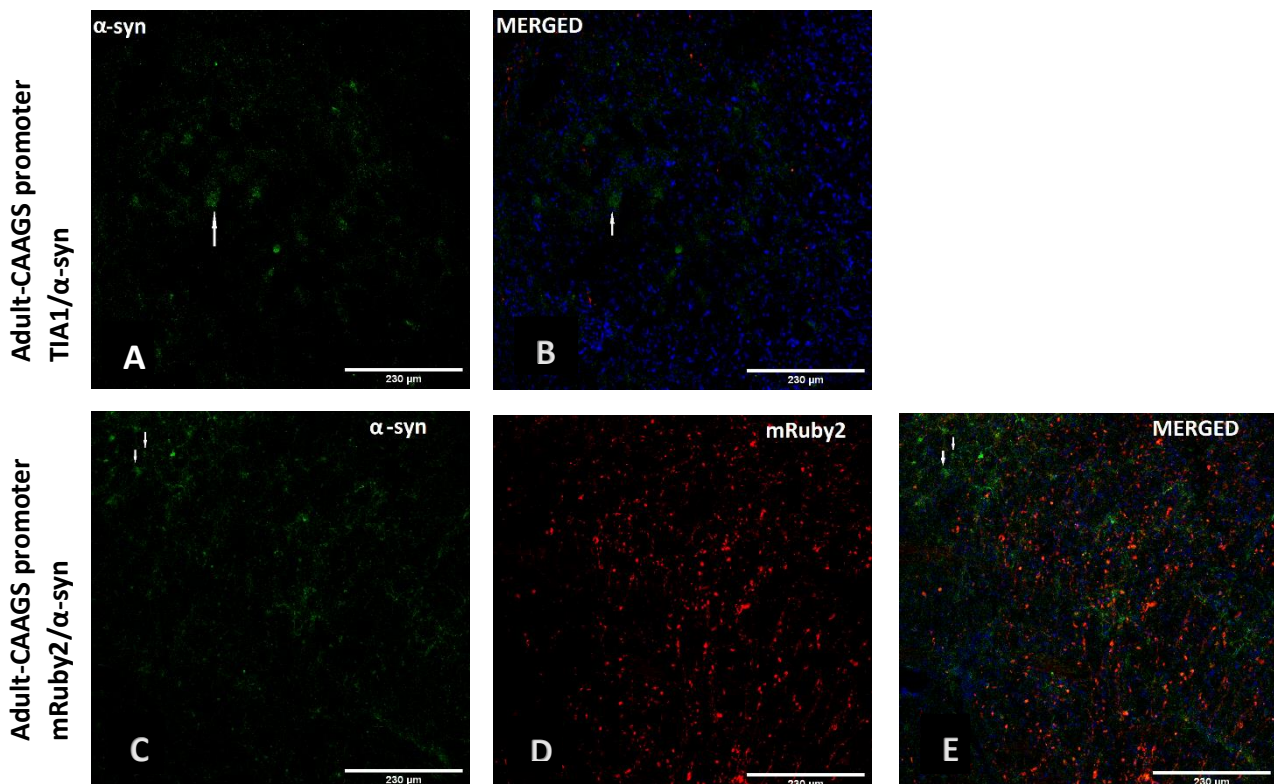
α-syn expression

Figure 4.2

Image A-B: α-syn expression in the substantia nigra of rat in the experimental hemisphere upon stereotactic injection with AAV vectors encoding for TIA1 and wild type human α-syn. Antibody used to detect α-syn: BD 610787. We report mediocre α-syn staining. Arrows point to cells where α-syn is possibly overexpressed.

Image C-E: α-syn expression in the substantia nigra of rat in the control hemisphere upon stereotactic injection with AAV vectors encoding for mRuby2 and wild type human α-syn. Antibody used to detect α-syn: BD 610787. We report mediocre α-syn staining; arrows point to cells where α-syn is expressed. mRuby2 expression suggests massive cell death and fragmentation.

GFAP expression

Figure 4.3

Image A-C: GFAP expression in the substantia nigra of rat in the experimental hemisphere upon stereotactic injection with AAV vectors encoding for TIA1 and wild type human α-syn. We report good GFAP staining; arrow point to characteristic astrocyte. We report contamination of the experimental hemisphere with the AAV vector encoding for mRuby2 and presence of fragmented cells.

Image D-F: GFAP expression in the substantia nigra of rat in the control hemisphere upon stereotactic injection with AAV vectors encoding for mRuby2 and wild type human α-syn. We report good GFAP staining; arrows point to characteristic astrocytes. mRuby2 expression suggests massive cell death and fragmentation.
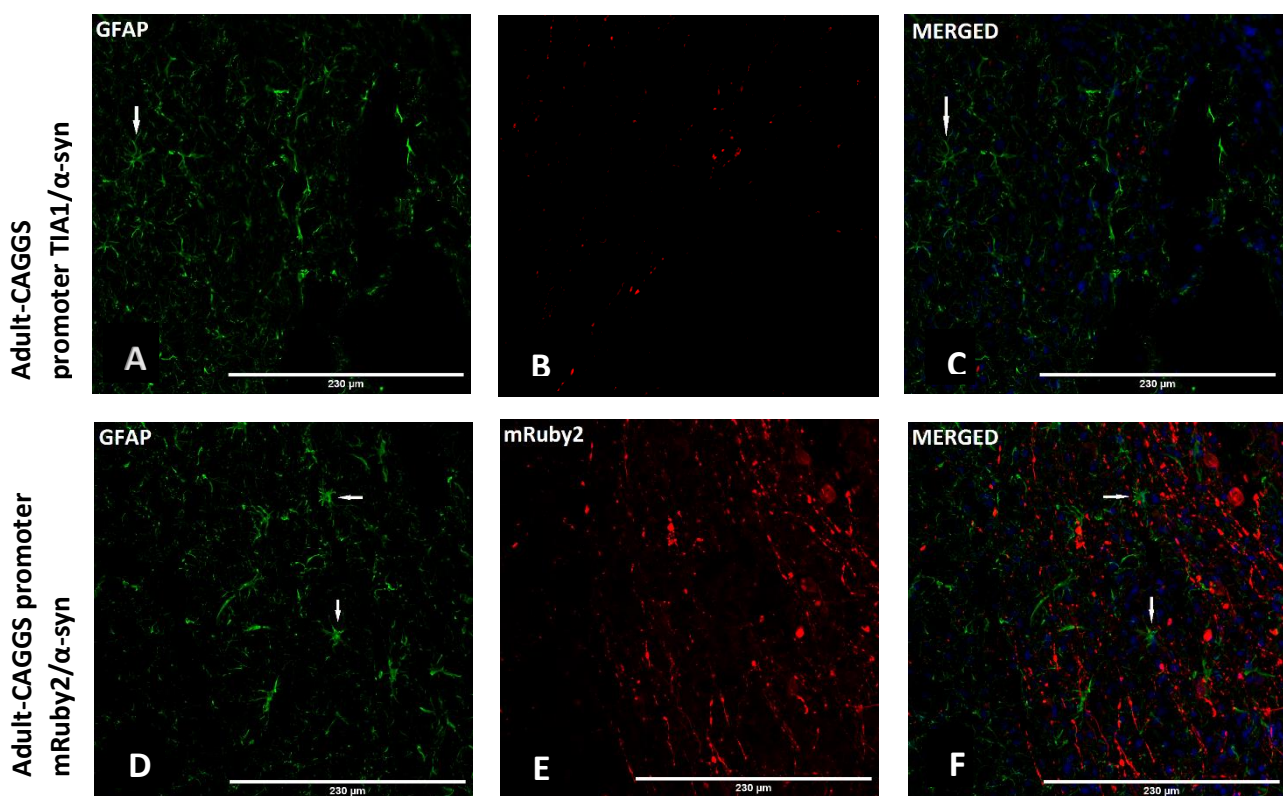
TIA1 expression
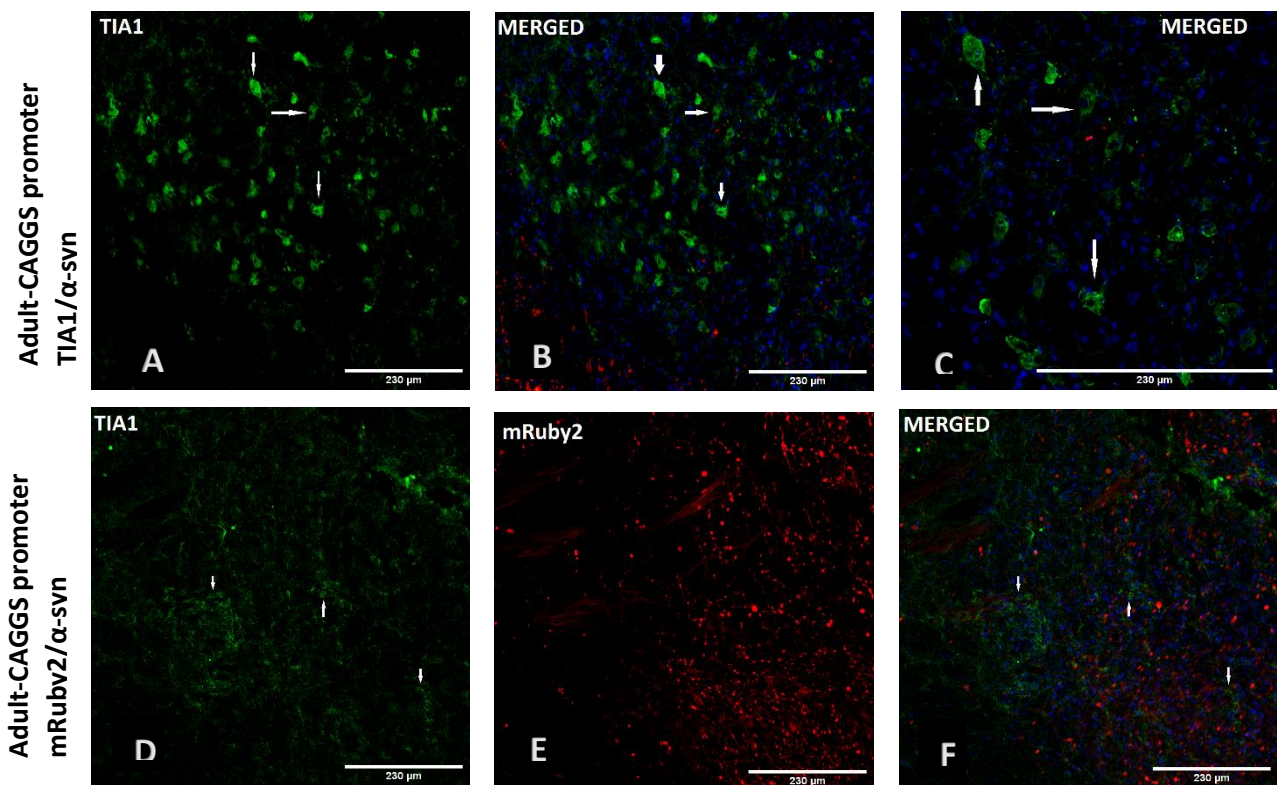
Figure 4.4

Image A-C: TIA1 expression in the substantia nigra of rat in the experimental hemisphere upon stereotactic injection with AAV vectors encoding for TIA1 and wild type human α-syn. Arrows point to cells where TIA1 is overexpressed. **Image C**: 40xlens.

Image D-F: TIA1 expression in the substantia nigra of rat in the control hemisphere upon stereotactic injection with AAV vectors encoding for mRuby2 and wild type human α-syn. We report good TIA1 staining. mRuby2 expression suggests massive cell death and fragmentation.

2.2.4. Applying the IHC protocol

After applying the finalized protocol, it was macroscopically conspicuous that in the control hemisphere the TH positive staining was notably decreased, hence indicating massive neuronal loss at this region. This observation was consistent with what we had previously reported upon IF staining.

IV. Finalized protocols and procedures

(materials and methods)

1. **Recombinant AAV viral vector construction**

1.1 Cell culture HEK293-T cells

1.1.1 Split: 30

Upon removing the growth medium from the 10cm culture plate-where the cells are approximately 80% confluent, add 2.8ml pre-warmed trypsin and incubate for 5'-minutes in order to detach the cells from surface of the plate. After gently pipetting over the cell layer surface, collect the cells in tubes and centrifuge them for 30 seconds. Discard trypsin and re-suspend the cells with 1ml pre-warmed DMEM/10%FBS growth medium. Prepare four 10cm culture plates with 10ml growth medium and add 250μl of the re-suspended cells. Let the cells recover for 5'-minutes and then place the culture plates in the incubator at 37°C.

1.1.2 Transfection:

Pre-warm trypsin and the growth medium DMEM/10%FBS. Prepare mixtures A and B for twelve 10cm culture plates and transfer 250μl from each mixture to a tube. Let the mixtures to fuse for 20'-minutes.

Mixture A: quantities for one 10cm culture plate	Mixture B: quantities for one 10cm culture plate
250μl optimum growth medium	250μl optimum growth medium
1.274ng PHP.e.b ICAP	16μl PEImax lipid
1.768ng Phelper	
958ng AAV plasmid	

Remove growth medium from the culture plates and add 2.8ml trypsin in each plate, incubate for 5'-minutes at 37°C. After pipetting over the cell

layer surface, collect the cells in tubes and centrifuge them for 30''-seconds. Discard the trypsin from the tubes and re-suspend the cells with 1ml growth medium DMEM/10%FBS per two tubes. Collect the cells and transfer 380µl cells to each tube containing mixtures A and B. Let them rest for 20'-minutes, while gently re-suspending every 7'minutes. Prepare twelve 10cm culture plates with 12ml growth medium DMEM/10%FBS, add the content of the tubes and insert them to the incubator at 37^{0}C. 24-hours post-transfection add 2ml growth medium DMEM/10%FBS to each culture plate. 48-hours post-transfection collect the supernatant media to a vessel and add 12ml of fresh DMEM/10%FBS media to each culture plate. Incubate for 48-hours.

Plasmid backbone used:
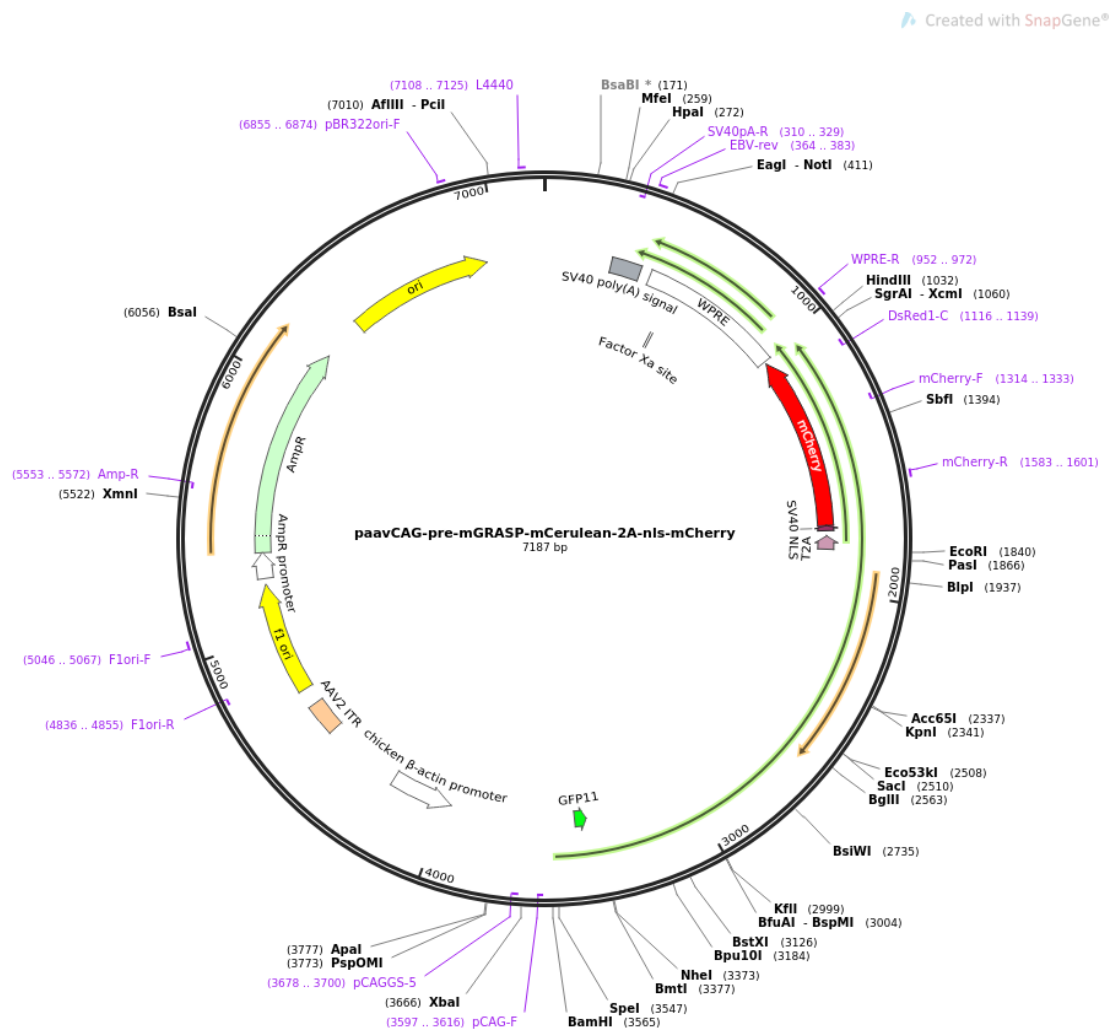
1.2 Purification and collection of the viral vector:

Prepare the precipitation solution (p.s) and the pellet re-suspension buffer (p.rs.b).

MIXTURE	INGREDIENTS	METHOD
Precipitation solution	400gr PEG-8000	Add PEG-8000 and NaCl to 400ml γ-H$_2$O and agitate until they dissolve. Add γ-H$_2$O up to 1L and let it to the magnetic agitator for 2hours.
	146.10gr NaCl	
	γ-H$_2$O up to 1L	
Pellet re-suspension buffer	14.6gr NaCl	Add NaCl to 400ml filtered γ-H$_2$O, agitate until it dissolves. Add γ-H$_2$O up to 1L.
	γ-H$_2$O filtered up to 1L	

Collect the media from the culture plates and repeat pipetting several times to remove all the cells. Wash sequentially all the culture plates with 10ml p.rs.b and transfer it along with the media to four 50ml falcons. Centrifuge at 3500rpm for 5'-minutes at 4^{0}C and collect the supernatant to the vessel from the previous steps.

Pellet: Re-suspend the pellet with 40ml of p.rs.b., vortex for 30''-seconds, freeze it in dry ice for 15'-minutes and thaw it in water-bath at 37^{0}C for 5'-minutes. Repeat the freeze thaw procedure three times to lyse the cells in order to release the intracellular viral vectors. Centrifuge at 4000rpm for 15'-minutes at 4^{0}C. Collect the supernatant and transfer it to four 50ml falcons, add to each falcon 10ml p.s and finally p.rs.b. up to 50ml. Place the falcons in ice for 3-hours.

*Supernatan*t: Filter the supernatant from the vessel with a 0.22μm filter and transfer it to eight 50ml falcons. Add to each falcon 10ml p.s and finally p.rs.b up to 50ml. Place the falcons in ice for 3-hours.

Collect all falcons from ice and centrifuge at 3500rpm for 40'-minutes at 4^0C. Discard supernatant, re-suspend the pellets sequentially with 10ml p.rs.b., for all twelve falcons , and transfer it to two 50ml falcons (5ml to each falcon). To each falcon add 4µl benzonase, 0.5µl RNAse, and 100µl protease inhibitors 50x. Place the falcons in water-bath at 37^0C for 1-hour. After gentle pipetting transfer the content to eight 50ml falcons, add 10ml p.s and finally p.rs.b. up to 50ml. Place the falcons in ice over-night.

Centrifuge at 3500rpm for 40'-minutes at 4^0C, discard the supernatant and re-suspend the pellet with 3.5ml p.rs.b. per falcon. Transfer to sixteen 2ml tubes and centrifuge at 13.000rpm for 10-15'-minutes at 4^0C. Transfer the supernatant to the ultra-centrifuge tubes, mark the side of the tube where the viral pellet will form, place the tubes inside the rotor and centrifuge at 50000rpm for 3-hours at 4^0C. Discard supernatant and re-suspend the pellet sequentially with 200µl p.rs.b for all the tubes. Collect at a 1.5ml tube, vortex gently and store at -20^0C.

1.3 Real-time PCR

Prepare the standard viral vector solutions

	pAAV mRuby2 vg/µl	γ-H_2O µl	pAAV mRuby2 vg/µl final
1	10µl of $2x10^8$	90	$2x10^7$
2	50µl of $2x10^7$	50	$1x10^7$
3	50µl of $1x10^7$	50	$0.5x10^7$
4	50µl of $0.5x10^7$	50	$0.25x10^7$
5	50µl of $0.25x10^7$	50	$0.125x10^7$
6	50µl of $0.125x10^7$	50	$0.0625x10^7$
7	50µl of $0.0625x10^7$	50	$0.03125x10^7$
8	50µl of $0.03125x10^7$	50	$0.015625x10^7$

Prepare the dilutions of the recombinant AAV viral vector to be tested

Dilution	
200x	3µl of the viral vector solution 597µl γ-H$_2$O
2.000x	10µl of the 200x viral vector solution 90µl γ-H$_2$O
20.000x	10µl of the 2.000x viral vector solution 90µl γ-H$_2$O
200.000x	10µl of the 20.000xviral vector solution 90µl γ-H$_2$O

Prepare Master-mix for 36 wells

	µl per well
γ-H$_2$O	5.6µl
Dream Taq. Buffer	2µl
dNTPs	0.4µl
SYBR green	0.9µl
Primers 5pm/µl 964-965	1µl
Taq polymerase	0.1µl

Transfer 10µl of each sample, standard or test, to three wells and add 10µl of the Master-mix to each well. Run qPCR. Based on standard samples create the standard curve and calculate the tested viral vector concentration.

1.4 Cell culture infection with the recombinant AAV viral vector

Upon removing the growth medium from the 60mm culture plate, where the cells are approximately 80% confluent, add 1.4ml pre-warmed trypsin

and incubate for 5'-minutes. After gentle pipetting, collect the cells in 1.5ml tubes and centrifuge them for 30 seconds. Discard the supernatant and re-suspend the cells with 400µl of the proper pre-warmed growth medium. For CAD cells use 2%FBS in DMEM/F12, for SH-SY5Y use 15%FBS in DMEM/F12, for Sk-N-SH cells use 10%FBS in DMEM. In a 15ml falcon add the growth medium (350µl per well for 48wells culture plate) and the differentiation medium.

 For CAD cells use forskolin:

 µl growth medium x 16µM forskolin/µM forskolin stock= µl forskolin total

For SH-SY5Y and Skin cells use retinoic acid (RA) in dark:

µl growth medium x 20µM R.A. /µM R.A. stock= µl R.A. total.

Vortex and add the re-suspended cells: 12µl cells per well for CAD cells, 8µl per well for SH-SY5Y, 10µl cells per well for Sk-N-SH cells. Upon gentle pipetting transfer the mixture to the wells and incubate for 24-hours. Add 2µl of the viral vectors per well, use one well for control and infect it with mRuby2 recombinant AAV virus, and incubate for 48-hours. Remove two-thirds of the media, add fresh growth medium and differentiation medium (calculate as described above), add 2µl of the viral vector per well and incubate for 48-72-hours. Repeat the procedure. Check the cells every day for signs of apoptosis. Up to the tenth day, at the control well approximately 80% of the cells should express the mRuby2 protein under fluorescent inverted microscope.

Prepare Master-mix. Calculate 100µl Master-mix per well. In tube add:

- protease inhibitors 50x: µl Master-mix/50 = µl protease inhibitors

- EDTA at final C=1.5mM: µl Master-mix x 1,5mM /mM stock = µl EDTA

- RIPA: add up to µl Master-mix

Remove media from the wells, add 100µl Master-mix per well, scrap the cell layer surface and collect the cells in tubes. Vortex for 10''-seconds, transfer the tubes in ice for 35'-minutes and repeat vortex every 5'minutes. Centrifuge at 13000rpm for 20'-minutes at 4°C.

 Transfer the loading dye 6x to clean tubes:

(100µl content per tube + µl loading dye 6x)/6 = µl loading dye 6x per tube.

Transfer the supernatant to the tubes containing the loading dye, vortex and store at -20°C.

1.5 Western blotting

Prepare the buffers

TBS 10x	24.2g Tris-base 87.8g NaCl add β-H$_2$O up to 1L	Agitate until they dissolve Adjust pH at 7.6
TBS-T	100ml TBS 10x 899ml β-H$_2$O 1ml Tween 20	Agitate well
Ponceau	0.5g Ponceau S 25ml acetic acid add β-H$_2$O up to 1L	Agitate well
Running buffer	144.0g glycine 10g SDS 30.3g Tris-base add β-H$_2$O up to 1L	Agitate well
Transfer buffer	14.4g glycine 3.03g Tris-base 200ml MetOH 800ml β-H$_2$O	Agitate well
Blocking buffer	5% nonfat dried milk in TBS-T	Agitate well

Prepare the gels

Resolving (running) gel (recipe for 12% , 7.5ml)	2.5 ml β-H_2O 3ml acrylamide 30% 1.9ml Tris 1.5M pH 8.8 75μl SDS 10% 75μl APS 10% 3μl TEMED	Add everything in a 50ml falcon except of the APS and the TMED that will be added just before pouring due to quick polymerization. Vortex.
Stack gel (recipe for 3ml)	2.1ml β-H_2O 0.5ml acrylamide 30% 0.38ml Tris 1M pH 6.8 30μl SDS 10% 30μl APS 10% 3μl TEMED	Add everything in a 50ml falcon except of the APS and the TMED that will be added just before pouring due to quick polymerization. Vortex

Pour the resolving gel between the glass plates of the rack for gel solidification, add 2-3ml isopropanol on top and let it solidify for 20'-minutes. Remove isopropanol and wash with γ-H_2O. Pour the stack gel and immerse a comb to form sample loading wells on stacking gel. Let it solidify for 10'-minutes. Adjust the heatblock surface at 110°C and insert the samples for 5'-minutes. Under tap water wash the glass plates with the gel and insert them to the electrophoretic apparatus. Place the electrophoretic apparatus into ice to maintain 4°C. Pour the running buffer inside the electrophoretic apparatus so as to completely cover the gel. Remove the comb carefully and rinse the inside of the wells with running buffer. Load 2.5μl of the ladder-marker and 17μl of each sample to the wells and connect the electrophoretic apparatus to the power supply. Apply 135Volt until the ladder runs and then apply 155Volt for 75'-minutes. Cut 4 Watman filter paper sheets to fit the measurement of the

gel, two sponges and one nitrocellulose membrane at the same dimensions; immerse them into transfer buffer. Take out of the electrophoretic apparatus the glass plates and separate them, retrieve the gel. Create a transfer sandwich by placing in the following order one sponge, two Watman filter paper sheets, the nitrocellulose membrane, the gel, two Watman filter paper sheets, and a sponge one on top of the other. Insert the transfer sandwich in the transfer apparatus, place it into ice and connect to the power supply. Adjust the settings at 390mA and let it transfer for 90-120'-minutes. Retrieve the nitrocellulose membrane, wash it with α-H$_2$O, pour ponceau buffer and check for the protein bands; de-stain with several washes with α-H$_2$O. Transfer the nitrocellulose membrane to the blocking buffer for 1hour. Prepare the primary antibodies at a dilution of 1:2000 to 3% nonfat dried milk in TBS-T. Cut the nitrocellulose membrane so as each piece to correspond only in one protein band. Add the primary antibodies and incubate overnight at 4°C. Perform three 5'-minute washes with TBS-T and the secondary antibodies in 3% nonfat dried milk in TBS-T. Incubate for 1-hour followed by three 5'-minute washes with TBS-T. Prepare the enhanced chemiluminescence (ECL) mix and incubate for 5'-minutes in dark. Visualize the result in the dark room.

2. <u>Intracerebroventricular injection to neonates</u>

The technique and the coordinates apply both for neonatal mice and rats. Approximately fifteen hours after birth, collect the pups and transfer them to ice for 5'-minutes before injection to achieve cryo-anesthesia. Upon movement cessation, place the pup on the surgical surface and perform the recombinant AAV injection bilaterally using a Hamilton syringe with a 32-gauge needle. The injection site is located two-fifths of the distance along the line between the eye and the Lambda intersection of the scull. Hold the needle perpendicularly to the scull, insert approximately 3mm and gradually release 2μl of the viral vector with rhythm 0.1μl per 15''-seconds. Leave the needle in place for 4-5'-minutes before retracting it. Place the pups in a warming pad to regain normal color and movement and transfer them back to their cage.
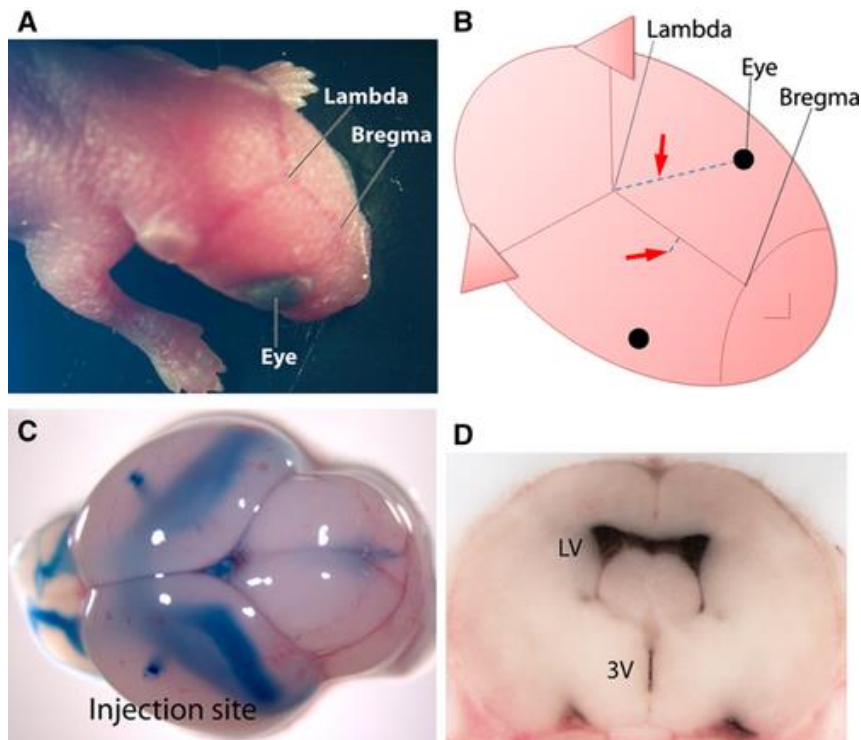
Figure IV. Injection site for intracerebroventricular injection to rodent pups and macroscopical view of whole brain tissue upon injection (Kim et al., 2013).

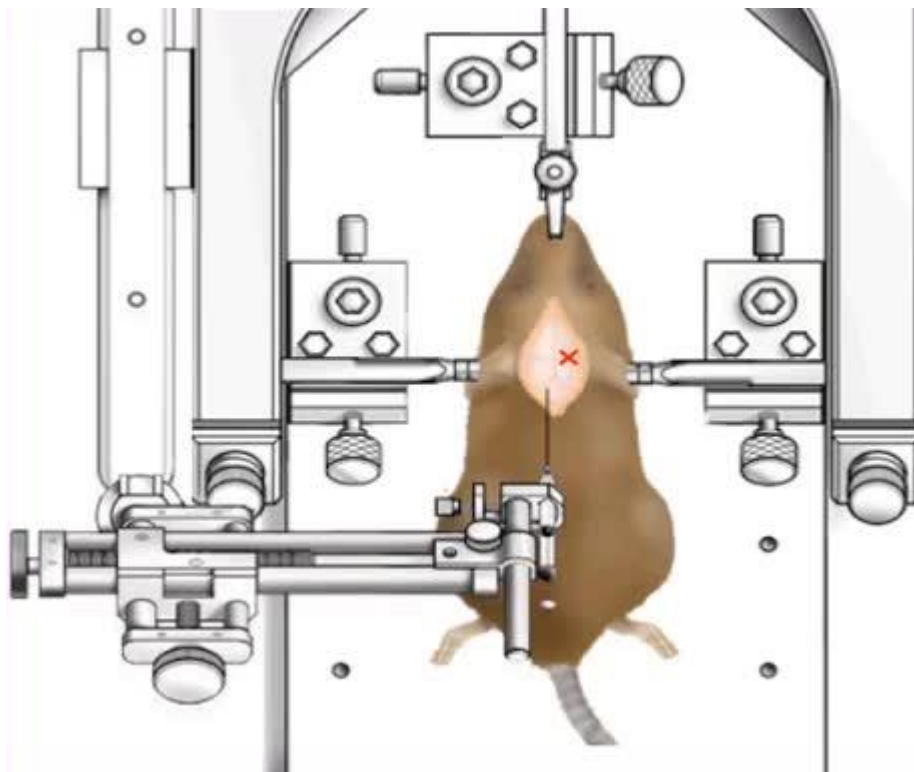### 3. Stereotactic injection to male 2-6months old Sprague-Dawley rats

Figure V. Stereotactic apparatus and rodents' position upon adjusting earbars and nosebar (jove science educational library)

Prepare the anesthesia mixture:

Ketamine (100mg/ml) / Xylazine (100mg/ml) 3:1

Adult male rats 2-6months old, with weight approximately 500gr, require 250-300µl for intraperitoneal injection of the anesthesia mixture. Upon injection, transfer the rat to the stereotactic apparatus and position the head in a way that the nose is inside the mask connected to isoflurane pump. Once the rat is no longer responsive to nociceptive stimuli, such pinching the toes, inject subcutaneously carpofen for analgesia and xylocaine as a local anesthetic for the scalp. Lead the ear bar inside the ear canal until the eye blink reflex appears and position the second ear bar to stabilize the head, screw the ear bars and the nosebar tightly. Apply lubricant eye ointment. Shave the fur of the skull and clean the skin with 70% ethanol. With a small blade scalpel make a midline incision and pull the skin aside to have a clear view of the Bregma and Lambda. With cotton swabs remove the periost and clean the skull with saline water and 3% hydrogen peroxide. Gently touch the skull with the injection capillary and measure Z coordinates for both the bregma and the lambda to ensure that the head is leveled at the rostral-caudal direction. If the Z coordinates are not corresponding, re-adjust the nosebar and repeat until the head is leveled. Find the exact center of the bregma and measure all the coordinates, this will be the zero point. Set the coordinates to target the area of choice; in our case for 2-6months old male Sprague-Dawley rat the coordinates for substantia nigra, based on Paxinos atlas, are: anteroposterior (AP): -5.0mm from bregma, mediolateral (ML): ±2.0mm from the midline, dorsoventral (DV): -7.2mm from dura mater. Using the AP and ML coordinates mark the exact spot where the hole will be drilled. Drill carefully with the handheld drill until you reach the dura matter, measure the Z coordinate and calculate the depth of the target area upon DV coordinates. Clear the hole from bone tissue and open the dura with a needle. Slowly insert the injection capillary up to the priorly calculated depth and inject the viral vectors solution at a rate of 0.1µl per 15''-seconds. Leave the injection capillary in place for 4'-minutes to prevent backflow. Retract the capillary slowly and repeat for the other hemisphere. Stich the scalp and place the rat in a clean cage on a heating

plate until it wakes up. Monitor the rat for a few days and if necessary apply analgesia.

4. Perfusion/fixation

Prepare the anesthesia mixture:

Ketamine (100mg/ml) / Xylazine (100mg/ml) 3:1

Adult rats weighting approximately 500gr require 500-600µl for intraperitoneal injection of the anesthesia mixture. Once the rat has reached a surgical plane of anesthesia and does not respond to nociceptive stimuli place it to the surgical surface. Make a 5-6cm lateral incision through the abdominal wall beneath the rib cage and carefully cut the diaphragm along the entire length of the rib cage to expose the pleural cavity. Using blunt scissors make a cut through the rib cage up to the collarbone in both sides. Lifting the sternum away cut any tissue connecting it to the heart. Use a hemostat to clump the heart and insert the needle connected to the perfusion pump to the left ventricle of the heart. Make an incision to the right atrium to create a large outlet. Open the valve of the pump and let the PBS perfusion buffer flow until it runs clear, mark the total quantity required. Observe the liver for discoloration as an indication of successful perfusion. Switch the PBS with 4% para-formaldehyde and note the fixation tremors to the limbs and tail of the rat, let the para-formaldehyde flow until corresponding quantity with the PBS has passed through the rat. Close the valve of the pump. The rat should be stiff at this stage.

5. Dissection-brain harvesting

Using scissors separate the head and make a midline incision with a scalpel to expose the skull. Remove any remaining muscles from the base of the skull. Insert the sharp end of a pair of scissors into the foramen magnum and slide along the inner surface of the skull. Make careful cuts to both ends of the incision and remove the skull from the cerebellum. Slide the scissors along the inner surface of the skull from the posterior edge of the skull to the anterior edge following the midline. Use the rongeurs to peel away the skull from the brain and trim the sides of the skull as well. Carefully cut the dura matter from the brain and gently tease

the brain away from its cavity using a spatula to sever the nervous connections and the olfactory bulb.

6. Snap-freezing protocol

After harvesting the brain transfer it to a 50ml falcon with approximately 30-40ml of 4% para-formaldehyde and leave overnight at 4°C. Remove the para-formaldehyde from the tissue with PBS and transfer the brain to 30-40ml of 15%sucrose solution overnight at 4°C. Replace the 15%sucrose solution with 30%sucroze solution and leave the brain until it sinks, approximately 48-hours, at 4°C. Fill a 50ml beaker with 40ml of 2-methyl-butane and place it deep in dry ice until it reaches temperature of -55°C. Instantly wash the brain with PBS to remove sucrose solution, dry it with a towel and place it into the 2-methyl-butane for 30''-seconds. Harvest the frozen tissue and store it to -80°C.

7. Cryo-sectioning

Once in cryostat, apply a thick layer of tissue tek O.C.T. on the tissue shelf and place the brain vertically until it freezes. Apply O.C.T. again and wait a few minutes to freeze. Repeat several times until the brain tissue is well stabilized and transfer the tissue shelf to the rotary microtome. Adjust the settings to 35µm thickness for sectioning and 50µm thickness for trimming. Start trimming, if necessary adjust the tissue so as to ensure that the sections are appropriate. Upon reaching the target area, switch from trimming to sectioning and collect the sections.
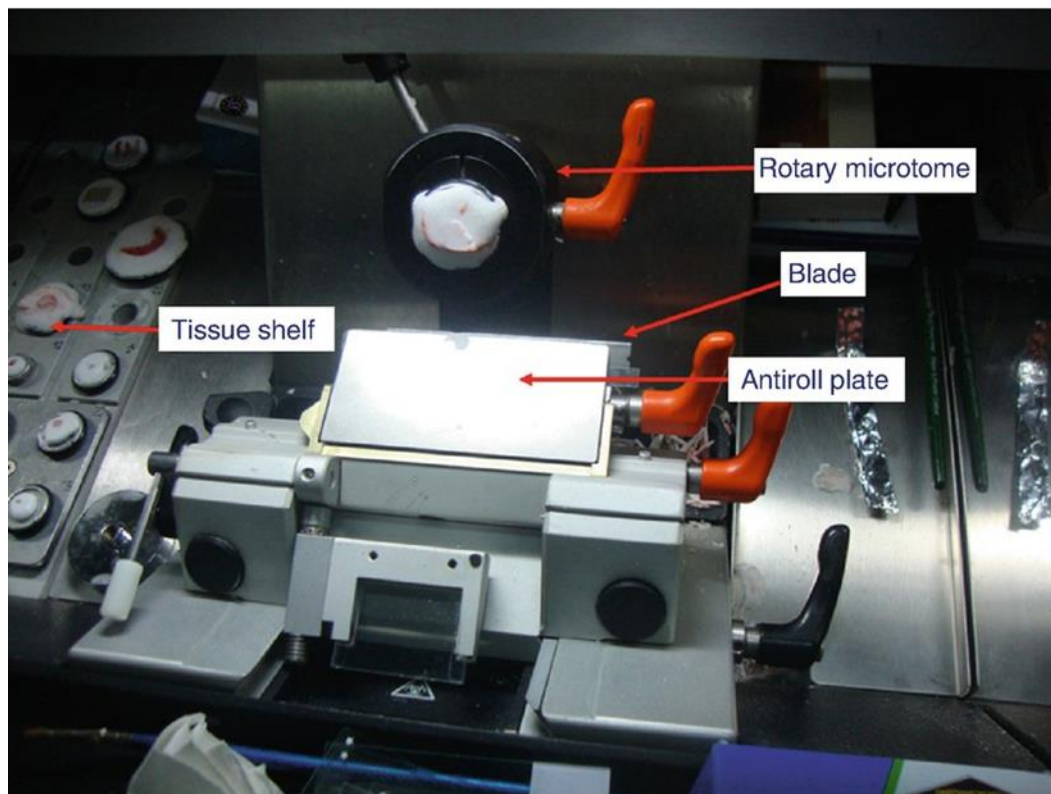
Figure VI. Cryostat parts. Image modified from (Dey, 2018)

To locate the Substantia nigra pars compacta region of the brain when taking coronal sections, observe the regions under the cerebral cortex for the hippocampal formation.
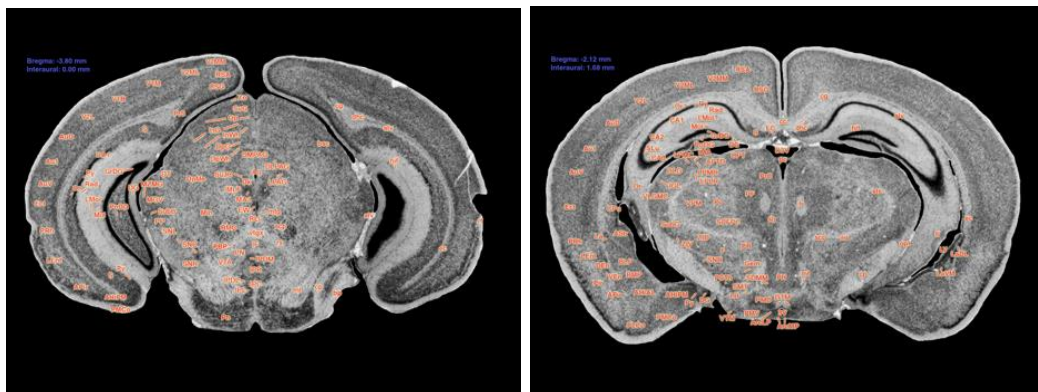
Figure VII. Enlarged macroscopic view of mouse brain coronal sections upon entering (left section) or exiting (right section) the substantia nigra pars compacta. Images from the mouse brain library. Same principles apply for rat brain.

When hippocampus is visible on the sides of the midbrain start collecting sections until the hippocampus is limited on the upper side of the sections.

Sink the sections into antifreeze solution and store them at -20°C.

For the antifreeze solution:

Prepare the 2xPO$_4$ 0.244M buffer :

- γ-H$_2$O   100ml
- NaOH   7.7g
- NaH$_2$PO$_4$ 29.28g

Agitate until NaOH and NaH$_2$PO$_4$ are dissolved.

Prepare the antifreeze solution

Ethylen-glycol	300ml	Mix the liquids and agitate well. Place to the magnetic agitator for 1hour. Store at 4°C.
Glycerol	300ml	
γ-H$_2$O	300ml	
2xPO$_4$ 0.244M buffer	100ml	

8. Immunofluorescence staining protocol

Prepare the PBS buffer, blocking buffer and citric acid solution

PBS 10x	80g NaCl 2.0g KCl 14.4g Na$_2$HPO$_4$ 2.4g KH$_2$PO$_4$ add β-H$_2$O up to 1L	Agitate well until they dissolve and adjust pH=7.4
PBS 1x	100ml PBS 10x 900ml γ-H$_2$O	Agitate well
Blocking buffer	5% BSA 0.1% Triton-x In PBS 1x	Agitate well and vortex
Citric acid 10Mm pH 6	0.294g Citric acid 100ml γ-H$_2$O	Agitate well Adjust pH=6

Place the sections in wells of a 24-well plate. Perform three 5'-minute washes with PBS. Transfer the section to the citric acid solution and place the plate into waterbath at 80°C for 45'-minutes. Let it at room temperature for 20'-minutes. Perform three 5'-minute washes with PBS and transfer the sections to the blocking buffer. Incubate for 1-hour with constant stirring. Prepare the primary antibodies in 2.5%BSA-0.1% Triton-X in PBS. Incubate the sections with the primary antibodies for 48-hours at 4°C with constant stirring.

Primary antibodies, dilutions

anti-TH Millipore AB152 (rabbit)	1:2000
anti-TIA Proteintech 12133-2-AP (rabbit)	1:100
anti-synuclein BD 610787 (mouse)	1:1000
anti-synuclein MJF Abcam ab138501 (rabbit)	1:100
anti-synuclein filamentous MJF Abcam ab209538 (rabbit host)	1:100
anti-GFAP Proteintech 16825-1-AP (rabbit)	1:100
anti-Iba1 Proteintech 10904-1-AP (rabbit)	1:100

Rinse with PBS three times for 5'-minutes. Prepare the secondary antibodies in 2.5%BSA/0.1%Triton-X in PBS. Incubate the sections with the secondary antibodies for 1-hour at room temperature with constant stirring.

Secondary antibodies dilutions

Donkey anti-Rabbit (DaR) Alexa fluor 488	1:1000
Donkey anti-Mouse (DaM) Alexa fluor 488	1:1000
DAPI	1:1000

Perform three 5'minute washes with PBS and proceed to mounting on the slides. Put the sections on slides that bind tissue electrostatically (superfrost plus). Let the sections dry, apply one drop of pre-warmed Mowiol mounting medium and attach the coverslip.

Mowiol mounting medium:

- Mix 2.4g mowiol powder with 6g glycerol and agitate until homogenization.
- Add γ-H_2O up to 6ml. Stir overnight.
- Add 12ml TrisHCl pH=8.5 and DABCO powder to reach final DABCO concentration 2.5%. Agitate well and store at -20°C.

9. Immunohistochemistry staining protocol

Prepare the buffers

Quenching buffer	3%H_2O_2 10%MetOH in PBS
Blocking buffer	5%BSA in PBS
Primary antibodies buffer	2.5%BSA in PBS anti-TH 1:2000
Biotin anti-rabbit buffer solution	1.5%BSA in PBS biotin anti-rabbit 1:1500
NeutrAvidin-HRP 31001 buffer solution	2.5%BSA in PBS NeutrAvidin-HRP 1:1000
Stock DAB solution	500mg 3,3'-diaminobenzidine-tetrahydrochloride (DAB) 100ml PBS
Working DAB solution	1ml stock DAB solution 9ml PBS 3.5µl 30% H_2O_2

Rinse the sections with PBS three times 5'-minutes each. Immerse the sections in the quenching buffer for 10'-minutes in dark. Perform three 5'-minute washes with PBS and transfer the sections to the blocking buffer for 1-hour with constant stirring. Place the sections to the primary

antibodies buffer for 48-hours with constant stirring at 4°C. Perform three 5'-minute washes with PBS and transfer the sections to the biotin anti-rabbit buffer solution for 1hour with constant stirring at room temperature. Rinse three times with PBS 5'-minutes each. Transfer the sections to the NeutrAvidin-HRP buffer solution for 1-hour with constant stirring at room temperature. Perform three 5'-minute washes with PBS. Immerse the sections into the working DAB solution for 7'-10'-minutes in dark at room temperature. After the seventh minute check the staining and if necessary stop the reaction adding β-H$_2$O. Rinse the sections with PBS three times 5'-minutes each. Place the section on electrostatic slides and let them dry overnight.

Perform the Nissl staining protocol by immersing the slide sequentially to the following solutions:

- 95% EtOH for 5'-minutes
- 100% Chloroform for 15'-minutes
- 95% EtOH for 15''-seconds to wash the chloroform
- 95% EtOH for 2'-minutes
- 70% EtOH for 1.5'-minutes
- γ-H$_2$O for 2'-minutes
- pre-warmed 0.3%cresyl violet/0.3%acetic acid glacial in γ-H$_2$O for 3'-5'-minutes until good staining is achieved
- wash under tap water to remove excess cresyl violet solution
- γ-H$_2$O for 2'-minutes
- 95% EtOH for 5'-minutes
- 100% EtOH for 5'-minutes
- Xylene first wash for 5'-minutes
- Xylene second wash for 5'-minutes

Let the slide dry overnight and continue with mounting and attaching the coverslip.

V. Discussion

α-syn is a neuronal protein that is expressed in the brain and is considered to be an intrinsically disordered protein that can adopt different conformations depending on the external stimuli. Although its normal function has yet to be fully understood, the ability to interact with membranes and other proteins along with its preferential localization in presynaptic terminals indicate a role in synaptic function. α-syn interaction with nuclear and mitochondrial components along with its implication in vesicle trafficking, lipid metabolism, SNARE complex assembly, and the dopamine system, including dopamine biosynthesis, storage, neurotransmission, and clearance, represent major functions. α-syn pathology that includes aggregation and toxic α-syn fibrils accumulation has been identified as part of the underlying cause in a broad spectrum of neurodegenerative disorders collectively referred to as α-synucleinopathies. Research has shown that α-syn aggregation is mainly attributed to point mutations, post-translational modifications and environmental factors. With regard to post-translational modifications, it has been reported that RBPs play a key role via targeting α-syn 3'untranslated region of its mRNA (Marchese et al., 2017). Members of our lab have focused in the study of the RBP TIA1 as it has been established as a major factor in several neurodegenerative diseases including ALS, ALS/FTD, AD, FTD-tau, and distal myopathy. In a long line of *in vitro* experiments they have shown that over-expression of TIA1 led to higher levels of α-syn phosphorylation and aggregation. Upon these findings, it was essential to generate an animal model and all analytic techniques and protocols to determine if these findings could be replicated *in vivo*.

Effort has been undertaken in order to develop a rodent model via intracerebroventricular injection in neonates with AAV vectors encoding for α-syn, TIA1, and a non-reactive fluorescent control protein (either GFP or mRuby2). However, the diffusion of the viral vectors proved to be inefficient and the target area substantia nigra was not infected. The hippocampal area was partially infected and immunofluorescence protocols were applied. Upon observation under confocal microscope, we were able to detect some cells where over-expressed TIA1 and possibly over-expressed α-syn co-localized, whereas in the control group no signal from over-expressed α-syn was detected. These findings however, could

be considered non-specific and thus we proceeded with targeted delivery of the viral vectors. At this point we have not been able to understand or explain the failure of all neonatal experiments. We expected that not a huge portion of the injected viral vectors would reach midbrain, however, in our line of experiments, the injected AAV vectors were mainly distributed to the cortex and olfactory system. The only plausible explanation is that our intracerebroventricular injections were not performed precisely at the correct site thus resulting to the diffusion of the AAV vectors only to brain regions close to the skull.

Hence, we next generated a rat model where AAV vectors were delivered via stereotactic injections directly to the SN of adult rats. One hemisphere was injected with viral vectors encoding for α-syn and TIA1 whereas the other hemisphere was injected with viral vectors encoding for α-syn and mRuby2. Stereotactic injections directly to SNc were accurate and delivery of the viral vectors was successful. The excess expression of the non-toxic mRuby2 protein, which lead to massive cell death and fragmentation, is attributed to the high titer of the AAV vectors we used. This outcome was not expected as data from the neonate models did not provide such indications; on the contrary, all neonates' data indicated inadequate delivery of our viral vectors leading us to conclude that the titers might be lower than required.

Taking these observations into consideration, we realized that it is crucial to take a step back in order to determine the appropriate dilution of the AAV vectors for stereotactic injections. For this purpose, we have now planned stereotactic injections to three adult male rats with AAV vectors encoding for a fluorescent protein (either GFP or mRuby2) with a TH promoter in three different dilutions. We believe that a targeted promoter is preferable over the universal CAGGS promoter to channel expression in dopaminergic neurons alone. The euthanasia will take place four weeks post-surgery and brain sections will be observed under fluorescent microscope. We will finally choose the titer that shows high infectivity, low levels of cell fragmentation, and low levels of contamination to the other brain hemisphere. Eventually, we will adjust the titers of all the AAV vectors and repeat the procedure that was described in the adult rat model section.

VI. References

Abbas, Y. M., Pichlmair, A., Górna, M. W., Superti-Furga, G., & Nagar, B. (2013). Structural basis for viral 5'-PPP-RNA recognition by human IFIT proteins. *Nature*, *494*(7435), 60–64. https://doi.org/10.1038/nature11783

Ahn, B.-H., Rhim, H., Kim, S. Y., Sung, Y.-M., Lee, M.-Y., Choi, J.-Y., Wolozin, B., Chang, J.-S., Lee, Y. H., Kwon, T. K., Chung, K. C., Yoon, S.-H., Hahn, S. J., Kim, M.-S., Jo, Y.-H., & Min, D. S. (2002). alpha-Synuclein interacts with phospholipase D isozymes and inhibits pervanadate-induced phospholipase D activation in human embryonic kidney-293 cells. *The Journal of Biological Chemistry*, *277*(14), 12334–12342. https://doi.org/10.1074/jbc.M110414200

Anderson, E. N., Hirpa, D., Zheng, K. H., Banerjee, R., & Gunawardena, S. (2019). The Non-amyloidal Component Region of α-Synuclein Is Important for α-Synuclein Transport Within Axons. *Frontiers in Cellular Neuroscience*, *13*, 540. https://doi.org/10.3389/fncel.2019.00540

Andringa, G., Du, F., Chase, T. N., & Bennett, M. C. (2003). Mapping of rat brain using the Synuclein-1 monoclonal antibody reveals somatodendritic expression of alpha-synuclein in populations of neurons homologous to those vulnerable to Lewy body formation in human synucleopathies. *Journal of Neuropathology and Experimental Neurology*, *62*(10), 1060–1075. https://doi.org/10.1093/jnen/62.10.1060

Antzoulatos, E., Jakowec, M. W., Petzinger, G. M., & Wood, R. I. (2010). Sex differences in motor behavior in the MPTP mouse model of Parkinson's disease. *Pharmacology, Biochemistry, and Behavior*, *95*(4), 466–472. https://doi.org/10.1016/j.pbb.2010.03.009

Apicco, D. J., Ash, P. E. A., Maziuk, B., LeBlang, C., Medalla, M., Al Abdullatif, A., Ferragud, A., Botelho, E., Ballance, H. I., Dhawan, U., Boudeau, S., Cruz, A. L., Kashy, D., Wong, A., Goldberg, L. R., Yazdani, N., Zhang, C., Ung, C. Y., Tripodis, Y., … Wolozin, B. (2018). Reducing the RNA binding protein TIA1 protects against tau-mediated neurodegeneration in vivo. *Nature Neuroscience*, *21*(1), 72–80. https://doi.org/10.1038/s41593-017-0022-z

Arimoto-Matsuzaki, K., Saito, H., & Takekawa, M. (2016). TIA1 oxidation inhibits stress granule assembly and sensitizes cells to stress-induced

apoptosis. *Nature Communications*, *7*, 10252.
https://doi.org/10.1038/ncomms10252

Atias, M., Tevet, Y., Sun, J., Stavsky, A., Tal, S., Kahn, J., Roy, S., & Gitler, D. (2019). Synapsins regulate α-synuclein functions. *Proceedings of the National Academy of Sciences of the United States of America*, *116*(23), 11116–11118. https://doi.org/10.1073/pnas.1903054116

Aznarez, I., Barash, Y., Shai, O., He, D., Zielenski, J., Tsui, L.-C., Parkinson, J., Frey, B. J., Rommens, J. M., & Blencowe, B. J. (2008). A systematic analysis of intronic sequences downstream of 5' splice sites reveals a widespread role for U-rich motifs and TIA1/TIAL1 proteins in alternative splicing regulation. *Genome Research*, *18*(8), 1247–1258. https://doi.org/10.1101/gr.073155.107

Beck, A. R., Medley, Q. G., O'Brien, S., Anderson, P., & Streuli, M. (1996). Structure, tissue distribution and genomic organization of the murine RRM-type RNA binding proteins TIA-1 and TIAR. *Nucleic Acids Research*, *24*(19), 3829–3835. https://doi.org/10.1093/nar/24.19.3829

Beck, A. R., Miller, I. J., Anderson, P., & Streuli, M. (1998). RNA-binding protein TIAR is essential for primordial germ cell development. *Proceedings of the National Academy of Sciences of the United States of America*, *95*(5), 2331–2336. https://doi.org/10.1073/pnas.95.5.2331

Beitz, J. M. (2014). Parkinson's disease: a review. *Frontiers in Bioscience (Scholar Edition)*, *6*, 65–74. https://doi.org/10.2741/s415

Bendor, J. T., Logan, T. P., & Edwards, R. H. (2013). The function of α-synuclein. *Neuron*, *79*(6), 1044–1066. https://doi.org/10.1016/j.neuron.2013.09.004

Benskey, M. J., Perez, R. G., & Manfredsson, F. P. (2016). The contribution of alpha synuclein to neuronal survival and function - Implications for Parkinson's disease. *Journal of Neurochemistry*, *137*(3), 331–359. https://doi.org/10.1111/jnc.13570

Bernal-Conde, L. D., Ramos-Acevedo, R., Reyes-Hernández, M. A., Balbuena-Olvera, A. J., Morales-Moreno, I. D., Argüero-Sánchez, R., Schüle, B., & Guerra-Crespo, M. (2019). Alpha-Synuclein Physiology and Pathology: A Perspective on Cellular Structures and Organelles. *Frontiers in Neuroscience*, *13*, 1399. https://doi.org/10.3389/fnins.2019.01399

Betancourt, E., Wachtel, J., Michaelos, M., Haggerty, M., Conforti, J., &

Kritzer, M. F. (2017). The impact of biological sex and sex hormones on cognition in a rat model of early, pre-motor Parkinson's disease. *Neuroscience*, *345*, 297–314. https://doi.org/10.1016/j.neuroscience.2016.05.041

Brenz Verca, M. S., Bahi, A., Boyer, F., Wagner, G. C., & Dreyer, J.-L. (2003). Distribution of alpha- and gamma-synucleins in the adult rat brain and their modification by high-dose cocaine treatment. *The European Journal of Neuroscience*, *18*(7), 1923–1938. https://doi.org/10.1046/j.1460-9568.2003.02913.x

Breydo, L., Wu, J. W., & Uversky, V. N. (2012). A-synuclein misfolding and Parkinson's disease. *Biochimica et Biophysica Acta*, *1822*(2), 261–285. https://doi.org/10.1016/j.bbadis.2011.10.002

Brinegar, A. E., & Cooper, T. A. (2016). Roles for RNA-binding proteins in development and disease. *Brain Research*, *1647*, 1–8. https://doi.org/10.1016/j.brainres.2016.02.050

Burré, J. (2015). The Synaptic Function of α-Synuclein. *Journal of Parkinson's Disease*, *5*(4), 699–713. https://doi.org/10.3233/JPD-150642

Burré, J., Sharma, M., Tsetsenis, T., Buchman, V., Etherton, M. R., & Südhof, T. C. (2010). Alpha-synuclein promotes SNARE-complex assembly in vivo and in vitro. *Science (New York, N.Y.)*, *329*(5999), 1663–1667. https://doi.org/10.1126/science.1195227

Burré, J., Vivona, S., Diao, J., Sharma, M., Brunger, A. T., & Südhof, T. C. (2013). Properties of native brain α-synuclein. *Nature*, *498*(7453), E4-6; discussion E6-7. https://doi.org/10.1038/nature12125

Butler, B., Sambo, D., & Khoshbouei, H. (2017). Alpha-synuclein modulates dopamine neurotransmission. *Journal of Chemical Neuroanatomy*, *83–84*, 41–49. https://doi.org/10.1016/j.jchemneu.2016.06.001

Carrascoso, I., Alcalde, J., Sánchez-Jiménez, C., González-Sánchez, P., & Izquierdo, J. M. (2017). T-Cell Intracellular Antigens and Hu Antigen R Antagonistically Modulate Mitochondrial Activity and Dynamics by Regulating Optic Atrophy 1 Gene Expression. *Molecular and Cellular Biology*, *37*(17). https://doi.org/10.1128/MCB.00174-17

Colla, E. (2019). Linking the Endoplasmic Reticulum to Parkinson's Disease and Alpha-Synucleinopathy. *Frontiers in Neuroscience*, *13*, 560. https://doi.org/10.3389/fnins.2019.00560

Creed, R. B., & Goldberg, M. S. (2018). New Developments in Genetic rat models of Parkinson's Disease. *Movement Disorders : Official Journal of the Movement Disorder Society*, *33*(5), 717–729. https://doi.org/10.1002/mds.27296

Curinha, A., Oliveira Braz, S., Pereira-Castro, I., Cruz, A., & Moreira, A. (2014). Implications of polyadenylation in health and disease. *Nucleus (Austin, Tex.)*, *5*(6), 508–519. https://doi.org/10.4161/nucl.36360

Dassi, E. (2017). Handshakes and Fights: The Regulatory Interplay of RNA-Binding Proteins. *Frontiers in Molecular Biosciences*, *4*, 67. https://doi.org/10.3389/fmolb.2017.00067

Dayton, R. D., Grames, M. S., & Klein, R. L. (2018). More expansive gene transfer to the rat CNS: AAV PHP.EB vector dose-response and comparison to AAV PHP.B. *Gene Therapy*, *25*(5), 392–400. https://doi.org/10.1038/s41434-018-0028-5

Dedmon, M. M., Lindorff-Larsen, K., Christodoulou, J., Vendruscolo, M., & Dobson, C. M. (2005). Mapping long-range interactions in alpha-synuclein using spin-label NMR and ensemble molecular dynamics simulations. *Journal of the American Chemical Society*, *127*(2), 476–477. https://doi.org/10.1021/ja044834j

Desplats, P., Spencer, B., Coffee, E., Patel, P., Michael, S., Patrick, C., Adame, A., Rockenstein, E., & Masliah, E. (2011). Alpha-synuclein sequesters Dnmt1 from the nucleus: a novel mechanism for epigenetic alterations in Lewy body diseases. *The Journal of Biological Chemistry*, *286*(11), 9031–9037. https://doi.org/10.1074/jbc.C110.212589

Dey, P. (2018). Frozen Section: Principle and Procedure. In *Basic and Advanced Laboratory Techniques in Histopathology and Cytology* (pp. 51–55). Springer Singapore. https://doi.org/10.1007/978-981-10-8252-8_6

Diao, J., Burré, J., Vivona, S., Cipriano, D. J., Sharma, M., Kyoung, M., Südhof, T. C., & Brunger, A. T. (2013). Native α-synuclein induces clustering of synaptic-vesicle mimics via binding to phospholipids and synaptobrevin-2/VAMP2. *ELife*, *2*, e00592. https://doi.org/10.7554/eLife.00592

Dixon, D. A., Balch, G. C., Kedersha, N., Anderson, P., Zimmerman, G. A., Beauchamp, R. D., & Prescott, S. M. (2003). Regulation of cyclooxygenase-2 expression by the translational silencer TIA-1. *The Journal of Experimental Medicine*, *198*(3), 475–481.

https://doi.org/10.1084/jem.20030616

Doxakis, E. (2014). RNA binding proteins: a common denominator of neuronal function and dysfunction. *Neuroscience Bulletin*, *30*(4), 610–626. https://doi.org/10.1007/s12264-014-1443-7

Fecchio, C., Palazzi, L., & de Laureto, P. P. (2018). α-Synuclein and Polyunsaturated Fatty Acids: Molecular Basis of the Interaction and Implication in Neurodegeneration. *Molecules (Basel, Switzerland)*, *23*(7). https://doi.org/10.3390/molecules23071531

Ferreon, A. C. M., Gambin, Y., Lemke, E. A., & Deniz, A. A. (2009). Interplay of alpha-synuclein binding and conformational switching probed by single-molecule fluorescence. *Proceedings of the National Academy of Sciences of the United States of America*, *106*(14), 5645–5650. https://doi.org/10.1073/pnas.0809232106

Förch, P., & Valcárcel, J. (2001). Molecular mechanisms of gene expression regulation by the apoptosis-promoting protein TIA-1. *Apoptosis : An International Journal on Programmed Cell Death*, *6*(6), 463–468. https://doi.org/10.1023/a:1012441824719

Fusco, G., De Simone, A., Gopinath, T., Vostrikov, V., Vendruscolo, M., Dobson, C. M., & Veglia, G. (2014). Direct observation of the three regions in α-synuclein that determine its membrane-bound behaviour. *Nature Communications*, *5*, 3827. https://doi.org/10.1038/ncomms4827

Gaugler, M. N., Genc, O., Bobela, W., Mohanna, S., Ardah, M. T., El-Agnaf, O. M., Cantoni, M., Bensadoun, J.-C., Schneggenburger, R., Knott, G. W., Aebischer, P., & Schneider, B. L. (2012). Nigrostriatal overabundance of α-synuclein leads to decreased vesicle density and deficits in dopamine release that correlate with reduced motor activity. *Acta Neuropathologica*, *123*(5), 653–669. https://doi.org/10.1007/s00401-012-0963-y

Gholizadeh, S., Tharmalingam, S., Macaldaz, M. E., & Hampson, D. R. (2013). Transduction of the central nervous system after intracerebroventricular injection of adeno-associated viral vectors in neonatal and juvenile mice. *Human Gene Therapy Methods*, *24*(4), 205–213. https://doi.org/10.1089/hgtb.2013.076

Gilks, N., Kedersha, N., Ayodele, M., Shen, L., Stoecklin, G., Dember, L. M., & Anderson, P. (2004). Stress granule assembly is mediated by prion-like aggregation of TIA-1. *Molecular Biology of the Cell*, *15*(12), 5383–5398. https://doi.org/10.1091/mbc.e04-08-0715

Goedert, M., Jakes, R., & Spillantini, M. G. (2017). The Synucleinopathies: Twenty Years On. *Journal of Parkinson's Disease*, *7*(s1), S51–S69. https://doi.org/10.3233/JPD-179005

Goers, J., Manning-Bog, A. B., McCormack, A. L., Millett, I. S., Doniach, S., Di Monte, D. A., Uversky, V. N., & Fink, A. L. (2003). Nuclear localization of alpha-synuclein and its interaction with histones. *Biochemistry*, *42*(28), 8465–8471. https://doi.org/10.1021/bi0341152

Gorbatyuk, O. S., Li, S., Nguyen, F. N., Manfredsson, F. P., Kondrikova, G., Sullivan, L. F., Meyers, C., Chen, W., Mandel, R. J., & Muzyczka, N. (2010). α-Synuclein expression in rat substantia nigra suppresses phospholipase D2 toxicity and nigral neurodegeneration. *Molecular Therapy : The Journal of the American Society of Gene Therapy*, *18*(10), 1758–1768. https://doi.org/10.1038/mt.2010.137

Gould, N., Mor, D. E., Lightfoot, R., Malkus, K., Giasson, B., & Ischiropoulos, H. (2014). Evidence of native α-synuclein conformers in the human brain. *The Journal of Biological Chemistry*, *289*(11), 7929–7934. https://doi.org/10.1074/jbc.C113.538249

Grigull, J., Mnaimneh, S., Pootoolal, J., Robinson, M. D., & Hughes, T. R. (2004). Genome-wide analysis of mRNA stability using transcription inhibitors and microarrays reveals posttranscriptional control of ribosome biogenesis factors. *Molecular and Cellular Biology*, *24*(12), 5534–5547. https://doi.org/10.1128/MCB.24.12.5534-5547.2004

Gueydan, C., Droogmans, L., Chalon, P., Huez, G., Caput, D., & Kruys, V. (1999). Identification of TIAR as a protein binding to the translational regulatory AU-rich element of tumor necrosis factor alpha mRNA. *The Journal of Biological Chemistry*, *274*(4), 2322–2326. https://doi.org/10.1074/jbc.274.4.2322

Guo, J. T., Chen, A. Q., Kong, Q., Zhu, H., Ma, C. M., & Qin, C. (2008). Inhibition of vesicular monoamine transporter-2 activity in alpha-synuclein stably transfected SH-SY5Y cells. *Cellular and Molecular Neurobiology*, *28*(1), 35–47. https://doi.org/10.1007/s10571-007-9227-0

Guo, Y., Rosati, B., & Scarlata, S. (2012). α-Synuclein increases the cellular level of phospholipase Cβ1. *Cellular Signalling*, *24*(5), 1109–1114. https://doi.org/10.1016/j.cellsig.2012.01.007

Hackman, P., Sarparanta, J., Lehtinen, S., Vihola, A., Evilä, A., Jonson, P. H., Luque, H., Kere, J., Screen, M., Chinnery, P. F., Åhlberg, G., Edström, L., & Udd, B. (2013). Welander distal myopathy is caused by a mutation

in the RNA-binding protein TIA1. *Annals of Neurology*, *73*(4), 500–509. https://doi.org/10.1002/ana.23831

Hammond, S. L., Leek, A. N., Richman, E. H., & Tjalkens, R. B. (2017). Cellular selectivity of AAV serotypes for gene delivery in neurons and astrocytes by neonatal intracerebroventricular injection. *PloS One*, *12*(12), e0188830. https://doi.org/10.1371/journal.pone.0188830

Hasegawa, M., Fujiwara, H., Nonaka, T., Wakabayashi, K., Takahashi, H., Lee, V. M.-Y., Trojanowski, J. Q., Mann, D., & Iwatsubo, T. (2002). Phosphorylated alpha-synuclein is ubiquitinated in alpha-synucleinopathy lesions. *The Journal of Biological Chemistry*, *277*(50), 49071–49076. https://doi.org/10.1074/jbc.M208046200

He, Y., Yu, Z., & Chen, S. (2019). Alpha-Synuclein Nitration and Its Implications in Parkinson's Disease. *ACS Chemical Neuroscience*, *10*(2), 777–782. https://doi.org/10.1021/acschemneuro.8b00288

Hentze, M. W., Castello, A., Schwarzl, T., & Preiss, T. (2018). A brave new world of RNA-binding proteins. *Nature Reviews. Molecular Cell Biology*, *19*(5), 327–341. https://doi.org/10.1038/nrm.2017.130

Ibrahim, F., Nakaya, T., & Mourelatos, Z. (2012). RNA dysregulation in diseases of motor neurons. *Annual Review of Pathology*, *7*, 323–352. https://doi.org/10.1146/annurev-pathol-011110-130307

Inglis, K. J., Chereau, D., Brigham, E. F., Chiou, S.-S., Schöbel, S., Frigon, N. L., Yu, M., Caccavello, R. J., Nelson, S., Motter, R., Wright, S., Chian, D., Santiago, P., Soriano, F., Ramos, C., Powell, K., Goldstein, J. M., Babcock, M., Yednock, T., … Anderson, J. P. (2009). Polo-like kinase 2 (PLK2) phosphorylates alpha-synuclein at serine 129 in central nervous system. *The Journal of Biological Chemistry*, *284*(5), 2598–2602. https://doi.org/10.1074/jbc.C800206200

Izquierdo, J. M., & Valcárcel, J. (2007). Two isoforms of the T-cell intracellular antigen 1 (TIA-1) splicing factor display distinct splicing regulation activities. Control of TIA-1 isoform ratio by TIA-1-related protein. *The Journal of Biological Chemistry*, *282*(27), 19410–19417. https://doi.org/10.1074/jbc.M700688200

Jackson, K. L., Dayton, R. D., Deverman, B. E., & Klein, R. L. (2016). Better targeting, better efficiency for wide-scale neuronal transduction with the synapsin promoter and AAV-PHP.B. *Frontiers in Molecular Neuroscience*, *9*(NOV2016), 1–11. https://doi.org/10.3389/fnmol.2016.00116

Järvelin, A. I., Noerenberg, M., Davis, I., & Castello, A. (2016). The new (dis)order in RNA regulation. *Cell Communication and Signaling : CCS*, *14*, 9. https://doi.org/10.1186/s12964-016-0132-3

Jiang, K., Rocha, S., Westling, A., Kesarimangalam, S., Dorfman, K. D., Wittung-Stafshede, P., & Westerlund, F. (2018). Alpha-Synuclein Modulates the Physical Properties of DNA. *Chemistry (Weinheim an Der Bergstrasse, Germany)*, *24*(58), 15685–15690. https://doi.org/10.1002/chem.201803933

Johnstone, O., & Lasko, P. (2001). Translational regulation and RNA localization in Drosophila oocytes and embryos. *Annual Review of Genetics*, *35*, 365–406. https://doi.org/10.1146/annurev.genet.35.102401.090756

Kalia, L. V, Kalia, S. K., Chau, H., Lozano, A. M., Hyman, B. T., & McLean, P. J. (2011). Ubiquitinylation of α-synuclein by carboxyl terminus Hsp70-interacting protein (CHIP) is regulated by Bcl-2-associated athanogene 5 (BAG5). *PloS One*, *6*(2), e14695. https://doi.org/10.1371/journal.pone.0014695

Karalok, H. M., Aydin, E., Saglam, O., Torun, A., Guzeloglu-Kayisli, O., Lalioti, M. D., Kristiansson, H., Duke, C. M. P., Choe, G., Flannery, C., Kallen, C. B., & Seli, E. (2014). mRNA-binding protein TIA-1 reduces cytokine expression in human endometrial stromal cells and is down-regulated in ectopic endometrium. *The Journal of Clinical Endocrinology and Metabolism*, *99*(12), E2610-9. https://doi.org/10.1210/jc.2013-3488

Kawakami, A., Tian, Q., Duan, X., Streuli, M., Schlossman, S. F., & Anderson, P. (1992). Identification and functional characterization of a TIA-1-related nucleolysin. *Proceedings of the National Academy of Sciences of the United States of America*, *89*(18), 8681–8685. https://doi.org/10.1073/pnas.89.18.8681

Keene, J. D. (2007). RNA regulons: coordination of post-transcriptional events. *Nature Reviews. Genetics*, *8*(7), 533–543. https://doi.org/10.1038/nrg2111

Kharraz, Y., Salmand, P.-A., Camus, A., Auriol, J., Gueydan, C., Kruys, V., & Morello, D. (2010). Impaired embryonic development in mice overexpressing the RNA-binding protein TIAR. *PloS One*, *5*(6), e11352. https://doi.org/10.1371/journal.pone.0011352

Kim, J.-Y., Ash, R. T., Ceballos-Diaz, C., Levites, Y., Golde, T. E., Smirnakis, S. M., & Jankowsky, J. L. (2013). Viral transduction of the neonatal brain

delivers controllable genetic mosaicism for visualising and manipulating neuronal circuits in vivo. *The European Journal of Neuroscience*, *37*(8), 1203–1220. https://doi.org/10.1111/ejn.12126

Kontopoulos, E., Parvin, J. D., & Feany, M. B. (2006). Alpha-synuclein acts in the nucleus to inhibit histone acetylation and promote neurotoxicity. *Human Molecular Genetics*, *15*(20), 3012–3023. https://doi.org/10.1093/hmg/ddl243

Kramer, M. L., & Schulz-Schaeffer, W. J. (2007). Presynaptic alpha-synuclein aggregates, not Lewy bodies, cause neurodegeneration in dementia with Lewy bodies. *The Journal of Neuroscience : The Official Journal of the Society for Neuroscience*, *27*(6), 1405–1410. https://doi.org/10.1523/JNEUROSCI.4564-06.2007

Lal, A., Mazan-Mamczarz, K., Kawai, T., Yang, X., Martindale, J. L., & Gorospe, M. (2004). Concurrent versus individual binding of HuR and AUF1 to common labile target mRNAs. *The EMBO Journal*, *23*(15), 3092–3102. https://doi.org/10.1038/sj.emboj.7600305

Lee, J. T., Wheeler, T. C., Li, L., & Chin, L.-S. (2008). Ubiquitination of alpha-synuclein by Siah-1 promotes alpha-synuclein aggregation and apoptotic cell death. *Human Molecular Genetics*, *17*(6), 906–917. https://doi.org/10.1093/hmg/ddm363

Lee, M. H., & Schedl, T. (2001). Identification of in vivo mRNA targets of GLD-1, a maxi-KH motif containing protein required for C. elegans germ cell development. *Genes & Development*, *15*(18), 2408–2420. https://doi.org/10.1101/gad.915901

Levine, P. M., Galesic, A., Balana, A. T., Mahul-Mellier, A.-L., Navarro, M. X., De Leon, C. A., Lashuel, H. A., & Pratt, M. R. (2019). α-Synuclein O-GlcNAcylation alters aggregation and toxicity, revealing certain residues as potential inhibitors of Parkinson's disease. *Proceedings of the National Academy of Sciences of the United States of America*, *116*(5), 1511–1519. https://doi.org/10.1073/pnas.1808845116

Lewis, Y. E., Galesic, A., Levine, P. M., De Leon, C. A., Lamiri, N., Brennan, C. K., & Pratt, M. R. (2017). O-GlcNAcylation of α-Synuclein at Serine 87 Reduces Aggregation without Affecting Membrane Binding. *ACS Chemical Biology*, *12*(4), 1020–1027. https://doi.org/10.1021/acschembio.7b00113

Li, J.-Q., Tan, L., & Yu, J.-T. (2014). The role of the LRRK2 gene in Parkinsonism. *Molecular Neurodegeneration*, *9*, 47.

https://doi.org/10.1186/1750-1326-9-47

Lindström, V., Fagerqvist, T., Nordström, E., Eriksson, F., Lord, A., Tucker, S., Andersson, J., Johannesson, M., Schell, H., Kahle, P. J., Möller, C., Gellerfors, P., Bergström, J., Lannfelt, L., & Ingelsson, M. (2014). Immunotherapy targeting α-synuclein protofibrils reduced pathology in (Thy-1)-h[A30P] α-synuclein mice. *Neurobiology of Disease*, *69*, 134–143. https://doi.org/10.1016/j.nbd.2014.05.009

López de Silanes, I., Galbán, S., Martindale, J. L., Yang, X., Mazan-Mamczarz, K., Indig, F. E., Falco, G., Zhan, M., & Gorospe, M. (2005). Identification and functional outcome of mRNAs associated with RNA-binding protein TIA-1. *Molecular and Cellular Biology*, *25*(21), 9520–9531. https://doi.org/10.1128/MCB.25.21.9520-9531.2005

Ltic, S., Perovic, M., Mladenovic, A., Raicevic, N., Ruzdijic, S., Rakic, L., & Kanazir, S. (2004). Alpha-synuclein is expressed in different tissues during human fetal development. *Journal of Molecular Neuroscience : MN*, *22*(3), 199–204. https://doi.org/10.1385/jmn:22:3:199

Lucas, H. R., & Fernández, R. D. (2020). Navigating the dynamic landscape of alpha-synuclein morphology: a review of the physiologically relevant tetrameric conformation. *Neural Regeneration Research*, *15*(3), 407–415. https://doi.org/10.4103/1673-5374.265792

Ludtmann, M. H. R., Angelova, P. R., Horrocks, M. H., Choi, M. L., Rodrigues, M., Baev, A. Y., Berezhnov, A. V, Yao, Z., Little, D., Banushi, B., Al-Menhali, A. S., Ranasinghe, R. T., Whiten, D. R., Yapom, R., Dolt, K. S., Devine, M. J., Gissen, P., Kunath, T., Jaganjac, M., … Gandhi, S. (2018). α-synuclein oligomers interact with ATP synthase and open the permeability transition pore in Parkinson's disease. *Nature Communications*, *9*(1), 2293. https://doi.org/10.1038/s41467-018-04422-2

Ludtmann, M. H. R., Angelova, P. R., Ninkina, N. N., Gandhi, S., Buchman, V. L., & Abramov, A. Y. (2016). Monomeric Alpha-Synuclein Exerts a Physiological Role on Brain ATP Synthase. *The Journal of Neuroscience : The Official Journal of the Society for Neuroscience*, *36*(41), 10510–10521. https://doi.org/10.1523/JNEUROSCI.1659-16.2016

Mackenzie, I. R., Nicholson, A. M., Sarkar, M., Messing, J., Purice, M. D., Pottier, C., Annu, K., Baker, M., Perkerson, R. B., Kurti, A., Matchett, B. J., Mittag, T., Temirov, J., Hsiung, G.-Y. R., Krieger, C., Murray, M. E., Kato, M., Fryer, J. D., Petrucelli, L., … Rademakers, R. (2017). TIA1 Mutations in

Amyotrophic Lateral Sclerosis and Frontotemporal Dementia Promote Phase Separation and Alter Stress Granule Dynamics. *Neuron*, *95*(4), 808-816.e9. https://doi.org/10.1016/j.neuron.2017.07.025

Maguire, C. A., Crommentuijn, M. H., Mu, D., Hudry, E., Serrano-Pozo, A., Hyman, B. T., & Tannous, B. A. (2013). Mouse gender influences brain transduction by intravascularly administered AAV9. In *Molecular therapy : the journal of the American Society of Gene Therapy* (Vol. 21, Issue 8, pp. 1470–1471). https://doi.org/10.1038/mt.2013.95

Marchese, D., Botta-Orfila, T., Cirillo, D., Rodriguez, J. A., Livi, C. M., Fernández-Santiago, R., Ezquerra, M., Martí, M. J., Bechara, E., & Tartaglia, G. G. (2017). Discovering the 3' UTR-mediated regulation of alpha-synuclein. *Nucleic Acids Research*, *45*(22), 12888–12903. https://doi.org/10.1093/nar/gkx1048

Mazzulli, J. R., Zunke, F., Isacson, O., Studer, L., & Krainc, D. (2016). α-Synuclein-induced lysosomal dysfunction occurs through disruptions in protein trafficking in human midbrain synucleinopathy models. *Proceedings of the National Academy of Sciences of the United States of America*, *113*(7), 1931–1936. https://doi.org/10.1073/pnas.1520335113

McKeith, I. G., Boeve, B. F., Dickson, D. W., Halliday, G., Taylor, J.-P., Weintraub, D., Aarsland, D., Galvin, J., Attems, J., Ballard, C. G., Bayston, A., Beach, T. G., Blanc, F., Bohnen, N., Bonanni, L., Bras, J., Brundin, P., Burn, D., Chen-Plotkin, A., … Kosaka, K. (2017). Diagnosis and management of dementia with Lewy bodies: Fourth consensus report of the DLB Consortium. *Neurology*, *89*(1), 88–100. https://doi.org/10.1212/WNL.0000000000004058

Meade, R. M., Fairlie, D. P., & Mason, J. M. (2019). Alpha-synuclein structure and Parkinson's disease - lessons and emerging principles. *Molecular Neurodegeneration*, *14*(1), 29. https://doi.org/10.1186/s13024-019-0329-1

Melo, T. Q., Copray, S. J. C. V. M., & Ferrari, M. F. R. (2018). Alpha-Synuclein Toxicity on Protein Quality Control, Mitochondria and Endoplasmic Reticulum. *Neurochemical Research*, *43*(12), 2212–2223. https://doi.org/10.1007/s11064-018-2673-x

Menges, S., Minakaki, G., Schaefer, P. M., Meixner, H., Prots, I., Schlötzer-Schrehardt, U., Friedland, K., Winner, B., Outeiro, T. F., Winklhofer, K. F., von Arnim, C. A. F., Xiang, W., Winkler, J., & Klucken, J. (2017). Alpha-synuclein prevents the formation of spherical

mitochondria and apoptosis under oxidative stress. *Scientific Reports*, *7*, 42942. https://doi.org/10.1038/srep42942

Meyer, C., Garzia, A., Mazzola, M., Gerstberger, S., Molina, H., & Tuschl, T. (2018). The TIA1 RNA-Binding Protein Family Regulates EIF2AK2-Mediated Stress Response and Cell Cycle Progression. *Molecular Cell*, *69*(4), 622-635.e6. https://doi.org/10.1016/j.molcel.2018.01.011

Miller, I. N., & Cronin-Golomb, A. (2010). Gender differences in Parkinson's disease: clinical characteristics and cognition. *Movement Disorders : Official Journal of the Movement Disorder Society*, *25*(16), 2695–2703. https://doi.org/10.1002/mds.23388

Moisan, F., Kab, S., Mohamed, F., Canonico, M., Le Guern, M., Quintin, C., Carcaillon, L., Nicolau, J., Duport, N., Singh-Manoux, A., Boussac-Zarebska, M., & Elbaz, A. (2016). Parkinson disease male-to-female ratios increase with age: French nationwide study and meta-analysis. *Journal of Neurology, Neurosurgery, and Psychiatry*, *87*(9), 952–957. https://doi.org/10.1136/jnnp-2015-312283

Mor, D. E., Ugras, S. E., Daniels, M. J., & Ischiropoulos, H. (2016). Dynamic structural flexibility of α-synuclein. *Neurobiology of Disease*, *88*, 66–74. https://doi.org/10.1016/j.nbd.2015.12.018

Mukherjee, N., Corcoran, D. L., Nusbaum, J. D., Reid, D. W., Georgiev, S., Hafner, M., Ascano, M. J., Tuschl, T., Ohler, U., & Keene, J. D. (2011). Integrative regulatory mapping indicates that the RNA-binding protein HuR couples pre-mRNA processing and mRNA stability. *Molecular Cell*, *43*(3), 327–339. https://doi.org/10.1016/j.molcel.2011.06.007

Müller-McNicoll, M., Rossbach, O., Hui, J., & Medenbach, J. (2019). Auto-regulatory feedback by RNA-binding proteins. *Journal of Molecular Cell Biology*, *11*(10), 930–939. https://doi.org/10.1093/jmcb/mjz043

Mund, T., Masuda-Suzukake, M., Goedert, M., & Pelham, H. R. (2018). Ubiquitination of alpha-synuclein filaments by Nedd4 ligases. *PloS One*, *13*(7), e0200763. https://doi.org/10.1371/journal.pone.0200763

Muntané, G., Ferrer, I., & Martinez-Vicente, M. (2012). α-synuclein phosphorylation and truncation are normal events in the adult human brain. *Neuroscience*, *200*, 106–119. https://doi.org/10.1016/j.neuroscience.2011.10.042

Nemani, V. M., Lu, W., Berge, V., Nakamura, K., Onoa, B., Lee, M. K., Chaudhry, F. A., Nicoll, R. A., & Edwards, R. H. (2010). Increased

expression of alpha-synuclein reduces neurotransmitter release by inhibiting synaptic vesicle reclustering after endocytosis. *Neuron*, *65*(1), 66–79. https://doi.org/10.1016/j.neuron.2009.12.023

Niibori, Y., Lee, S. J., Minassian, B. A., & Hampson, D. R. (2020). Sexually Divergent Mortality and Partial Phenotypic Rescue After Gene Therapy in a Mouse Model of Dravet Syndrome. *Human Gene Therapy*, *31*(5–6), 339–351. https://doi.org/10.1089/hum.2019.225

Ninkina, N. N., Tarasova, T. V, Chaprov, K. D., Goloborshcheva, V. V, Bachurin, S. O., & Buchman, V. L. (2019). Synuclein Deficiency Decreases the Efficiency of Dopamine Uptake by Synaptic Vesicles. *Doklady. Biochemistry and Biophysics*, *486*(1), 168–170. https://doi.org/10.1134/S1607672919030025

Niu, Z., Pontifex, C. S., Berini, S., Hamilton, L. E., Naddaf, E., Wieben, E., Aleff, R. A., Martens, K., Gruber, A., Engel, A. G., Pfeffer, G., & Milone, M. (2018). Myopathy With SQSTM1 and TIA1 Variants: Clinical and Pathological Features. *Frontiers in Neurology*, *9*, 147. https://doi.org/10.3389/fneur.2018.00147

Nonaka, T., Iwatsubo, T., & Hasegawa, M. (2005). Ubiquitination of alpha-synuclein. *Biochemistry*, *44*(1), 361–368. https://doi.org/10.1021/bi0485528

Okochi, M., Walter, J., Koyama, A., Nakajo, S., Baba, M., Iwatsubo, T., Meijer, L., Kahle, P. J., & Haass, C. (2000). Constitutive phosphorylation of the Parkinson's disease associated alpha-synuclein. *The Journal of Biological Chemistry*, *275*(1), 390–397. https://doi.org/10.1074/jbc.275.1.390

Paiva, I., Jain, G., Lázaro, D. F., Jerčić, K. G., Hentrich, T., Kerimoglu, C., Pinho, R., Szegő, È. M., Burkhardt, S., Capece, V., Halder, R., Islam, R., Xylaki, M., Caldi Gomes, L. A., Roser, A.-E., Lingor, P., Schulze-Hentrich, J. M., Borovečki, F., Fischer, A., & Outeiro, T. F. (2018). Alpha-synuclein deregulates the expression of COL4A2 and impairs ER-Golgi function. *Neurobiology of Disease*, *119*, 121–135. https://doi.org/10.1016/j.nbd.2018.08.001

Payton, J. E., Perrin, R. J., Woods, W. S., & George, J. M. (2004). Structural determinants of PLD2 inhibition by alpha-synuclein. *Journal of Molecular Biology*, *337*(4), 1001–1009. https://doi.org/10.1016/j.jmb.2004.02.014

Peng, X., Tehranian, R., Dietrich, P., Stefanis, L., & Perez, R. G. (2005).

Alpha-synuclein activation of protein phosphatase 2A reduces tyrosine hydroxylase phosphorylation in dopaminergic cells. *Journal of Cell Science*, *118*(Pt 15), 3523–3530. https://doi.org/10.1242/jcs.02481

Perez, R. G., Waymire, J. C., Lin, E., Liu, J. J., Guo, F., & Zigmond, M. J. (2002). A role for alpha-synuclein in the regulation of dopamine biosynthesis. *The Journal of Neuroscience : The Official Journal of the Society for Neuroscience*, *22*(8), 3090–3099. https://doi.org/10.1523/JNEUROSCI.22-08-03090.2002

Piecyk, M., Wax, S., Beck, A. R., Kedersha, N., Gupta, M., Maritim, B., Chen, S., Gueydan, C., Kruys, V., Streuli, M., & Anderson, P. (2000). TIA-1 is a translational silencer that selectively regulates the expression of TNF-alpha. *The EMBO Journal*, *19*(15), 4154–4163. https://doi.org/10.1093/emboj/19.15.4154

Pinho, R., Paiva, I., Jercic, K. G., Fonseca-Ornelas, L., Gerhardt, E., Fahlbusch, C., Garcia-Esparcia, P., Kerimoglu, C., Pavlou, M. A. S., Villar-Piqué, A., Szego, É., Lopes da Fonseca, T., Odoardi, F., Soeroes, S., Rego, A. C., Fischle, W., Schwamborn, J. C., Meyer, T., Kügler, S., … Outeiro, T. F. (2019). Nuclear localization and phosphorylation modulate pathological effects of alpha-synuclein. *Human Molecular Genetics*, *28*(1), 31–50. https://doi.org/10.1093/hmg/ddy326

Pirc, K., & Ulrih, N. (2011). Alpha-Synuclein Interactions with Membranes. In *Etiology and Physiology of Parkinson's Disease*. https://doi.org/10.5772/16816

Pirc, K., & Ulrih, N. P. (2015). α-Synuclein interactions with phospholipid model membranes: Key roles for electrostatic interactions and lipid-bilayer structure. *Biochimica et Biophysica Acta*, *1848*(10 Pt A), 2002–2012. https://doi.org/10.1016/j.bbamem.2015.06.021

Pozo Devoto, V. M., & Falzone, T. L. (2017). Mitochondrial dynamics in Parkinson's disease: a role for α-synuclein? *Disease Models & Mechanisms*, *10*(9), 1075–1087. https://doi.org/10.1242/dmm.026294

Pronin, A. N., Morris, A. J., Surguchov, A., & Benovic, J. L. (2000). Synucleins are a novel class of substrates for G protein-coupled receptor kinases. *The Journal of Biological Chemistry*, *275*(34), 26515–26522. https://doi.org/10.1074/jbc.M003542200

Ramirez, E. P. C., & Vonsattel, J. P. G. (2014). Neuropathologic changes of multiple system atrophy and diffuse Lewy body disease. *Seminars in Neurology*, *34*(2), 210–216. https://doi.org/10.1055/s-0034-1381732

Rappley, I., Gitler, A. D., Selvy, P. E., LaVoie, M. J., Levy, B. D., Brown, H. A., Lindquist, S., & Selkoe, D. J. (2009). Evidence that alpha-synuclein does not inhibit phospholipase D. *Biochemistry*, *48*(5), 1077–1083. https://doi.org/10.1021/bi801871h

Ravanidis, S., Kattan, F.-G., & Doxakis, E. (2018). Unraveling the Pathways to Neuronal Homeostasis and Disease: Mechanistic Insights into the Role of RNA-Binding Proteins and Associated Factors. *International Journal of Molecular Sciences*, *19*(8). https://doi.org/10.3390/ijms19082280

Rayman, J. B., Hijazi, J., Li, X., Kedersha, N., Anderson, P. J., & Kandel, E. R. (2019). Genetic Perturbation of TIA1 Reveals a Physiological Role in Fear Memory. *Cell Reports*, *26*(11), 2970-2983.e4. https://doi.org/10.1016/j.celrep.2019.02.048

Rayman, J. B., Melas, P. A., Schalling, M., Forsell, Y., Kandel, E. R., & Lavebratt, C. (2020). Single-nucleotide polymorphism in the human TIA1 gene interacts with stressful life events to predict the development of pathological anxiety symptoms in a Swedish population. *Journal of Affective Disorders*, *260*, 597–603. https://doi.org/10.1016/j.jad.2019.09.018

Romanelli, M. G., Diani, E., & Lievens, P. M.-J. (2013). New insights into functional roles of the polypyrimidine tract-binding protein. *International Journal of Molecular Sciences*, *14*(11), 22906–22932. https://doi.org/10.3390/ijms141122906

Samuel, F., Flavin, W. P., Iqbal, S., Pacelli, C., Sri Renganathan, S. D., Trudeau, L.-E., Campbell, E. M., Fraser, P. E., & Tandon, A. (2016). Effects of Serine 129 Phosphorylation on α-Synuclein Aggregation, Membrane Association, and Internalization. *The Journal of Biological Chemistry*, *291*(9), 4374–4385. https://doi.org/10.1074/jbc.M115.705095

Sánchez-Jiménez, C., & Izquierdo, J. M. (2013). T-cell intracellular antigen (TIA)-proteins deficiency in murine embryonic fibroblasts alters cell cycle progression and induces autophagy. *PloS One*, *8*(9), e75127. https://doi.org/10.1371/journal.pone.0075127

Schulz-Schaeffer, W. J. (2010). The synaptic pathology of alpha-synuclein aggregation in dementia with Lewy bodies, Parkinson's disease and Parkinson's disease dementia. *Acta Neuropathologica*, *120*(2), 131–143. https://doi.org/10.1007/s00401-010-0711-0

Seo, J.-H., Rah, J.-C., Choi, S. H., Shin, J. K., Min, K., Kim, H.-S., Park, C. H.,

Kim, S., Kim, E.-M., Lee, S.-H., Lee, S., Suh, S. W., & Suh, Y.-H. (2002). Alpha-synuclein regulates neuronal survival via Bcl-2 family expression and PI3/Akt kinase pathway. *FASEB Journal : Official Publication of the Federation of American Societies for Experimental Biology*, *16*(13), 1826–1828. https://doi.org/10.1096/fj.02-0041fje

Sheng, J., & Wu, L.-G. (2012). Cysteine string protein α: a new role in vesicle recycling. *Neuron*, *74*(1), 6–8. https://doi.org/10.1016/j.neuron.2012.03.013

Shin, Y., Klucken, J., Patterson, C., Hyman, B. T., & McLean, P. J. (2005). The co-chaperone carboxyl terminus of Hsp70-interacting protein (CHIP) mediates alpha-synuclein degradation decisions between proteasomal and lysosomal pathways. *The Journal of Biological Chemistry*, *280*(25), 23727–23734. https://doi.org/10.1074/jbc.M503326200

Sorrentino, Z. A., & Giasson, B. I. (2020). The emerging role of α-synuclein truncation in aggregation and disease. *The Journal of Biological Chemistry*, *295*(30), 10224–10244. https://doi.org/10.1074/jbc.REV120.011743

Sorrentino, Z. A., Vijayaraghavan, N., Gorion, K.-M., Riffe, C. J., Strang, K. H., Caldwell, J., & Giasson, B. I. (2018). Physiological C-terminal truncation of α-synuclein potentiates the prion-like formation of pathological inclusions. *The Journal of Biological Chemistry*, *293*(49), 18914–18932. https://doi.org/10.1074/jbc.RA118.005603

Stefanis, L., Emmanouilidou, E., Pantazopoulou, M., Kirik, D., Vekrellis, K., & Tofaris, G. K. (2019). How is alpha-synuclein cleared from the cell? *Journal of Neurochemistry*, *150*(5), 577–590. https://doi.org/10.1111/jnc.14704

Südhof, T. C., & Rothman, J. E. (2009). Membrane fusion: grappling with SNARE and SM proteins. *Science (New York, N.Y.)*, *323*(5913), 474–477. https://doi.org/10.1126/science.1161748

Sun, J., Wang, L., Bao, H., Premi, S., Das, U., Chapman, E. R., & Roy, S. (2019). Functional cooperation of α-synuclein and VAMP2 in synaptic vesicle recycling. *Proceedings of the National Academy of Sciences of the United States of America*, *116*(23), 11113–11115. https://doi.org/10.1073/pnas.1903049116

Swant, J., Goodwin, J. S., North, A., Ali, A. A., Gamble-George, J., Chirwa, S., & Khoshbouei, H. (2011). α-Synuclein stimulates a dopamine transporter-dependent chloride current and modulates the activity of

the transporter. *The Journal of Biological Chemistry*, *286*(51), 43933–43943. https://doi.org/10.1074/jbc.M111.241232

Taguchi, K., Watanabe, Y., Tsujimura, A., & Tanaka, M. (2016). Brain region-dependent differential expression of alpha-synuclein. *The Journal of Comparative Neurology*, *524*(6), 1236–1258. https://doi.org/10.1002/cne.23901

Tak, H., Eun, J. W., Kim, J., Park, S. J., Kim, C., Ji, E., Lee, H., Kang, H., Cho, D.-H., Lee, K., Kim, W., Nam, S. W., & Lee, E. K. (2017). T-cell-restricted intracellular antigen 1 facilitates mitochondrial fragmentation by enhancing the expression of mitochondrial fission factor. *Cell Death and Differentiation*, *24*(1), 49–58. https://doi.org/10.1038/cdd.2016.90

Tian, Q., Streuli, M., Saito, H., Schlossman, S. F., & Anderson, P. (1991). A polyadenylate binding protein localized to the granules of cytolytic lymphocytes induces DNA fragmentation in target cells. *Cell*, *67*(3), 629–639. https://doi.org/10.1016/0092-8674(91)90536-8

Tofaris, G. K., Kim, H. T., Hourez, R., Jung, J.-W., Kim, K. P., & Goldberg, A. L. (2011). Ubiquitin ligase Nedd4 promotes alpha-synuclein degradation by the endosomal-lysosomal pathway. *Proceedings of the National Academy of Sciences of the United States of America*, *108*(41), 17004–17009. https://doi.org/10.1073/pnas.1109356108

Totterdell, S., Hanger, D., & Meredith, G. E. (2004). The ultrastructural distribution of alpha-synuclein-like protein in normal mouse brain. *Brain Research*, *1004*(1–2), 61–72. https://doi.org/10.1016/j.brainres.2003.10.072

Ulmer, T. S., Bax, A., Cole, N. B., & Nussbaum, R. L. (2005). Structure and dynamics of micelle-bound human alpha-synuclein. *The Journal of Biological Chemistry*, *280*(10), 9595–9603. https://doi.org/10.1074/jbc.M411805200

van der Wateren, I. M., Knowles, T. P. J., Buell, A. K., Dobson, C. M., & Galvagnion, C. (2018). C-terminal truncation of α-synuclein promotes amyloid fibril amplification at physiological pH. *Chemical Science*, *9*(25), 5506–5516. https://doi.org/10.1039/c8sc01109e

van Vliet, A. R., & Agostinis, P. (2018). Mitochondria-Associated Membranes and ER Stress. *Current Topics in Microbiology and Immunology*, *414*, 73–102. https://doi.org/10.1007/82_2017_2

Vanderweyde, T., Apicco, D. J., Youmans-Kidder, K., Ash, P. E. A., Cook,

C., Lummertz da Rocha, E., Jansen-West, K., Frame, A. A., Citro, A., Leszyk, J. D., Ivanov, P., Abisambra, J. F., Steffen, M., Li, H., Petrucelli, L., & Wolozin, B. (2016). Interaction of tau with the RNA-Binding Protein TIA1 Regulates tau Pathophysiology and Toxicity. *Cell Reports*, *15*(7), 1455–1466. https://doi.org/10.1016/j.celrep.2016.04.045

Vargas, J. Y., Grudina, C., & Zurzolo, C. (2019). The prion-like spreading of α-synuclein: From in vitro to in vivo models of Parkinson's disease. *Ageing Research Reviews*, *50*, 89–101. https://doi.org/10.1016/j.arr.2019.01.012

Villar-Piqué, A., Lopes da Fonseca, T., & Outeiro, T. F. (2016). Structure, function and toxicity of alpha-synuclein: the Bermuda triangle in synucleinopathies. *Journal of Neurochemistry*, *139 Suppl*, 240–255. https://doi.org/10.1111/jnc.13249

Walsh, D. M., Lomakin, A., Benedek, G. B., Condron, M. M., & Teplow, D. B. (1997). Amyloid beta-protein fibrillogenesis. Detection of a protofibrillar intermediate. *The Journal of Biological Chemistry*, *272*(35), 22364–22372. https://doi.org/10.1074/jbc.272.35.22364

Wang, L., Das, U., Scott, D. A., Tang, Y., McLean, P. J., & Roy, S. (2014). α-synuclein multimers cluster synaptic vesicles and attenuate recycling. *Current Biology : CB*, *24*(19), 2319–2326. https://doi.org/10.1016/j.cub.2014.08.027

Wang, Y., & Mandelkow, E. (2016). Tau in physiology and pathology. *Nature Reviews. Neuroscience*, *17*(1), 5–21. https://doi.org/10.1038/nrn.2015.1

Wani, W. Y., Chatham, J. C., Darley-Usmar, V., McMahon, L. L., & Zhang, J. (2017). O-GlcNAcylation and neurodegeneration. *Brain Research Bulletin*, *133*, 80–87. https://doi.org/10.1016/j.brainresbull.2016.08.002

Wollerton, M. C., Gooding, C., Wagner, E. J., Garcia-Blanco, M. A., & Smith, C. W. J. (2004). Autoregulation of polypyrimidine tract binding protein by alternative splicing leading to nonsense-mediated decay. *Molecular Cell*, *13*(1), 91–100. https://doi.org/10.1016/s1097-2765(03)00502-1

Wood, S. J., Wypych, J., Steavenson, S., Louis, J. C., Citron, M., & Biere, A. L. (1999). alpha-synuclein fibrillogenesis is nucleation-dependent. Implications for the pathogenesis of Parkinson's disease. *The Journal of Biological Chemistry*, *274*(28), 19509–19512. https://doi.org/10.1074/jbc.274.28.19509

Zhang, J., Li, X., & Li, J.-D. (2019). The Roles of Post-translational Modifications on α-Synuclein in the Pathogenesis of Parkinson's Diseases. *Frontiers in Neuroscience*, *13*, 381. https://doi.org/10.3389/fnins.2019.00381

Zhang, T., Delestienne, N., Huez, G., Kruys, V., & Gueydan, C. (2005). Identification of the sequence determinants mediating the nucleo-cytoplasmic shuttling of TIAR and TIA-1 RNA-binding proteins. *Journal of Cell Science*, *118*(Pt 23), 5453–5463. https://doi.org/10.1242/jcs.02669

Zheng, S., & Black, D. L. (2013). Alternative pre-mRNA splicing in neurons: growing up and extending its reach. *Trends in Genetics : TIG*, *29*(8), 442–448. https://doi.org/10.1016/j.tig.2013.04.003

Zhu, M., Li, J., & Fink, A. L. (2003). The association of alpha-synuclein with membranes affects bilayer structure, stability, and fibril formation. *The Journal of Biological Chemistry*, *278*(41), 40186–40197. https://doi.org/10.1074/jbc.M305326200